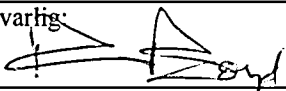NGU Rapport 98.090

The Hydrogeochemistry of the Shira Region,
Republic of Khakassia, Southern Siberia,
Russian Federation - Data Report

NGU

Norges geologiske undersøkelse
Geological Survey of Norway

Postboks 3006 - Lade
7002 TRONDHEIM
Tlf. 73 90 40 11
Telefaks 73 92 16 20

RAPPORT

Rapport nr.: 98.090	ISSN 0800-3416	Gradering: Åpen

Tittel:

The Hydrogeochemistry of the Shira Region, Republic of Khakassia, Southern Siberia, Russian Federation - Data Report

Forfatter: Banks, D., Parnachev, V.P., Berezovsky, A.Y. & Garbe-Schönberg, D.	Oppdragsgiver: NGU, Tomsk State University (Russia), Local Administration of Shira Region (Khakassia, Russian Federation), University of Kiel (Germany)
Fylke: Khakassia, Russian Federation	Kommune: Shirinskii region
Kartblad (M=1:250.000)	Kartbladnr. og -navn (M=1:50.000)
Forekomstens navn og koordinater:	Sidetall: 99 Pris: 120,- Kartbilag:

Feltarbeid utført: August 1996	Rapportdato: 16.06.98	Prosjektnr.: 2716.00	Ansvarlig:

Sammendrag:

The groundwater chemistry of the aquifers around and within the Devonian rift basin of the Shira area is very different from that of the Permian Oslo Rift. The anionic chemical composition in the Russian Devonian aquifers is often dominated by apparently evaporite-derived sulphate and chloride salinity. The composition of the more saline ground- and lake-waters is typically of sodium sulphate (-chloride) type. This sodium sulphate signature appears be present even in non-evaporite-bearing aquifers and to pervade the entire hydrological cycle, probably by the presence of evaporite-dust and lake spray in local precipitation. It is postulated that the sodium-sulphate-(chloride) hydrochemical signature is characteristic for inland, semi-arid, partially closed drainage basins, being derived from silicate water-rock interaction, halite and gypsum dissolution, coupled with calcium, magnesium and bicarbonate removal via calcite/dolomite precipitation. Evaporite-derived saline groundwaters feed lake systems, where further evaporative up-concentration occurs such that maximum salinities of over 100 g/L are reported in the most saline lake (Lake Tus). The Khakassian groundwaters do not, even in the granitoids, contain the high levels of natural health-related minor/trace elements (F, U, Th, Be, Tl) characteristic of the granites in and around the Oslo rift. Fluoride concentrations exceeding drinking water norms are not encountered in the Shira region, even in the granitoid complexes. In town areas in the Shira region, nitrate concentrations often exceed drinking water norms, suggesting possible contamination from latrines or sewerage. This result suggests that a systematic microbiological survey of the region's public supply wells for faecal micro-organisms would be advisable.

Emneord: Geokjemi	Hydrogeologi	Borebrønn
Fjell	Evaporitt	Granitt
Grunnvannskvalitet	Helse	Kartlegging

CONTENTS

Figures

Part 2

Figure 2.1. Sketch map of the Minusinsky intermontane trough within the Altai-Sayan mountain region, southern Siberia, Russia (after Luchitsky 1960).

Figure 2.2. Map showing geology and locations of sampled wells, boreholes and springs in the Shirinsky district.

Figure 2.3. Durov diagram illustrating the main water types of the sampled groundwaters.

Figure 2.4. Boxplots indicating the dependence of groundwater temperature (at sampling point) on lithology and source-type.

Figure 2.5. Boxplots indicating the dependence of selected hydrochemical parameters on lithology.

Figure 2.6. Plots illustrating the dependence of sulphate, alkalinity, calcium, magnesium and sodium concentrations on chloride, and of sodium concentrations on sulphate.

Figure 2.7. Plot of Br/Cl ratio versus Cl for varying nitrate concentrations in the sampled groundwaters.

Figure 2.8. Boxplots illustrating distribution of concentrations of nitrate and potassium in the sampled groundwaters according to land-use type.

Figure 2.9. Boxplots illustrating the dependence of selected minor and trace parameters on lithology in the sampled groundwaters.

Figure 2.10. Boxplots illustrating the distributions of selected parameters in granitic groundwaters from the Cambro-Ordovician Khakassian granites (this paper), the Carboniferous granite of the Isles of Scilly, U.K. (Banks et al. 1997), the Precambrian Iddefjord Granite of southern Norway (Banks et al. 1995a,b, 1997) and the Permian Drammen Granite of the Oslo Rift, southern Norway (Reimann et al. 1996).

Part 4

Figure 4.1. Schematic map of the structure of the Minusinsky intermontane trough. (Inset: position of the Minusinsky Trough within the Altai-Sayan mountain region of southern Siberia (Russian Federation)).

Figure 4.2. Schematic map of sampled groundwater sources (boreholes, wells and springs) in the Shira district.

Part 8

Figure 8.1: Boxplots showing distribution of elements Al, Ba, Ca, Ce, Cu, Fe, K, Li, Mg, Mn, Mo and Na, as analysed by ICP-AES.

Figure 8.2: Boxplots showing distribution of elements P, Pb, Si, Sr, Ti, V, Zn, Zr, as analysed by ICP-AES, and also As by atomic adsorption, sum of anions (chloride + alkalinity +

sulphate + nitrate) and sum of cations (sodium + potassium + magnesium + calcium + iron [assumed +II]).

Figure 8.3: Boxplots showing distribution of parameters pH (field), temperature (°C - field), Eh (mV - field), alkalinity (meq/l - field), Br, Cl, F, NO_3^-, $SO_4^=$ (all mg/l, by ion chromatography), $log_{10}Cl$ and $log_{10}SO_4^=$.

Figure 8.4: Boxplots showing distribution of the mass ratios Sr/Ca, Na/Cl, Na/Ca and $SO_4^=$/Cl according to geological units.

Figure 8.5: x-y plots showing distribution of the mass ratios Sr/Ca, Na/Cl, Na/Ca and $SO_4^=$/Cl according to geological units and pH.

Figure 8.6: x-y plots showing distribution of the mass ratios Sr/Ca, Na/Cl, Na/Ca and $SO_4^=$/Cl according to geological units and chloride.

Figure 8.7: x-y plots showing Na vs. Cl, Na vs. $SO_4^=$, Mg vs. Ca and Mg vs. $SO_4^=$, according to geological units.

Figure 8.8: x-y plots showing P vs. NO_3^-, K vs. NO_3^-, Fe vs. NO_3^- and Br/Cl mass ratio vs. NO_3^- according to surrounding land use.

Figure 8.9: x-y plots showing (top) distribution of ion balance error versus sum of anions (meq/l) according to geological unit, (bottom) Br/Cl mass ratio vs. Cl (mg/l).

Figure 8.10: x-y plots showing $SO_4^=$ vs. Cl, K vs. Cl, Ca vs. Cl, and Mg vs. Cl according to geological units.

Figure 8.11: x-y plots showing alkalinity vs. Cl, Na/K (meq ratio) vs. Cl, Ca/Mg (meq ratio) vs. Cl, and Ca/alkalinity (meq ratio) vs. Cl according to geological units.

Figure 8.12: x-y plots showing Na/Cl (meq ratio) vs. Cl, Na/$SO_4^=$ (meq ratio) vs. $SO_4^=$, Na vs. Cl, and Na vs. $SO_4^=$ according to geological units.

Figure 8.13: Boxplots showing distribution of Na/$SO_4^=$ mass ratio according to geological units.

Figure 8.14: x-y plots showing $SO_4^=$ vs. Cl, Sr vs. Ca, Ba vs. $SO_4^=$, and Ca vs F according to geological units.

Figure 8.15: "Draftsman" presentation of correlations between different parameters.

Figure 8.16: Boxplots showing distribution of selected elements analysed by ICP-MS (and fluoride by ion chromatography), according to geological units.

Figure 8.17 Boxplots comparing pH, alkalinity, calcium, sodium, uranium, fluoride, copper, zinc, Na/Ca mass ratio and lead for four different granites.

Figure 8.18 Boxplots comparing iron, manganese and beryllium for the four different granites (as for Fig. 8.17).

Figure 8.19 Durov diagram based only on meq/l concentrations of Na, Mg, Ca, $SO_4^=$, Cl, and alkalinity (HCO_3^-) (i.e. not NO_3^- and K), sorted according to geological units.

Figure 8.20 x-y diagrams comparing eight selected parameters analysed by ICP-AES and ICP-MS techniques.

Figure 8.21 x-y diagrams comparing six selected parameters analysed by ICP-AES, AA and ICP-MS techniques.

Figures 8.22 and 8.23 Boxplots showing distributions of concentrations according to geological units for all elements analysed by ICP-MS.

Tables

Table 2.1. The chemical composition of 6 saline lakes and one freshwater lake (Itkul) in the Shira region.

PART 1 - INTRODUCTION

Groundwater sampling was carried out in the Shira region of Khakassia during the period 16th - 21st August 1996, by David Banks (NGU), Prof. Valery Petrovich Parnachev (Dept. of Dynamic Geology, Tomsk State University) and Alexander Y. Berezovsky (Tomsk State University / Shira Regional Administration). Alkalinity, pH, Eh and temperature were measured in the field, while filtered (0.45 μm) samples were returned to NGU for analysis by ICP-AES and ion chromatography methods. Samples were also sent to Germany for analysis by ICP-MS techniques by Dr. Dieter Garbe-Schönberg of the University of Kiel.

This report is intended to document the raw data produced during the study. To introduce the data, Part 2 of the report consists of the first version of a paper prepared for submission to an international scientific journal.

Summaries of selected aspects of the data have already been published by Parnachev et al. (1997a) as an extended abstract in NGU Bulletin and by Banks et al. (1998) as a report to a conference in Tomsk. For readers interested in acquiring more information about the geology, hydrochemistry, limnochemistry and state of the environment in the Shira Region, the recent monograph by Parnachev et al. (1997b) may be consulted.

Banks, D., Makarenko, N.A., Bukatin, I.V. & Berezovsky, A.Y. (1998). Gidrogeokhimicheskie ossobennosti podzemnikh vod Shirinskovo raiona (Respublika Khakassia) *[Hydrogeochemical characteristics of groundwaters of the Shira region, Republic of Khakassia - in Russian]. In* Aktualynie voprosi geologii i geografii Sibiri: Tom 1: Obshaya i regionalnaya geologiya. Stratigrafiya. Paleontologiya. Problemi i zadachi geologicheskovo obrazovannie *[Current issues of geology and geography of Siberia. Vol. 1: General and regional geology. Stratigraphy. Palaeontology. Problems and aims of geological education].* Proc. Conference 1-4th April 1998, Tomsk State University, p. 36-38.

Parnachev, V.P., Banks, D. & Berezovsky, A.Y. (1997a). The anionic composition of groundwaters in extensional tectonic environments: the Shira Region, Khakassia, southern Siberia. *Norges* geologiske *undersøkelse Bulletin,* **433,** 62-63.

Parnachev, V.P., Balakhchin, V.L., Berezovsky, A.Y., Bukatin, I.V., Banks, D., Vidrina, S.M., Dmitriev, V.E., Kurbatsky, V.N., Larichev, V.E., Makarenko, N.A., Nekratov, N.A., Petrov, A.N., Prokofiev, S.M. & Tanzibaev, M.G. (1997b). Zhemchuzhina Khakassii: Prirodnii kompleks Shirinskovo raiona *[Khakassian pearl: the natural system of the Shira region - in Russian].* Khakas State University , Abakan, 180 pp. ISBN 5-7810-0052-6.

PART 2 - THE HYDROCHEMICAL COMPOSITION OF GROUNDWATERS IN AN EXTENSIONAL TECTONIC ENVIRONMENT: THE SHIRA REGION, KHAKASSIA, SOUTHERN SIBERIA

V. P. Parnachev[1], D. Banks[2], A. Y. Berezovsky[1], D. Garbe-Schönberg[3]

[1]Department of Dynamic Geology, Tomsk State University, Lenina prospekt 36, TOMSK, 634050 Russia.

[2]Norges Geologiske Undersøkelse, Postboks 3006 Lade, N-7002 TRONDHEIM, Norway.

[3]Geologisch-Paläontologisches Institut und Museum, Christian-Albrechts-Universität zu Kiel, Olshausenstraße 40-60, D-24118 KIEL, Germany.

2.1   Introduction

Extensional tectonic environments are often associated with esoteric groundwater chemistry. Some of the naturally occurring hydrochemical components may be toxic to humans. The reasons for the problematic hydrogeochemistry are at least three-fold:

(i) extensional environments are usually related to igneous activity, often involving unusual petrochemistry (alkaline suites).

(ii) extension may be associated with subsidence and rifting. In inland, arid climates this may result in poor surface drainage, evaporative up-concentration of waters and, sometimes, saline lakes, saline groundwaters and evaporite formation.

(iii) extensional settings are often associated with high geothermal gradients and mineralised, thermal springs

For example, the East African Rift is associated with highly saline lakes and fluoride-rich groundwaters. Some of the earliest cases of fluorosis (1000 AD - Shupe et al. 1979) are reported from Iceland. Recently, a survey by Reimann et al. (1996) of bedrock groundwaters associated with the Oslo Rift, revealed disturbingly high concentrations of potential toxins

such as fluoride, radon, uranium, beryllium and thallium. In fact, on the basis of only a few parameters, over 50 % of Reimann et al.'s groundwaters failed accepted drinking water quality norms (Morland et al. 1997., Banks et al. *in press*).

It is thus of great importance to gain a better understanding of groundwater evolutionary processes in extensional tectonic environments. Many traditional geologists assume that petrochemistry is always the dominant factor controlling groundwater composition. Detailed studies have suggested that other factors may be at least as important, such as: climate, proximity to the coast, weathering and glacial history, topography, hydrodynamic factors (Banks et al. 1997) and common thermodynamic equilibria (e.g. calcite saturation).

This project aims to assess the groundwater chemistry of a rifting environment not geologically dissimilar to the Oslo Graben, namely the Khakassian Graben system (the so-called Minusinsk Trough structure) in Southern Siberia. The geographical location and climatic conditions of Oslo and Southern Siberia are, needless to say, somewhat different, permitting an evaluation of the relative importance of geological versus climatic/geographic factors on groundwater chemistry.

2.2   The Study Area

Khakassia is a small republic of the Russian Federation. The Republic is situated in the central part of the Altai-Sayan Mountain region in southern Siberia (Figure 2.1). The study area lies within the Minusinsk intermontane trough, bounded by the mountain areas of Kuznetsk-Alatau in the west, and the Western and Eastern Sayans in the south and the east. The trough itself, containing Upper Palaeozoic sediments and volcanics, is divided, from north to south, into four sub-basins by east-west ridges of Precambrian/Lower Palaeozoic rocks: the Nazarovskaya, Chebakovo-Balakhtinskaya, Sydo-Eribinskaya and Yuzhno-Minusinskaya basins (Luchitski 1960, Parnachev et al. 1992). The intervening ridges are offshoots of the Kuznetsk Alatau and Eastern Sayan ranges and include the Solgonsky and the Batenevsky ridges. From a tectonic perspective, the Minusinsk Trough is considered an early Devonian palaeorift structure (Parnachev et al. 1996a). The geology is, however, indicative of repeated phases of rifting activity; in the Cambrian-Ordovician, in the Lower Devonian and, most

recently, in the Palaeogene-Quaternary (fault reactivation, volcanic activity). This study will focus on the region around the town of Shira (Figure 2.2).

The climate is semi-arid (annual average rainfall = 312 mm at Shira, ratio of rainfall to potential evaporation = 0.5-1.5; Feshbach et al. 1995). At Shira, the majority of the rainfall occurs in the months June to September. The mean monthly temperature fluctuates between +20 and -20°C with a yearly mean close to 0°C. The area is not permafrosted (Feshbach et al. 1995); it and the surrounding mountain areas were not extensively glaciated during the Weichselian (Nalivkin 1960). The semi-arid climate results in a low density of surface water drainage, although the region lies on one of Siberia's major water divides, that between the Ob' and Yenisei catchments.

The Shira region of Khakassia lies on the southern margin of the second Devonian sub-basin, the Chebakovo-Balakhtinskaya basin. The topography within the basin ranges from ca. 320 - 670 m and largely consists of hilly steppe, with dominant grass and low shrub vegetation and sparse trees. The land use ranges from open grassland and pasture used for free-range cattle-herding to relatively low intensity agriculture - various grains and sunflowers being prominent crops. The boundaries of the basin are formed by lower Palaeozoic and Precambrian rocks (up to around 1300 m), where a more taiga-like vegetation dominates. The Tuim granite complex south of Shira forms an area of intermediate hilly topography with a vegetation and appearance resembling closely that of southern Norway - low to medium density woodland of mixed conifer and birch. The Tuim granite area yields poor agricultural soils and is dominantly used for free-range cattle herding.

In Shira town the land use is largely residential with some light - to - medium industry, including engineering. The Tuim Plant produces metal-wares while mining and some smelting have historically occurred for a variety of metals including Cu, Mo and W, dominantly associated with the granite complex. Alluvial gold mining is currently carried out in the SW mountains of the Shira area.

2.3   Geology

The region is particularly interesting in as much as it presents a very varied geology consisting of Precambrian and Palaeozoic metamorphic, sedimentary and igneous rocks (Figure 2.2). The Kuznetsk-Alatau and Eastern Sayan ranges are comprised of Precambrian and Lower Palaeozoic formations (including volcanics, clastic and carbonate sedimentary rocks and granitoids), as are the Batenevsky and Solgonsky ridges which define the borders of the Chebakovo-Balakhtinskaya Basin. The Basin itself is a large (250 x 100 km) synclinorium, infilled by Devonian and Lower Carboniferous volcanics, evaporites and sediments, with a complex internal structure.

Lower Devonian deposits are represented by the sedimentary-volcanogenic Byskarskaya series, which unconformably overlaps the Riphean-Vendian and Cambrian-Ordovician rocks bordering the Basin. The Byskarskaya series contains alternating horizons of volcanic and sedimentary rocks. The volcanics consist of interbedded acidic and basic (homodromous trachyrhyodacite-trachybasalt) rocks, while sedimentary horizons are generally discontinuous layers of red-bed sandstones, siltstones, tuffites and occasional conglomerates and gritstones. The deposits tend to reflect continental conditions, while the occurrence of evaporite minerals (halite and gypsum imprints) suggests deposition in enclosed lagoon or lake basins. The thickness of the series is estimated to be 1800 - 2000 m.

The Middle Devonian is represented by the Saragashskaya and Beiskaya suites. The former transgressively overlies Lower Devonian deposits and contains thin interlayers of gritstone at the base of the sequence. These are replaced upwards by interbedded yellow- and greenish siltstones, sandstones, mudstones, marls and limestones. The thickness of the Saragashskaya Formation varies from 150 to 300 m and is conformably overlain by the Beiskaya Formation (60-250 m thick), comprising grey limestones, with interlayers of dolomites, marls, occasional calcareous sandstones, siltstones and mudstones.

Upper Devonian deposits include the terrigenous red-bed sedimentary rocks of the Oidanovskaya, Kokhaiskaya and Tubinskaya Formations. The Oidanovskaya Formation is some 200 - 600 m thick, conformably overlies the Beiskaya limestones and consists of

siltstones, mudstones and occasional cross-bedded gritstones. The Kokhaiskaya Formation (30 - 600 m thick) is dominated by intercalated greyish siltstones and mudstones (containing thin beds of sandstones), marls and algal and brecciated limestones. The Tubinskaya Formation (200 to 1200 m thick) is composed of red sandstones, with interlayers of siltstones, mudstones and conglomerates.

The Lower Carboniferous system (Tournaisian Stage) is represented by the Bystryanskaya and Altaiskaya Formation. The Bystryanskaya Formation (total thickness 275 m) conformably overlies the Tubinskaya red-beds, and comprises grey, yellowish and greenish sandstones, limestones, siltstones, mudstones and tuffites. A gradual upwards transition introduces the Altaiskaya Formation (50-135 m thick), comprising red-brown and yellowish-violet tuffs, tuffites, siltstones and sandstones.

The sedimentary rocks of the Middle (Saragashskaya, Beiskaya) and Upper (Oidanovskaya, Kokhaiskaya, Tubinskaya) Devonian and Lower Carboniferous are believed to have been laid down in a post-rift sedimentary basin under shallow-water marine and lagoonal (Middle Devonian and Carboniferous) or continental (Upper Devonian) conditions. Indicator-minerals of evaporite conditions (interbeds of gypsum, barite and fluorite, imprints of rock salt) are known from Middle, Upper Devonian and Lower Carboniferous deposits.

The modern structure of the sub-basins of the Minusinsk Trough is traversed by sublatitudinal faults. The most recent displacements on these faults, accompanied by the formation of volcanic pipes, took place 28 - 78 Ma ago (Parnachev et al. 1996b).

2.4   Saline Lakes and Water Supply

The popularity of the Shira region of Khakassia as a holiday destination for Siberians is partly due to the abundance of lakes, both fresh and salt. Probably the most saline is Lake Tus, reported to have a mineralisation of over 100 g/l. Other saline lakes are detailed in Table 2.1. The hydrochemical type of the lakes is variable, but the more saline are typically dominated by sodium sulphate. The saline lakes tend to be associated with Upper Devonian (D_3) and Lower Devonian (D_1) deposits which contain evaporite minerals and saline groundwaters. The

salinity of the lakes is further enhanced by the lack of surface water flux through the lakes and high evaporation. Modern evaporites (whose nature is uncertain) are also observed forming on the margins of several of the saline lakes. Freshwater lakes tend to occur on strata older than D_3 without evaporite sequences. Lake Itkul, for example, on D_2 carbonates, forms the backbone of Shira Town's water supply.

2.5   Field techniques and Data Analysis

Groundwater sampling in Khakassia was performed during the period 16th - 21st August 1996. Samples were taken either from bedrock groundwater springs or bedrock boreholes in regular use for water supply (both in rural and urban areas). It was not possible to sample all boreholes directly at the well-head; some samples were acquired from the header tank above the borehole, from a household tap fed by the borehole or from a communal electric pump on a borehole-fed ring-main. In all cases the tap was run for at least 5 minutes prior to sampling. pH and temperature of water were measured in the field using a Palintest Micro 900 pH meter, calibrated regularly against standard solutions of pH 7 and 10. Alkalinity was determined using an Aquamerck field titration kit, with indicator of end-point pH=4.3, with an estimated accuracy of ± 0.2 mmol/l. Duplicate determinations were carried out and the mean value used. Logistical constraints restricted sampling to a single 1x100 ml polyethene flask of groundwater, filtered at 0.45 µm with disposable Millipore "Millex" filters.

The samples were transported to Norway and c. 10 ml of each sample was decanted for analysis at the Geological Survey of Norway (NGU) for the anions SO_4^{2-}, PO_4^{3-}, F$^-$, NO_3^-, Cl$^-$, Br$^-$ and NO_2^- by Ion Chromatography (IC). The remaining 90 ml of sample was shipped to the University of Kiel, where it was acidified with concentrated ultrapure nitric acid in-flask and analysed for a range of trace elements by Inductively Coupled Plasma Mass Spectrometry (ICP-MS) techniques. The acidified samples were then returned to Norway for analysis on NGU's Inductively Coupled Plasma Atomic Emission Spectroscopy (ICP-AES) equipment. For the purposes of statistical analysis, analytical values below experimental detection limit were assigned a value equal to half the detection limit.

Samples were allocated to their most likely bedrock type (Figure 2.2):

13

V-C = Vendian / Cambrian volcanogenic and carbonate sedimentary series

C-O = Cambrian / Ordovician igneous complex. Dominated by alkaline granitoid massifs.

D_1 = Lower Devonian. Interbedded volcanics and sediments with some evaporite minerals.

D_2 = Middle Devonian. Carbonate rich sediments, including limestones and dolomites.

D_3 = Upper Devonian. Sedimentary sequence with frequent red-beds and evaporite-bearing horizons.

C_1 = Lower Carboniferous. Sandstones, siltstones, mudstones, limestones and tuffites.

Fours wells, numbers 8, 14, 20 and 31, lie very close to lithological boundaries. For the purpose of statistical analysis they are allocated to groups D_1, D_3, D_2 and D_3 respectively. Some wells, including 24 and 25, may also receive some input of groundwater from Quaternary deposits.

2.6   Water Types

The waters exhibit a large range in hydrochemical type, as illustrated by the Durov diagram in Figure 2.3. The waters from the C-O igneous complex are dominantly calcium-bicarbonate waters of low ionic content, suggesting waters following a standard silicate- and carbonate-dissolution evolutionary pathway.

The waters from the Carboniferous aquifers are of sodium bicarbonate type.

The waters from the Devonian and Vendian-Cambrian sedimentary aquifers have a wide range of water type, from Ca-Mg-HCO_3, through Mg-SO_4 to Na-SO_4 and Na-Cl. The Ca-Mg-HCO_3 waters probably reflect carbonate weathering in sedimentary sequences rich in dolomite. The predominance of Mg, SO_4, Na and Cl in some waters is likely to reflect the influence of evaporite minerals such as dolomite, gypsum, anhydrite and halite.

All waters are saturated with respect to calcite (i.e. saturation index SI between -0.2 and +0.7). The waters tend to be saturated or supersaturated with respect to dolomite, the Carboniferous waters and the most saline Devonian and V-C waters exhibiting the highest saturation indices.

The magnesium-poor waters are undersaturated with respect to magnesite, but the Carboniferous waters and most saline Devonian and V-C waters are saturated. Waters are generally unsaturated with respect to gypsum and anhydrite, although the two most saline waters from D_1 and D_3 do approach saturation.

2.7   pH and Temperature

Figures 2.4 and 2.5 indicate the distribution of selected parameters with aquifer lithology and source type (spring/borehole). Groundwater temperatures are generally lower in springs than boreholes, possibly reflecting geothermal gradient with depth, but more likely reflecting warming in pumps and pipelines from boreholes. Temperatures of water in springs are around 3 - 4°C, reflecting annual average air temperature. There is a slight tendency to lower temperatures in groundwaters of the C-O igneous complex than the D_3 and C_1 aquifers. This may be due to the generally higher altitude of the C-O complex but more likely reflects the prevalence of boreholes in the D_3 and C_1 aquifers, as opposed to more springs in the igneous complex.

pH values are generally in the interval 7 -8, with the notable exception of the boreholes in the C_1 aquifer, all three of which exhibit pH values in excess of 8.

2.8   Anionic Composition

Alkalinity varies greatly (from 3 to 13 meq/L) which, surprisingly, shows no clear correlation with pH. The lowest alkalinities tend to be found in groundwaters from the C-O igneous complex, reflecting their generally leucocratic, siliceous nature.

Chloride and sulphate exhibit a high degree of co-variance. The highest concentrations of both parameters are found in the D_3 aquifers, with one particularly high outlier in D_1. The lowest median values tend to be found in the C-O igneous complex, reflecting a lack of lithological sources for these parameters. Levels of a few mg/L chloride are explainable by salts in rainfall. Many samples have higher concentrations which must be explained either by significant evapotranspirative up-concentration, possible pollution or dissolution of

15

evaporites. The latter explanation must be invoked to explain the particularly high values from the D_1 and D_3 sequences. Interestingly, the chloride and sulphate contents of the main Lake Tus spring (sample 30, 2850 and 3230 mg/L, respectively) suggest a considerably lower spring salinity than the Lake water itself (reported to be 100 g/L). This suggests that the Lake's salinity is derived from the dissolved Devonian evaporite salts in spring water feeding the Lake, but significantly concentrated by evaporation in the Lake basin itself.

A plot of chloride versus sulphate (Figure 2.6) indicates a significant enrichment of sulphate relative to the sea-water dilution line. This is in accord with the lake compositions shown in Table 1 and may indicate a prevalence of sulphate evaporites over halite in the Devonian sequences. The sulphate enrichment is, however, observed in almost all samples, even those from Cambro-Ordovician granite areas. It is postulated that the chloride and sulphate content in groundwater from non-evaporite-containing aquifers is derived both from dry fallout of salts and dissolved salts in rainfall. In the extremely inland environment of Khakassia this salt fallout is likely to be dominated by salts derived from terrigenous sources (evaporites, lakes) rather than marine sources. Hence, the salt fallout retains an evaporite (sulphate-enriched) signature, rather than a marine signature as is the case in maritime regions (e.g. Norway and SW England - see below).

Plots of Br/Cl mass ratio yield values of around 0.0035 for the more saline waters, equivalent to the current average sea-water ratio (Edmunds 1996). Such a ratio, or lower, is also compatible with evaporite-derived brines. Higher apparent Br/Cl ratios occur at lower chloride concentrations, for which there are two possible explanations (i) analytical error (i.e. greater relative error in Br determination in low-salinity waters) or (ii) another, non-marine, non-evaporitic source of bromide and chloride (Andreasen & Fleck 1997). Figure 2.7 suggests, if we ignore the two most saline waters, that there is some correlation between high NO_3^- concentrations and elevated chloride, supporting the idea of such a second-source. It is known that many nitrate-rich sources of contamination (sewage, landfills, fertiliser), also contain elevated chloride.

The various groundwater sources have been divided into rural, agricultural (incl. cattle station) and urban land use categories (Figure 2.8). The rural and agricultural sources exhibit concentrations of nitrate of < 45 mg/L (Russian GOST drinking water limit - Kirjuhin et al.

1993), while the median urban concentration is around 57 mg/L, with a maximum of 189 mg/L in Vlasyevo town supply (sample 6). Such a level is regarded as being potentially hazardous for young children. Clearly, an urban source should be invoked for the worst instances of nitrate contamination. The most likely source is sewage / leaking latrines, although other sources such as refuse tips may contribute. The results suggest that a microbiological investigation of urban groundwater sources in Khakassia should be prioritised.

2.9   Cationic Composition

The various lithologies have rather similar distributions of calcium concentrations (Figure 2.5), with the exception of the Carboniferous aquifer, where calcium concentrations are significantly lower. The Carboniferous groundwaters also exhibit relatively high strontium concentrations, high Sr/Ca ratios and high sodium concentrations. These tend to be suggestive of either (a) ion exchange of sodium for calcium, possibly related to the zeolite mineralisation found in the aquifer system or (b) calcium removal at high pH by calcite saturation and precipiation. Magnesium and sodium concentrations are higher in the sedimentary/volcanic sequences than in the Cambro-Ordovician igneous complex, indicating the importance of evaporite dissolution for groundwater chemistry in the sediments.

Potassium exhibits concentrations which are significantly higher in the D_3 aquifer system than in D_1. Concentrations in the Carboniferous aquifer are notably low. Potassium concentrations are also significantly greater in the urban groundwaters than in the rural or agricultural area waters, possibly (like nitrate) being derived from pollution.

Several ratios shed interesting light on the evolution of the water types. The Sr/Ca ratio in many systems is rather constant reflecting congruent dissolution of Sr and Ca from mineral phases such as carbonate. An elevated Sr/Ca ratio is typical of calcium removal, either by calcite saturation and precipitation (as calcite typically reaches saturation earlier than strontium carbonates or sulphates) or by ion exchange, or by dissolution of specific minerals with a high Sr/Ca ratio (possibly evaporite minerals). In the Khakassian waters the lowest

Sr/Ca ratios are in the C-O igneous complex (where the ratio is very constant) and also in the V-C sediments and D_1 complex. Elevated ratios occur in the D_2, D_3 and C_1 aquifers.

A similar pattern is seen in the Na/Ca ratio, with the highest values being observed in the C_1 system.

The Na/Cl ratio is often seen as an indicator of water rock reaction (Figure 2.6). The mass ratio in sea-water is 0.60 (equivalent ratio 0.93) and in halite 0.65 (equivalent ratio 1.0). A ratio higher than this in groundwater implies that Na is being contributed by sources other than halite dissolution or marine salts in precipitation. A sodium excess is often derived from feldspar weathering (e.g. in granites or immature sediments) or by cation exchange. Significant sodium excesses are observed, particularly in the sedimentary aquifers and the question naturally arises - where is this sodium coming from ?

2.10   Groundwater Chemical Signatures

A clue is found in a plot of Na versus SO_4^{2-} (Figure 2.6), where an almost perfect linear relationship is observed. In other words, a clear background Na-SO_4^{2-} signature is observed in all the waters from Khakassia in much the same way that a clear Na-Cl signature is observed in many groundwaters from Norway due to that land's coastal proximity.

In Norway, the Na-Cl signature may be derived from one of three sources:

(1) Direct intrusion of sea-water

(2) Dry or wet fallout of marine salts as precipitation

(3) Leaching of pore water in marine sediments in coastal areas

We have already seen that the saline lakes in the Shira region tend to be sodium-sulphate in composition. The Na-SO_4^{2-} hydrochemical background could be explained by:

(1) direct intrusion of lake water

18

(2) Dry or wet fallout of Na-SO$_4^{2-}$ dominated salts in precipitation (Shira is about as far from the coast as it is possible to get, so no marine signature would be expected in precipitation). These salts may be derived from soil dust or spray from lakes.

(3) Accumulation of precipitated salts in soils due to fallout and evaporation followed by leaching to groundwater; or even leaching of Na and SO$_4^{2-}$ from evaporite minerals in the rocks themselves.

The suggestion raises some interesting postulates: if a non-marine, non-anthropogenic (presumably geogenic) component of sulphate dominates precipitation and the hydrosphere in Khakassia, could the same also be true in Europe ? Do some of the solutes we see in so-called "acid-rain" have a geogenic origin (sulphate) or even an origin in wind-blown dust from fertilised arable land (NO$_3^-$ or NH$_4^+$) ? This aspect will not be pursued further here, as a more fundamental question remains to be answered in the Khakassian situation - what is the ultimate source of the sodium-sulphate in the saline waters ? If the sodium comes from halite - where has the chloride gone ? If the sulphate comes from the gypsum, where is the calcium ?

2.11   A Partially Closed Hydrological and Chemical System ?

The origin of sodium sulphate saline lakes and groundwaters remains problematic for the hydrogeologist and the limnologist, although it has been discussed by, for example, Grossman (1968), Eugster & Hardie (1978), Eugster (1980), Hardie (1984) and Harben & Kuzvart (1996). It is perhaps no coincidence that the world's greatest reserves of natural sodium sulphate evaporite minerals occur in the interior of the worlds largest continents (North America and Asia), in partially closed, poorly drained basins in semi-arid climates. In the Plains of Alberta, Canada, extensive deposits of recent sodium sulphate evaporites occur, believed to have been deposited from post-glacial saline lakes (the crystallisation of mirabilite having been promoted by periodic freezing of the lake water). The location of the deposits coincides with underlying evaporite-bearing late Devonian sediments (Grossman 1968). The climate is not dissimilar to Siberia and the area is believed to have been partially hydraulically closed in post-glacial times, permitting evaporative up-concentration of saline groundwaters derived from Devonian strata in the lake basins.

19

Major deposits of sodium sulphate also occur in connection with saline lakes in North Dakota, Utah and California (USA), in Transbaikal, and in several places in Khazakhstan and western Siberia, such as the Kulunda Steppe and the major deposit of Lake Kuchuk, near Novosibirsk. The latter covers 155 km^2, contains some 600 million tons sodium sulphate and precipitates 640,000 tons mirabilite each winter (Harben & Bates 1990, Harben & Kuzvart 1996).

Some or all of the above-named sodium sulphate provinces share numerous similarities with the Minusinsk Trough area of Khakassia:

(i) inland areas, far from the sea.

(ii) wholly or partially hydrologically and/or topographically closed basins with low surface water through-flow

(iii) semi arid or arid climate

(iv) a high potential for up-concentration of solutes in lake basins

(v) the presence of evaporite-bearing formations at depth.

The dominance of the sodium sulphate signature has, however, not yet been adequately explained. The sources of sodium may partially be (i) halite dissolution, but in order to explain the Na/Cl excess a second source must be postulated, such as (ii) feldspar weathering (either within the depositional basin or the marginal igneous complexes) or (iii) ion exchange (Harben & Kuzvart, 1996, suggest ion exchange between gypsum and alkali silicates). Both (ii) and (iii) typically produce sodium bicarbonate waters. The source of sulphate is most likely to be gypsum dissolution (contributing both calcium and sulphate), although sulphide oxidation may be a secondary source.

These processes thus release Na^+, Cl^-, HCO_3^-, SO_4^{2-} and Ca^{2+} to the hydrosphere. We have seen that groundwaters are saturated with respect to dolomite and calcite but generally not with respect to gypsum. The groundwater/lake environment may thus act as a sink for calcium, some magnesium and bicarbonate, but only to a lesser extent for sulphate. Sodium, sulphate and chloride persist preferentially in the water phase, sodium retaining an excess over chloride due to the existence of non-evaporite sources, whereas chloride probably has an evaporite source (halite).

Such a hypothesis is supported by Figure 2.6, which illustrates good linear relationships between Na, Cl⁻ and SO_4^{2-}. If, for example, Cl⁻, is taken as an indicator of evolution of waters by evaporite dissolution and evapotranspirative up-concentration, it may be surmised from their linear relationship that no sink exists for these species and that they persist in the hydrosphere. Both calcium and alkalinity show a very low rate of increase with Cl⁻, indicating that these may be removed from groundwaters by carbonate precipitation. The somewhat higher rate of increase of magnesium with Cl⁻ testifies to the greater solubility of dolomite or epsomite, saturation being reached at a later stage of groundwater evolution.

The declining Na/Cl⁻ ratio with increasing salinity (Figure 2.6) is indicative of some external source of Na, such a source being most prominent in the least saline waters. The almost perfectly linear Na/SO_4^{2-} relationship suggests the controlling role of a sodium sulphate mineral phase in controlling groundwater chemical composition. Even in non-evaporitic aquifers (e.g. the granites), the 1:1 $Na:SO_4^{2-}$ relationship persists, suggesting the dominance of a sodium sulphate salt in windblown dust and as dissolved salts in precipitation.

2.12   Groundwater and Health

2.12.1 In Khakassia

Figure 2.9 compares the content of a number of potentially health-related minor and trace elements for the different aquifer systems identified in the study. None of the Russian groundwater samples exceed the Russian GOST drinking water limit of 1.5 mg/L for fluoride (Kirjuhin et al. 1993), even in the C-O igneous complex.

For beryllium, all the Khakassian samples lie below the analytical detection limit of 1 μg/L by ICP-AES. Russia operates with a limit of 0.2 μg/L for beryllium (Kirjuhin et al. 1993), although this must be regarded as very ambitious in the light of available analytical detection limits and the American MAC of 4 μg/L (Fetter 1994, USEPA 1997). For thallium, all except two samples are below the analytical detection limit of ICP-MS, namely 0.03 μg/L. All samples satisfy both the Russian (0.1 μg/L) and American (2 μg/L) drinking water standards (Kirjuhin et al. 1993, USEPA 1997).

For uranium, no samples exceed the Russian drinking water standard of 1700 µg/L (Kirjuhin et al. 1993), the highest value being 28 µg/L in sample 9. Apart from this sample, all other lie below the American and Canadian drinking water standard of 20 µg/L (Fetter 1994, Barnes 1986). For all samples, thorium occurs at concentrations less than the analytical detection limit of 0.03 µg/L.

Neither Cu, Zn, Pb or Cd reach concentrations in the Khakassian groundwaters which are likely to have health consequences. It is of interest to note that both W and Cu show somewhat elevated concentrations in the granitic (C-O) aquifer, which contains known W and Cu mineralisations.

2.12.2 Compared with other Granitic Groundwaters

In the Oslo rift region, granitic groundwaters very often exceed recognised drinking water standards with respect to several toxic elements such as radioelements (radon, uranium), fluoride, beryllium and thallium. Figure 2.10 compares the Khakassian C-O granite complex groundwaters with groundwaters from (i) the Permian granites of the Oslo Rift (dominated by the Drammen granite), (ii) the Precambrian Iddefjord Granite of Hvaler, lying just east of the Oslo Rift, and (iii) the Scilly Isles granite of Great Britain. Data for these granitic groundwaters are taken from Reimann et al. (1996), Banks et al. (1995a,b) and Banks et al. (1997), respectively. Immediately it becomes obvious that the Khakassian granite groundwaters differ significantly from the Norwegian. The former are generally more calcic (while the Norwegian waters are typically sodium bicarbonate), higher in alkalinity and are also poorer in most health related solutes (F, U, Be, Tl, Th). For example, the modest fluoride concentrations of the Khakassian granites are in contrast to the Oslo and Bergen areas (Reimann et al. 1996) where concentrations of up to 9 mg/L are found in crystalline bedrock aquifers.

Figure 2.10 amply demonstrates that granitic groundwaters display a wide variety of chemical compositions, ranging from the calcium bicarbonate waters of Khakassia, through the dominantly sodium bicarbonate waters of Norway to the marine dominated, immature sodium-chloride waters of the Scilly Islands in open Atlantic. The low concentrations of

health-related trace parameters in the Scilly granite has been ascribed by Banks et al. (1997) to the immaturity of these waters resulting from short residence times and the removal of many mineral phases by prolonged subaerial exposure and weathering in this unglaciated terrain. The relative enrichment of the Norwegian granitic groundwaters in many interesting minor and trace elements may be due to long residence times and the fresh nature of the recently glacially scoured granite, with reactive mineral phases still presumed to be intact. These explanations are only partially adequate for the Khakassian waters which, although poor in health-related minor and trace elements and not exposed to extensive recent glaciation, bear some signs of maturity (e.g. high alkalinity).

2.13   Conclusion

The anionic chemical composition in the Devonian aquifers of the Shira region of Khakassia is dominated by apparently evaporite-derived sulphate and chloride salinity. The composition of the more saline ground- and lake-waters are typically of sodium sulphate (-chloride) type. This sodium sulphate signature appears be present even in non-evaporite-bearing aquifers and to pervade the entire hydrological cycle, probably by the presence of evaporite-dust and lake spray in local precipitation. It is postulated that the sodium-sulphate-(chloride) hydrogeological signature is characteristic for inland, semi-arid, partially closed drainage basins, being derived from feldspar weathering and/or Ca/Na ion exchange and halite and gypsum dissolution, coupled with calcium, magnesium and bicarbonate removal via calcite/dolomite precipitation.

Evaporite-derived saline groundwaters feed lake systems, where further evaporative up-concentration occurs such that maximum salinities of over 100 g/L are reported in the most saline lake (Lake Tus).

The Khakassian groundwaters do not, even in the granitoids, contain the high levels of natural health-related minor/trace elements (F, U, Th, Be, Tl) so characteristic of the granites in and around the Oslo rift. Fluoride concentrations exceeding drinking water norms are not encountered in the Shira region, even in the granitoid complexes.

In town areas in the Shira region, nitrate concentrations often exceed drinking water norms, suggesting possible contamination from latrines or sewerage. This result suggests that a systematic microbiological survey of the region's public supply wells for faecal micro-organisms would be advisable.

2.14 Acknowledgements

2.15 References

Andreasen, D.C. & Fleck, W.B. (1997): Use of bromide:chloride ratios to differentiate potential sources of chloride in a shallow, unconfined aquifer affected by brackish-water intrusion. *Hydrogeology Journal* 5, No. 2, 17-26.

Banks, D., Reimann, C., Røyset, O., Skarphagen, H. & Sæther, O.M. (1995a): Natural concentrations of major and trace elements in some Norwegian bedrock groundwaters. *Applied Geochemistry* 10, 1-16.

Banks, D., Røyset, O., Strand, T. & Skarphagen, H. (1995b): Radioelement (U, Th, Rn) concentrations in Norwegian bedrock groundwaters. *Environmental Geology* 25, 165-180.

Banks, D., Midtgård, Aa.K., Morland, G., Reimann, C., Strand, T., Bjorvatn, K. & Siewers, U. (in press): Is pure groundwater safe to drink ? Natural "contamination" of groundwater in Norway. Accepted for publication in *Geology Today* (in press).

Banks, D., Reimann, C., Skarphagen, H. & Watkins, D. (1997): The comparative hydrogeochemistry of two granitic island aquifers: the Isles of Scilly, UK and the Hvaler Islands, Norway. *Norges Geol. Unders. Report* 97.070.

Barnes, A.J. (1986): Water pollution control; national primary drinking water regulations; radionuclides. *U.S. Federal Register,* **51/189, 30/9/86,** 34836-34862.

Edmunds, W.M. (1996): Bromine geochemistry of British groundwaters. *Mineralogical Magazine,* **60,** 275-284.

Eugster, H.P. & Hardie, L.A. (1978): Saline lakes. *In* Lerman, A. (ed.), *"Lakes: chemistry, geology and physics",* Springer verlag. 237-293.

Eugster, H.P. (1980): Geochemistry of evaporite lacustrine deposits. *Am. Rev. of Earth & Planet. Science* **8,** 35-63.

Feshbach, M., Abrosimova, Y.Y., Artyukhov, V.V., Martynov, A.S., Ermakov, S.P., Prokhorov, B.B. & Guroff (1995): Environmental and health atlas of Russia. Paims Publishing House.

Fetter, C.W. (1994): *Applied Hydrogeology (3rd edn.).* Macmillan, New York. 691 pp.

Grossman, I.G. (1968): Origin of the sodium sulfate deposits of the northern great plains of Canada and the United States. *U.S. Geol. Surv. Prof. Paper* **600-B,** B104-B109.

Harben, W. & Bates, R.L. (1990): *Industrial minerals; geology and world deposits.* Metal Bulletin plc, London, 312 pp.

Harben, P.W. & Kuzvart, M. (1996): *Global geology. A: Industrial minerals.* Industrial Minerals Information Ltd., Metal Bulletin plc., London. 462 pp.

Hardie, L.A. (1984): Evaporites; marine or non-marine ?*American J. Science* **284,**193-240.

Kirjuhin, V.A., Korotkov, A.N. & Shvartsev, C.L. (1993): *Gidrogeohimija [Hydrogeochemistry - in Russian],* Nedra, Moscow, 383 pp.

Luchitsky, I.V. (1960): *Vulcanism and Devonian Tectonics of the Minusinsk Basin.* Akademija Nauk, Moscow.

Morland, G., Reimann, C., Strand, T., Skarphagen, H., Banks, D., Bjorvatn, K., Hall, G.M. and Siewers, U. (1997): The hydrochemistry of Norwegian bedrock groundwater - selected parameters (pH, F⁻, Rn, U, Th, B, Na, Ca) in samples from Vestfold and Hordaland, Norway. *Norges Geologiske Undersøkelse Bulletin* **432,** 103-118.

Nalivkin, D.V. (1960): *The geology of the USSR: a short outline* (Ch. 6 Angara Geosyncline). Pergamon Press, 170 pp.

Parnachev, V.P., Vasilev, B.D. & Ivankin, G.A. and others (1992): *Geology and minerals of Northern Khakassia [in Russian].* Izd-vo Tomsk State University, 166 pp.

Parnachev, V.P., Vilzan, I.A., Makarenko, N.A. and others (1996a): *Devonian riftogenic formations in southern Siberia [in Russian].* Izd-vo Tomsk State University, 239 pp.

Parnachev, V.P., Vilzan, I.A., Makarenko, N.A. and others (1996b): *Continental riftogenesis and post-rift sedimentary basins in the geological history of southern Siberia [in Russian].* Izd-vo Tomsk State University, 100 pp.

Parnachev, V.P., Balakhchin, V.L., Berezovsky, A.Y., Bukatin, I.V., Banks, D., Vidrina, S.M., Dmitriev, V.E., Kurbatsky, V.N., Larichev, V.E., Makarenko, N.A., Nekratov, N.A., Petrov, A.N., Prokofiev, S.M. & Tanzibaev, M.G. (1997): Zhemchuzhina Khakassii: Prirodnii kompleks Shirinskovo raiona *[Khakassian pearl: the natural system of the Shira region - in Russian].* Khakas State University , Abakan, 180 pp. ISBN 5-7810-0052-6.

Reimann, C., Hall, G.E.M., Siewers, U., Bjorvatn, K., Morland, G., Skarphagen, H. & Strand, T. (1996): Radon, fluoride and 62 elements as determined by ICP-MS in 145 Norwegian hard rock groundwater samples. *Science of the Total Environment*, **192**, 1-19.

Shupe, J.L., Arland, E.O. & Sharma, R.P. (1979): Effects of fluorides in domestic and wild animals. *In:* Oehme, F.W. (ed.) «*Toxicity of heavy metals in the environment - Part 2*», Marcel Dekker, New York.

USEPA (1997): *National primary drinking water regulations. Contaminant Specific Fact Sheets. Inorganic Chemicals - Technical Version.* United States Environmental Protection Agency world wide web site: http://www.epa.gov/OGWDW/dwh/t-ioc.html

Table 1. The chemical composition of 6 saline lakes and one freshwater lake (Itkul) in the Shira region.

[1] data after Parnachev et al. (1992).
[2] data after Parnachev et al. (1997).

Lake	Area (km²)	Maximum depth (m)	Water composition. Kurlov formula (M = mineralisation in g/L: major ions as % equivalents)	pH
Shira[1,2]	36	21.8	$M_{21.0}$ [$SO4_{71}Cl_{21}HCO3_4$ / $(Na+K)_{60}Mg_{38}$]	8.7-9.2
Byelyo[2]	75	48.2	$M_{8.7}$ [$SO4_{57}Cl_{24}$ / $(Na+K)_{58}Mg_{38}$]	8.9-9.2
Tus[2]	2.65	2.0	M_{110} [$SO4_{51}Cl_{46}(HCO3+CO_3)_3$ / $Mg_{49}(Na+K)_{48}Ca_3$]	8.3-8.4
Shunyet[2]	0.46	3.0	$M_{12.0}$ [$Cl_{60}SO4_{33}$ / $Mg_{56}(Na+K)_{41}$]	8.4
Utichye-1[1]	0.5	2.0	M_6 [$SO4_{61}Cl_{22}$ / $Na_{61}Mg_{37}$]	
Utichye-3[1]	1.4	3.0	$M_{14.2}$ [$SO4_{60}Cl_{36}$ / $Na_{57}Mg_{26}$]	
Itkul[2]	23	17	$M_{0.7}$ [$(HCO3+CO3)_{74}SO4_{19}$ / $Mg_{55}Na_{18}Ca_{16}$]	

Figure 1. Sketch map of the Minusinsky intermontane trough within the Altai-Sayan mountain region, southern Siberia, Russia (after Luchitsky 1960). Key: I boundary of the Minusinsk trough; II the main Devonian sub-basins; III Horst/ridge areas between sub-basins; IV,V depressions; VI horst/ridge area, beneath cover of Devonian volcanogenic rocks; VII ditto, beneath cover of Mesozoic (mainly Jurassic) deposits; VIII Chulimskaya synclinorium (Mesozoic sediments); IX Pre-Devonian magmatic and metamorphic formations surrounding the Minusinsk trough (i.e. basement); X basement, beneath cover of mid-Palaeozoic sedimentary rocks.
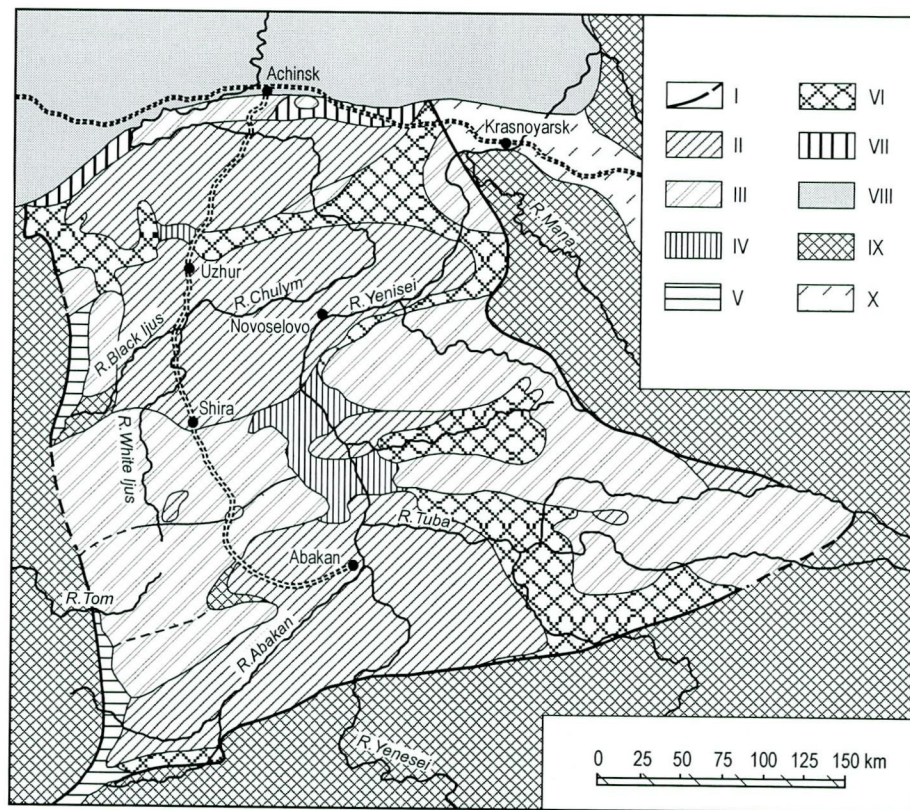
Figure 2. Map showing geology and locations of sampled wells, boreholes and springs in the Shirinsky district.
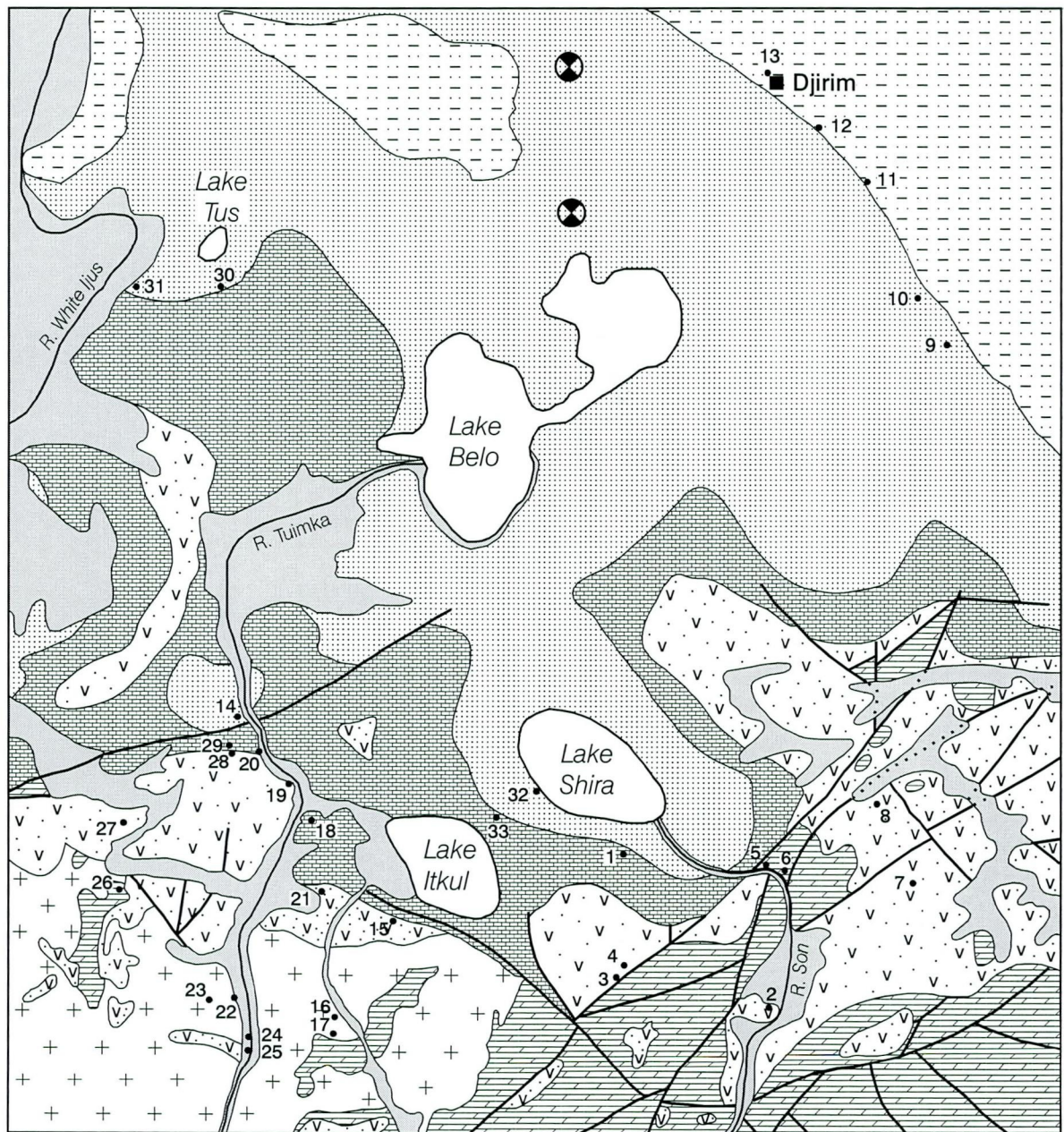
KEY
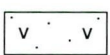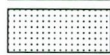
Quaternary	Lower Devonian
Carboniferous	Cambrian - Ordovician igneous complex
Upper Devonian	Riphaean / Vendian / Cambrian sedimentary complex
Middle Devonian	Palaeogene / Quaternary volcanic pipes

Figure 3. Durov diagram illustrating the main water types of the sampled groundwaters.
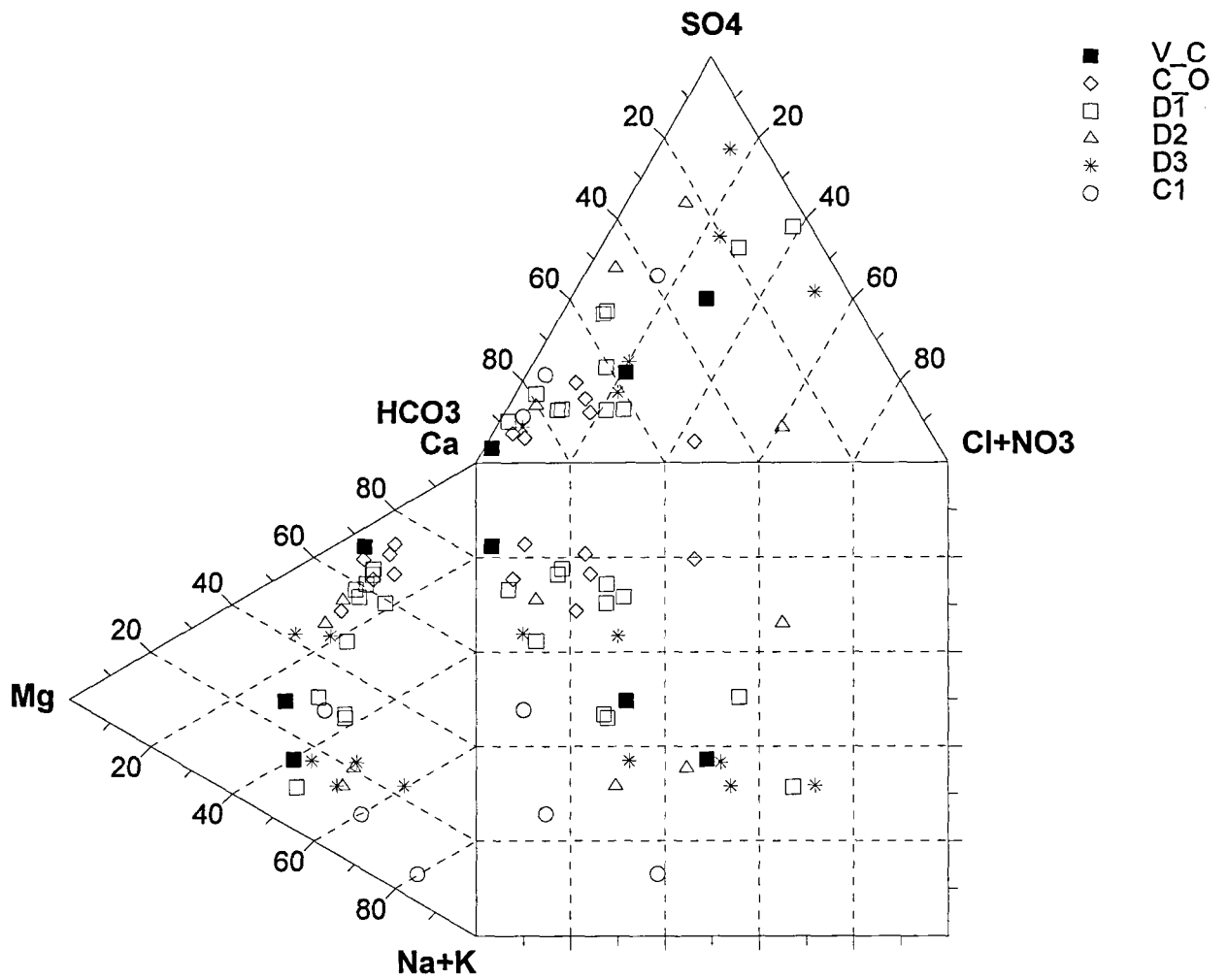
Figure 4. Boxplots indicating the dependence of groundwater temperature (at sampling point) versus lithology and source-type. Box-plots comparing groundwater chemistry for selected parameters. Each box-plot represents well/springs in a given lithology. # = number of samples, the box shows the inter-quartile range, with a horizontal line at the median value. "Whiskers" show the extra-quartile data, excluding near and far outliers, shown as squares and crosses, respectively. Horizontal "brackets" show 95% confidence interval around the median value.
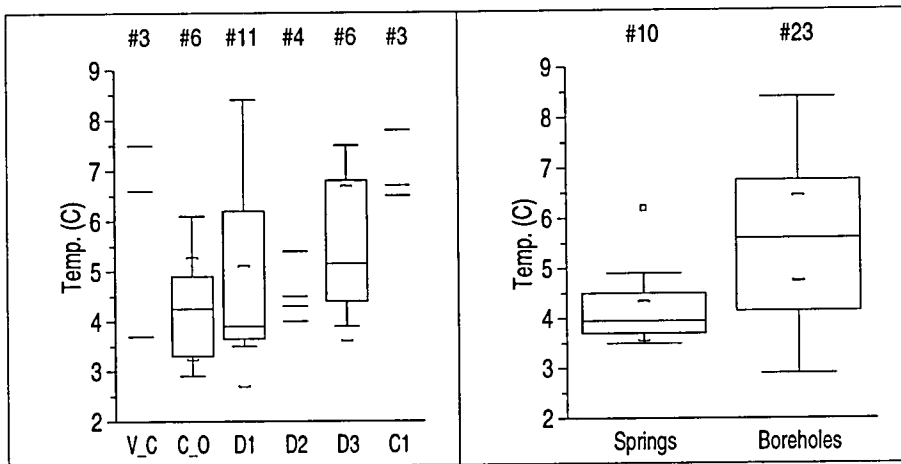
Figure 5. Boxplots indicating the dependence of selected hydrochemical parameters on lithology.
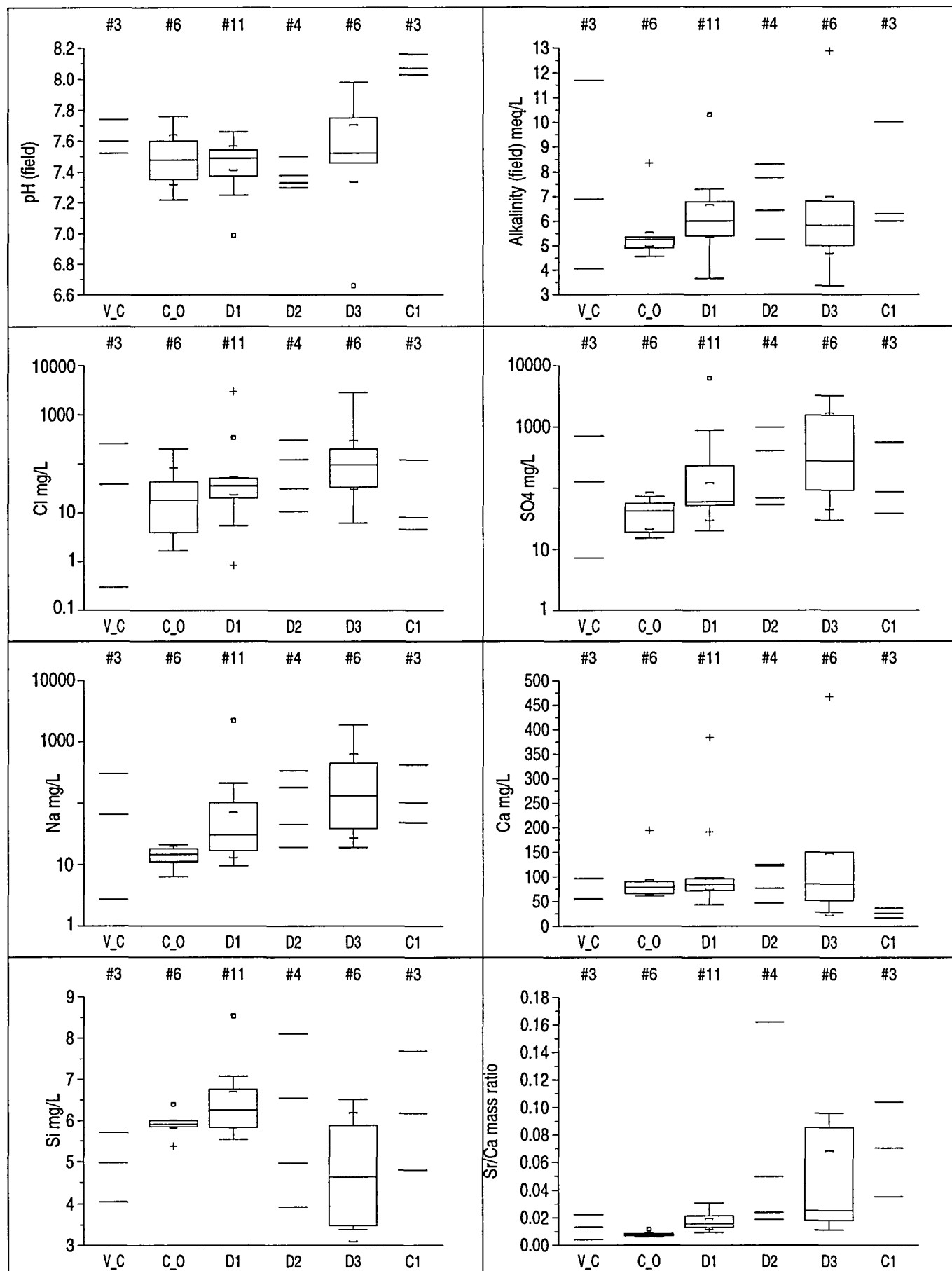
Figure 6. Plots illustrating the dependence of sulphate, alkalinity, calcium, magnesium and sodium concentrations on chloride, and of sodium concentrations on sulphate. Lines show sea-water dilution lines.
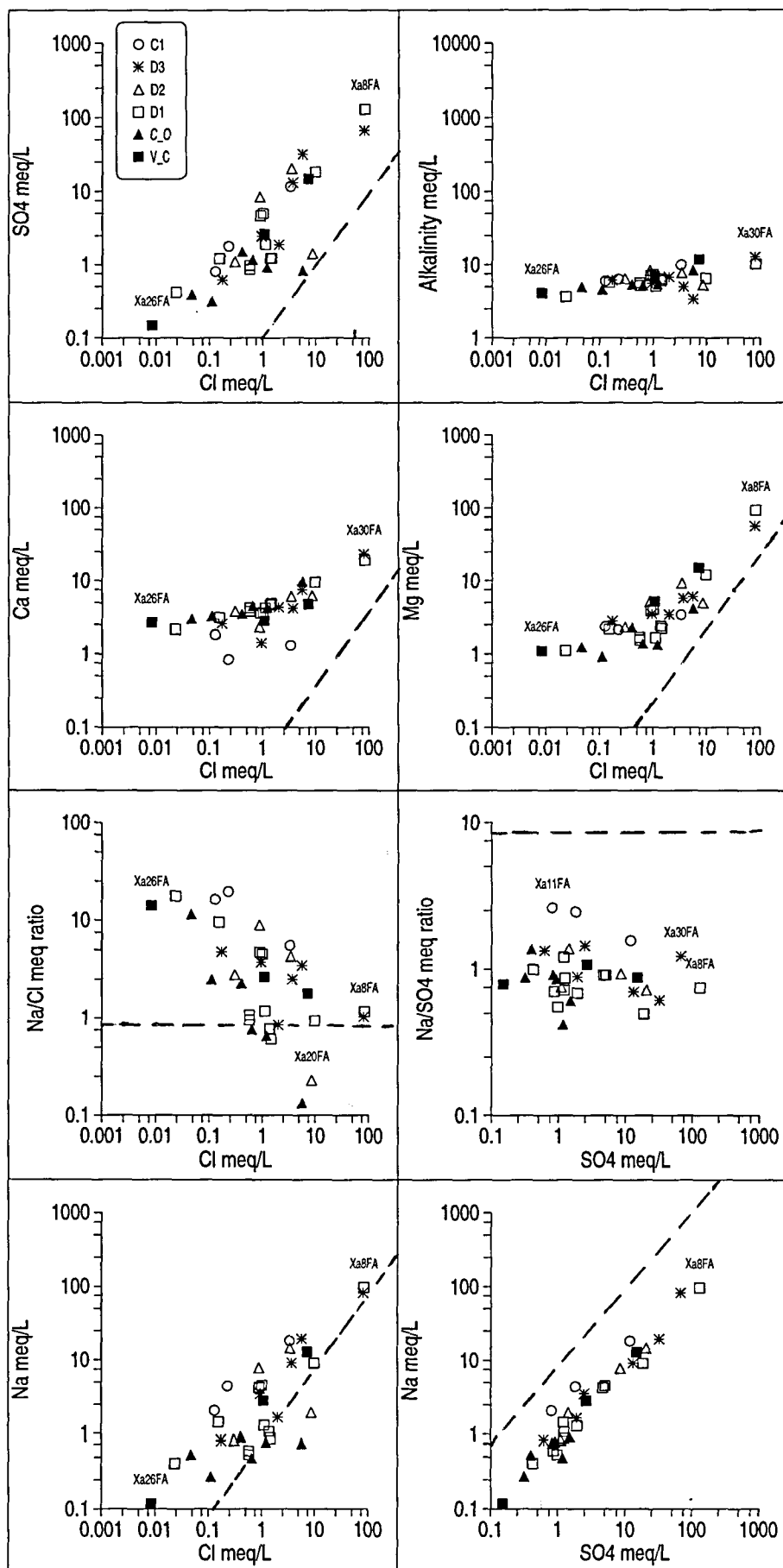
Figure 7. Plot of Br/Cl ratio versus Cl for varying nitrate concentrations in the sampled groundwaters.
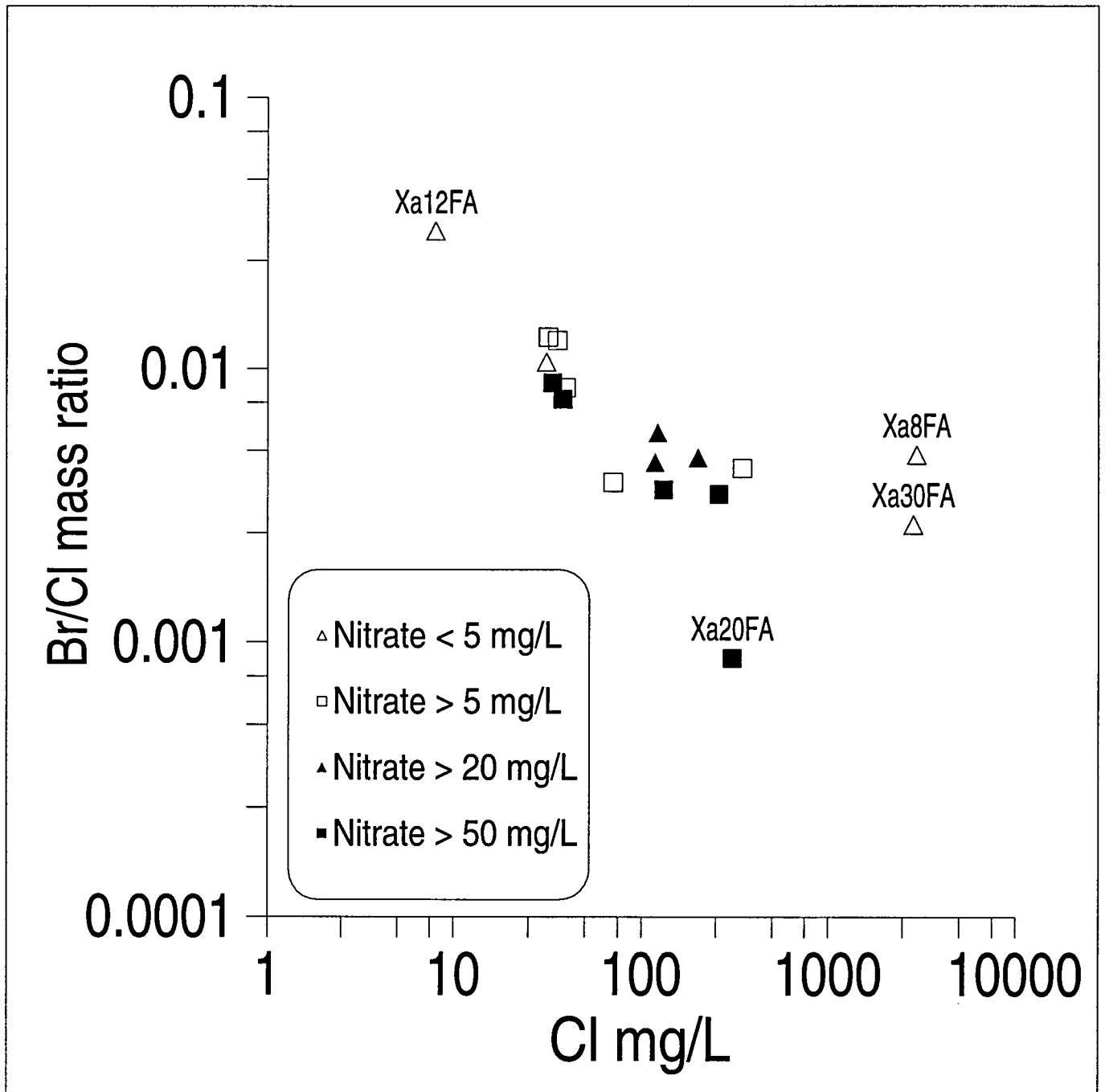
Figure 8. Boxplots illustrating distribution of concentrations of nitrate and potassium in the sampled groundwaters according to land-use type.
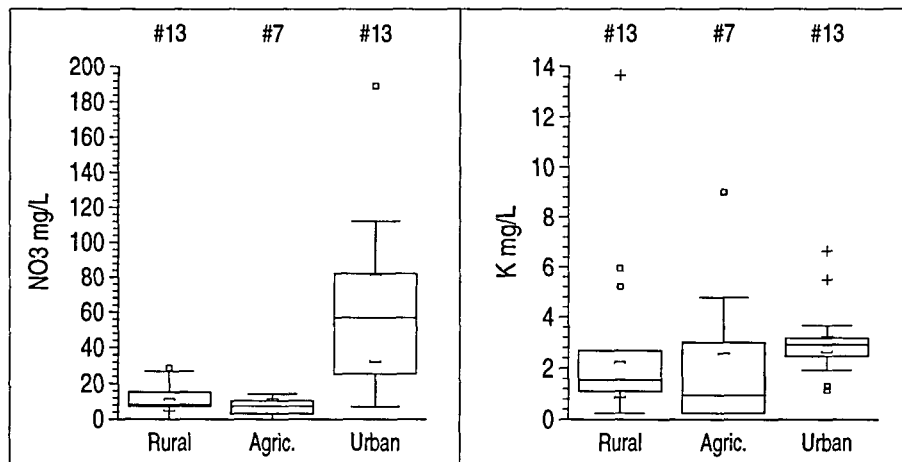
Figure 9. Boxplots illustrating the dependence of selected minor and trace parameters on lithology in the sampled groundwaters.
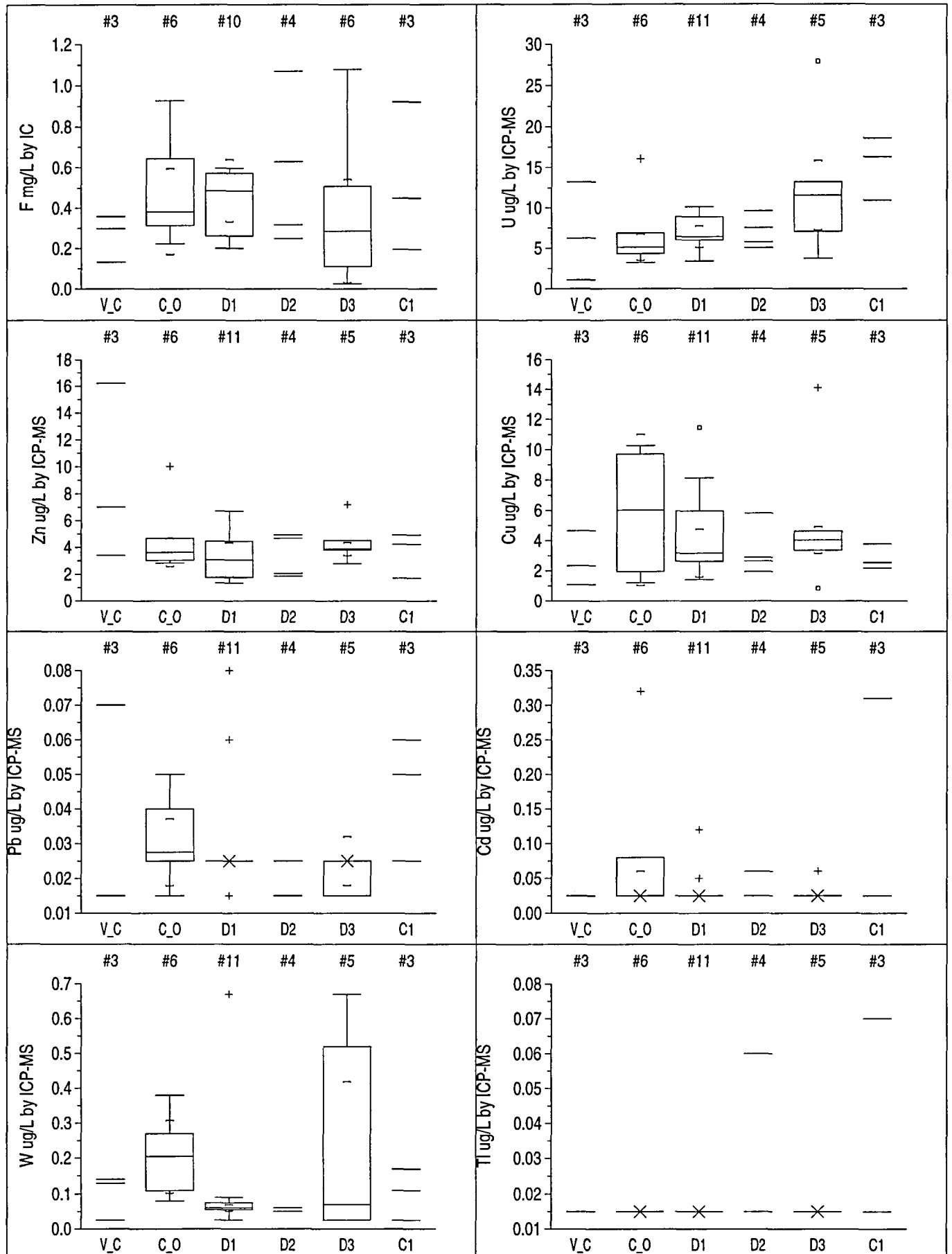
Figure 10. Boxplots illustrating the distributions of selected parameters in granitic groundwaters from the Cambro-Ordovician Khakassian granites (this paper), the Carboniferous granite of the Isles of Scilly, U.K. (Banks et al. 1997), the Precambrian Iddefjord Granite of southern Norway (Banks et al. 1995a,b, 1997) and the Permian Drammen Granite of the Oslo Rift, southern Norway (Reimann et al. 1996).
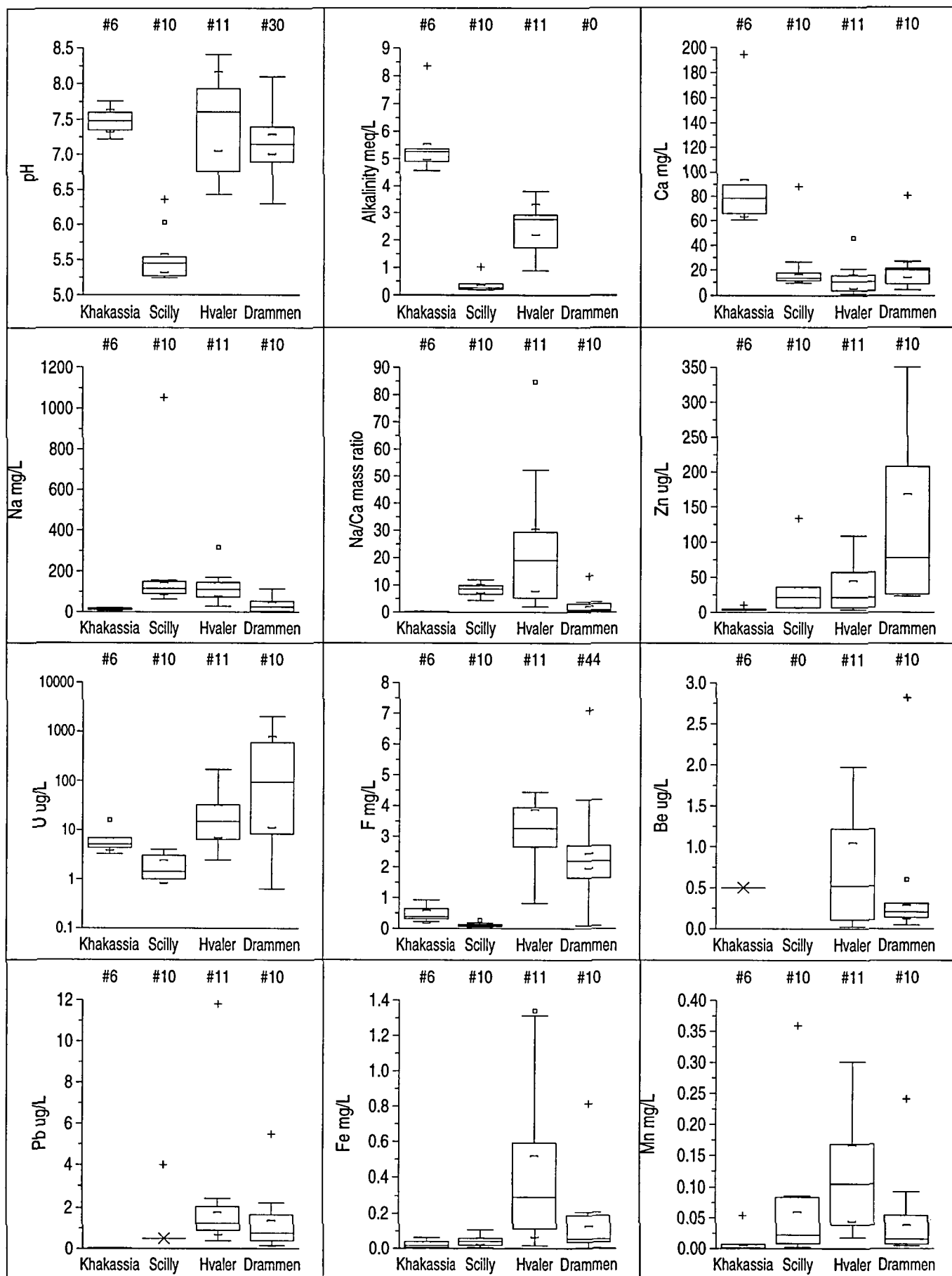
PART 3 - DESCRIPTION OF SAMPLE LOCALITIES

by D. Banks

Samplenr	*Rocktype	*Type	Depth	Flow_ls	*Location	Rockcode
1	D2(Q)	S	1.5			4
2	D1 basalt	B	47			3
3	D1 trachyrhyolite tuff in basalts	S	0	0.5		3
4	D1 trachyrhyolite tuff in basalts	S	0	0.35		3
5	V-C carbonate/dolomite	B	100		Borets	1
6	V-C carbonate/dolomite	B	70		Vlasyevo	1
7	D1 seds	B	50		Stary Borets	3
8	D1 seds (carbonates / evaps)	B				3
9	D3 ORS	B	350		Vorota	5
10	D3 ORS	B				5
11	C1 (carbonate/tuffite/zeolite)	B			Djirim no. 2/5	6
12	C1 (carbonate/tuffite/zeolite)	B			Djirim no. 2/1	6
13	C1 (carbonate/tuffite/zeolite)	B			Djirim town	6
14	D3 ORS/ D2	B			Tselinni	5
15	D1 dolerite sill	S	0		Lake Itkul	3
16	C-O Granite	B	32		TPU Baza	2
17	C-O Granite	S	0		Lake Sakuchik	2
18	D1 volcanics	B			Shira stadium	3
19	D1 volcanics	B	10		Private, Shira	3
20	D2 carbonates	B			Shira North	4
21	D1 volcanics	B			Malii Spirin	3
22	C-O Granodiorite etc.	B			Tupik Vostok	2
23	C-O Granodiorite etc.	B			Tupik Zapad	2
24	C-O Granite + Q	B	19		Tuim town - centre	2
25	C-O Granite + Q	B	20		Tuim town - south	2
26	Cam1 carbonates / basic volcanics	S	0		TGU field centre	1
27	D1 basalt	B			Martsengash	3
28	D1 volcanics and sst	S	0		Oz. Kruglaya S.	3
29	D2 carbonates	S	0		Oz. Kruglaya W.	4
30	D3 ORS	S	0		Oz. Tus S.	5
31	D3/D2 + Q	B			Solyonozyornoe	5
32	D3 ORS	B	100		Oz. Shira kurort	5
33	D2 carbonates	S	0		Novosibirsk Univ. field centre	4
34	D3 ORS	B	100		Oz. Shira kurort (unfiltered)	5

IC results entered and checked 14/1/97
Field data and locations entered 14/1/97 and checked 15/1/97

Sample 34 is also referred to as 32U

S = spring
B = borehole
Depth in m
Estmated Flow in l/s

Rock code
1 = Vendian/Cambrian
2 = Cambro-Ordovician igneous complex
3 = Lower Devonian D_1
4 = Middle Devonia D_2
5 = Upper Devonian D_3
6 = Carboniferous C_1

Sample Site Description:

16/8/96

Site 1: Spring chamber composed of concrete rings with (flowing) overflow. Approx. 1.5 m deep and 1.5 m diameter. Believed to be in D_2 sediments, probably with thin Quaternary cover. Surrounding area composed of open steppe and marshy land.

Site 2: Borehole at cattle farm. Sampled from tap in kitchen. Reported to be 47 m deep in D_1 basaltic volcanics. Borehole pumped by electric pump.

Site 3: Piped spring emerging from hillside from D_1 trachyrhyolitic tuff in a sequence with few D_1 basalts. Surrounded by unfarmed steppe.

Site 4: As above, situated ca. 100 m away from site 3. Flow from spring ca. 0.3-0.4 l/s. Possible to take Eh reading by constricting pipe opening with sawn off neck of a plastic bottle (to form a simple throughflow cell).

Site 5: Boryets village groundwater supply. Sampled from electrical hand pump from a pipe-fed sump (or possibly ring-main) in turn fed by borehole. Reported to be ca. 100 m deep from Vendian-Cambrian carbonates/dolomite.

18/8/96

Site 6: Vlasyevo village groundwater supply. Taken from electric hand pump on ring main nearest to the boreholes themselves. Water is abstracted from (at least two) boreholes drilled some 70 m deep into Vendian-Cambrian carbonates. The villagers do not (for some undisclosed reason) use this water for drinking but travel to Boryets to obtain drinking water.

Site 7: Stariy Boryets (Old Boryets). Water tower fed by ca. 50 m deep borehole in D_1 sedimentary rocks. The water tower is used in turn to fill lorry-driven bowsers. Main surrounding land-use is arable agriculture.

Site 8: Dairy station. Apparently unmanned hillside cattle/dairy station. Sample taken from hose in dairy from a storage tank fed by the bore. The water is somewhat salty. The bore is in D_1 sediments (carbonates/evaporites) and the wellhead is poorly protected. Rather little arable land in surrounding area - mainly pasture/steppe. Some iron precipitation on the 0.45 µm filter.

Site 9: Vorota town supply. Taken from electric hand pump on ring main supplied by around 4 boreholes drilled some 300-400 m deep into D_3 sandstones. The town mayor says that there are some problems due to salt content.

Site 10: Sample from hose directly from borehole of a hillside cattle station. D_3 sediments.

Site 11: Dzhirim log. 5: Hillside cattle station. Sample from tank to which bore pumps. Drilled in C_1 carbonates and tuffites (with zeolite minerals).

Site 12: Dzhirim log. 1: Hillside cattle station. Sampled from leak of water at top of rising main during pumping. Some iron precipitation on the 0.45 µm filter.

Site 13: Dzhirim town supply: Taken from electric hand pump on ring main supplied by borehole(s) in C_1.

Site 14: Tselinij town supply: Taken from electric hand pump on ring main supplied by borehole(s) in D_3 sandstones or D_2 (or, quite conceivably, D_3 overlying D_2 carbonates at shallow depth). The borehole is believed to be very close to the Chulym River.

19/8/96

Site 15: Spring near Lake Itkul. Powerful spring emerging from outcrop of an intrusive dolerite (rhomb-porphyritic alkaline dolerite/trachydolerite) sill within D_1. Several l/s flow.

Site 16: Baza TPU. Tomsk Polytechnic University field study centre. Sampled directly from hose from bore, pumped by electric pump. Bore in Cambro-Ordovician granite, 32 m deep.

Site 17: Spring near Lake Sabuchik. Large seepage-type spring from Cambro-Ordovician granites. No discrete point of emergence so sampled in streamlet where a good, clear, fast-flowing sample could be obtained. Forest.

20/8/96

Site 18: Pump at Shira Town Stadium, near Orlova Lake. Sampled from an electric hand-pump drawing on a ring main fed, in turn, by a borehole in D_1 volcanics.

Site 19: Domestic borehole at Prof. Parnachev's friend's house, Shira. Borehole is reported as 10 m deep. The water is believed to be derived from D_1 volcanics, but a portion may conceiably come from overlying Quaternary sediments. The house's pit latrine is situated som 15 m away. Sampled directly from hose from borehole.

Site 20: Shira Town North. Sampled from an electric hand-pump drawing on a sump (or ring main) fed, in turn, by a borehole in D_2 carbonates. Surrounding area is residential with some fairly heavy industry nearby.

Site 21: Malij Spirin village. Village borehole in D_1 volcanics. Sampled direct from bore via outside hose.

Site 22: Tupik Vostok (East Tupik) village supply: Sampled from hose from header tank above borehole. Drilled in Cambro-Ordocian granodiorite/syenite/monzonite/diorite.

Site 23: Tupik Zapad (West Tupik) village supply: Sampled directly from hose from borehole. Drilled in Cambro-Ordocian granodiorite/syenite/monzonite/diorite.

Site 24: Tu-im village waterworks (central). 5 bores are drilled to depths of 18-20 m through the flood-plain sediments of the Tu-im River into the underlying Cambro-Ordovician granitoids. The water is probably a mixture of Quaternary and granitic groundwater. The

sample was taken from the entry point of pumped borehole water to one of the waterworks' storage reservoirs.

Site 25: Tu-im village waterworks (south). 6 bores are drilled to depths of ca. 20 m probably through the flood-plain sediments of the Tu-im River into the underlying Cambro-Ordovician granitoids. The water is probably a mixture of Quaternary and granitic groundwater. The sample was taken from an electric hand-pump near to (and fed by) the waterworks.

Site 26: Baza TGU. Tomsk State University field study centre. Sample from large seepage spring derived from lower Cambrian carbonates and basic volcanics. The spring is belived to be a karstic spring in the carbonates, but may also contain a component of groundwater derived from overlying Quaternary deposits.

Site 27: Martsengash. Farm with artesian borehole in D_1 basalts. Sample taken from artesian overflow hose from borehole.

Site 28: South shore Lake Kruglaya. Substantial seepage spring emerging from D_1 basaltic volcanics with red siltstones and sandstones. Little farmland around lake.

Site 29: West shore Lake Kruglaya. V. strong seepage/upwelling microkarst spring derived from D_2 silty carbonates. Little farmland around lake.

Site 30: Spring, south side of Lake Tus. Powerful upwelling spring from D_3 feeding Lake Tus.

Site 31: Solyonoozyornoe Village. Sampled from an electric hand-pump drawing on a ring main fed, in turn, by 2 boreholes. Geology uncertain: probably D_3, maybe D_2 (or both). May also be a component of water from overlying Quaternary.

21/8/96

Site 32: Borehole, Kurort, Ozera Shira. Sampled directly from D_3 borehole, 100 m deep. A lot of iron in the water, which van be seen to precipitate out on the 0.45 μm filter. Two samples were therefore taken, one filtered and one unfiltered. *

Site 33: Spring near Novosibirsk University field centre, between Lake Itkul and Lake Shira. Spring wells up inside concrete rings (and overflow) in pasture/steppe area. Sandy soil overlies D_2 carbonates. Possibly a faint smell of H_2S.

* The unfiltered sample is referred to as either 32U or 34

Rural: Sample nos. 1, 3, 4, 15, 16, 17, 24, 25, 26, 28, 29, 30, 33. N = 13
Agricultural: 2, 7, 8, 10, 11, 12, 27. N = 7
Urban: 5, 6, 9, 13, 14, 18, 19, 20, 21, 22, 23, 31, 32. N = 13.

PART 4 - DESCRIPTION OF GEOLOGY OF THE SHIRA REGION

by Prof. V.P. Parnachev and A.Y. Berezovsky

4.1   Geological Setting

The study area is situated in the central part of the Altai-Sayan Mountain region in southern Siberia, Russia (Fig. 4.1). More specifically, it lies within the Minusinsk intermontane trough, bounded by the mountain areas of Kuznetsk-Alatau in the west, and the Western and Eastern Sayans in the south and the east. The trough itself, containing Upper Palaeozoic sediments and volcanics, is divided, from north to south, into four sub-basins by ridges of Precambrian/Lower Palaeozoic rocks: the Nazarovskaya, Chebakovo-Balakhtinskaya, Sydo-Eribinskaya and Yuzhno-Minusinskaya basins. The intervening ridges are offshoots of the Kuznetsk Alatau and Eastern Sayan ranges and include the Solgonsky and the Batenevsky ridges. From a tectonic perspective, the Minusinsk Trough is considered an early Devonian palaeorift structure (Parnachev et al., 1996).

This report considers the chemical quality of groundwater in the rocks of the Chebakovo-Balakhtinskaya Basin (and earlier rocks adjacent to the basin), in the vicinity of the town of Shira. The topography of the area is dominated by plains, hills and low mountains. Topographic depressions are occupied by numerous fresh- and saline lakes. The elevation within the Basin varies from ca. 320 - 350 m asl at the shores of the lakes to 670 m asl on hilltops. Outside the Basin, more mountainous topography prevails, achieving elevations of up to 800 - 1300 m asl.

The region is particularly interesting inasmuch as it presents a very varied geology consisting of Precambrian and Paleozoic metamorphic, sedimentary and igneous rocks (Fig. 4.2). The Kuznetsk-Alatau and Eastern Sayan ranges are comprised of Precambrian and Lower Palaeozoic formations (including volcanics, clastic and carbonate sedimentary rocks and granitoids), as are the Batenevsky and Solgonsky ridges which define the borders of the Basin. The Chebakovo - Balakhtinskaya depression itself is a large (250 x 100 km) synclinorium, infilled by Devonian and Lower Carboniferous volcanics, evaporites and sediments, with a complex internal structure.

Lower Devonian deposits are represented by the sedimentary-volcanogenic Byskarskaya series, which unconformably overlaps the Riphean-Vendian and Cambrian-Ordovician rocks bordering the Basin. The Byskarskaya series contains alternating horizons of volcanic and sedimentary rocks. The volcanics consist of interbedded acidic and basic (homodromous

trachyrhyodacite-trachybasalt) rocks, while sedimentary horizons are generally discontinuous layers of red-bed sandstones, siltstones, tuffites and occasional conglomerates and gritstones. The deposits tend to reflect continental conditions, while the occurrence of evaporite minerals (halite and gypsum imprints) suggests deposition in enclosed lagoon or lake basins The thickness of the series is estimated to be 1800 - 2000 m.

The Middle Devonian is represented by the Saragashskaya and Beiskaya suites. The former transgressively overlies Lower Devonian deposits and contains thin interlayers of gritstone at the base of the sequence. These are replaced upwards by interbedded yellow- and greenish siltstones, sandstones, mudstones, marls and limestones. The thickness of the Saragashskaya Formation varies from 150 to 300 m and is conformably overlain by the Beiskaya Formation, comprising grey limestones, with interlayers of dolomites, marls, occasional calcareous sandstones, siltstones and mudstones. The thickness of the Beiskaya Formation varies from 60 to 250 m.

Upper Devonian deposits include the terrigenous red-bed sedimentary rocks of the Oidanovskaya, Kokhaiskaya and Tubinskaya Formations. The Oidanovskaya Formation is some 200 - 600 m thick, conformably overlies the Beiskaya limestones and consists of siltstones, mudstones and occasional cross-bedded gritstones. The Kokhaiskaya Formation is is 30 - 600 m thick and is dominated by intercalated greyish siltstones and mudstones (containing thin beds of sandstones), marls and algal and brecciated limestones. The Tubinskaya Formation varies from 200 to 1200 m in thickness and is composed of red sandstones, with interlayers of siltstones, mudstones and conglomerates.

The Lower Carboniferous system (Turnaisian Stage) is represented by the Bystryanskaya and Altaiskaya Formation. The Bystryanskaya Formation conformably overlies the Tubinskaya red-beds, and comprises grey, yellowish and greenish sandstones, limestones, siltstones, mudstones and tuffites, with a total thickness of some 275 m. A gradual upwards transition introduces the Altaiskaya Formation, comprising red-brown and yellowish-violet tuffs, tuffites, siltstones and sandstones, which is 50 - 135 metres thick.

The sedimentary rocks of the Middle (Saragashskaya, Beiskaya) and Upper (Oidanovskaya, Kokhaiskaya, Tubinskaya) Devonian and Lower Carboniferous are believed to have been laid down in a post-rift sedimentary basin under shallow-water marine and lagoonal (Middle Devonian and Carboniferous) or continental (Upper Devonian) conditions. Indicator-minerals of evaporite conditions (interbeds of gypsum, barite and fluorite, imprints of rock salt) are known from Middle, Upper Devonian and Lower Carboniferous deposits.

The modern structure of the sub-basins of the Minusinsky Trough is traversed by sublatitudinal faults. The most recent displacements on these faults, accompanied by the

formation of volcanic pipes, took place in the interval 28 - 78 Ma ago (Parnachev et al., 1996b).

4.2 Hydrogeology

According to Russian hydrogeological systematics, the study area is dominantly located in the Chebakovo-Balakhtinsky «2nd-order» groundwater basin, a part of the Altai-Sayan «hydrogeological region» (Hydrogeology of the USSR, 1972). The Chebakovo-Balakhtinsky Basin is surrounded by mountain massifs of the Kuznetsky Alatau and Eastern Sayan Ranges, and the Batenevsky and Solgonsky ridges. These massifs are composed of intensively dislocated and metamorphosed terrigenous, carbonaceous and volcanogenic deposits dating from the Upper Proterozoic and Lower Cambrian, and also of Early Palaeozoic granitoid plutons. Fresh groundwater is found here in fracture and karst systems.

The Chebakovo-Balakhtinsky groundwater basin itself is formed by Devonian and Carboniferous volcanogenic, terrigenous and carbonaceous rocks, some of which were deposited in evapotite environments. Groundwater flow tends to be dominated by fracture flow and its chemistry is characterised by highly variable mineralisation. The structure within the Basin is complex and 3rd or 4th order basins can be identified, such as the Itkulsky, Shirinsky, Djirimsky and Solenoozerny basins.

Within the Chebakovo-Balakhtinsky hydrogeological basin and its surroundings, the following aquifer units are distinguished:

1. V-C Water-bearing horizons of the Vendian-Cambrian volcanogenic-carbonate series (samples no. 5, 6, 26).
2. C-O Fracture aquifers within the Cambrian-Ordovician granitoid massifs (samples no. 16, 17, 22, 23, 24, 25).
3. D_1 Water-bearing horizons within the riftogenic Lower Devonian red-bed volcanic-sedimentary sequence (samples no. 2, 3, 4, 7, 15, 18, 19, 20(?), 21).
4. D_2 Water-bearing horizons within the post-rift Middle Devonian grey terrigenic-carbonate sequence (Saragashskaya and Beiskaya Formations) (samples no. 1, 14(?), 20(?), 29).
5. D_3 Water-bearing horizons within the post-rift Upper Devonian red-bed terrigenic sequence (Oidanovskaya, Kokhaiskaya, Tubinskaya Formations) (samples no. 9, 10, 30, 31(?)).
6. C_1 Water-bearing horizons within the post-rift Lower Carboniferous grey carbonate-terrigenic sequence (Bystryanskaya and Altaiskaya suites) (samples no. 11, 12, 13).

In the case of some samples it has proven difficult to definitively assign them to a specific aquifer unit:

Sample 8 - Vendian-Cambrian carbonate series (dolomites) on the map; conceivably carbonate or dolomite horizon (evaporitic?) within the D_1 sedimentary-volcanogenic series. Samples 14 and 31 - on the boundary between D_2 and D_3.

Sample 20 - terrigenous-carbonate formation D_2 on the map, sedimentary-volcanogenic formation D_1 is possible.

4.3   References

1. Hydrogeology of the USSR (1972). Vol. 18. *Krasnoyarsky krai i Tuvinskaya ASSR. M.:* Nedra publishers, 1972. - 479 pp.

2. Parnachev V.P., Vilzan I.A., Makarenko N.A. et al. (1996). *Devonian riftogenic formations in the south of Siberia.* Tomsk: Izd-vo Tomsk State University, 1996. - 239 pp.

3. Parnachev V.P., Vilzan I.A., Makarenko N.A. et al. *Continental riftogenesis and postrift sedimentation basins in the geological history of Southern Siberia.* Tomsk: Izd-vo Tomsk State University, 1996. - 100 pp.

Fig. 4.1. Schematic map of the structure of the Minusinsky intermontane trough. (Inset: position of the Minusinsky Trough within the Altai-Sayan mountain region of southern Siberia (Russian Federation).

1-2 - the Altai-Sayan mountain region, 2 - Minusinsky intermontane trough; 3 - mountain massifs surrounding the Minusinsky trough; 4 - sub-basins of the Minusinsky Trough (figures in brackets): 1 - Nazarovskaya, 2 - Chebakovo-Balakhtinskaya, 3 - Sido-Erbinskaya, 4 - Yuzhno-Minusinskaya; 5 - disjunctive boundaries of depressions; 6 - the study area.
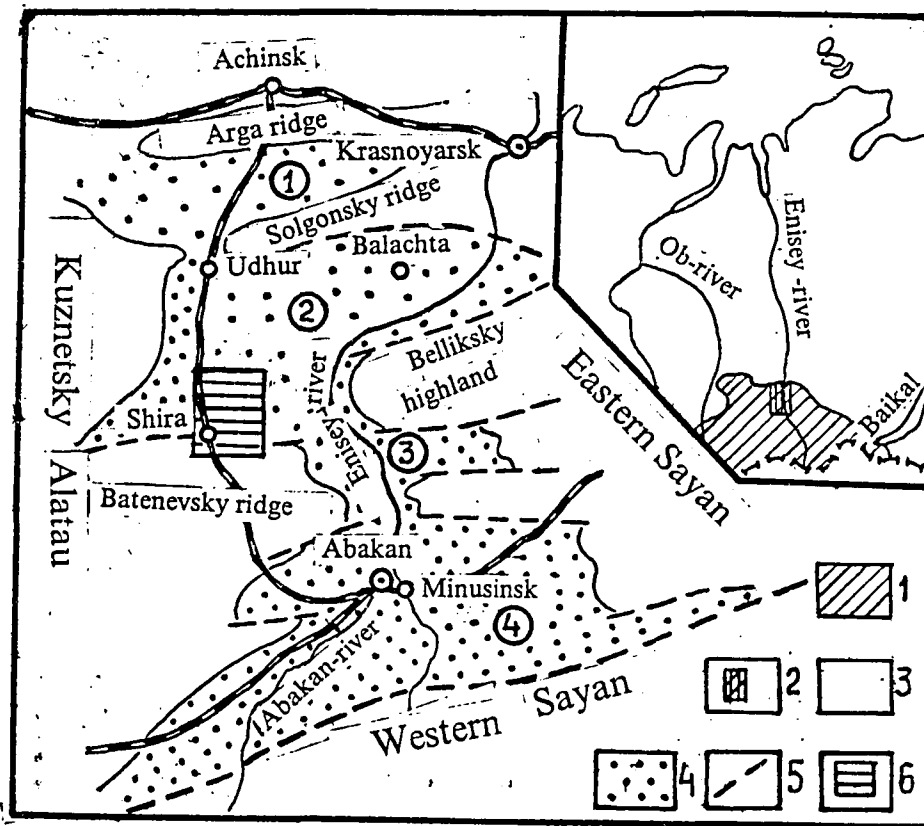
Fig. 4.2. Schematic map of sampled groundwater sources (boreholes, wells and springs) in the Shira district.

Lower Carbonaceous (1-3): *1 - Visean stage: grey-coloured sandstones, siltstones; 2 - Turnaisian-Visean stages: undisjuncted: variegated tuffs, sandstones, limestones; 3 - Turnaisian stage: yellowish-grey tuffs, sandstones, siltstones.*

Upper Devonian (4-6): *4 - Tubinskaya Formation: red-coloured sandstones, siltstones, mudstones; 5 - Kokhaiskaya Formation: grey-coloured siltstones, mudstones; 6 - Oidanovskaya Formation: red-coloured sandstones, siltstones, mudstones, gritstones.*

Middle Devonian (7-8): *7 - Beiskaya Formation: grey-coloured limestones, marls, rarely dolomites: 8 - Saragashskaya Formation: yellowish-grey siltstones, sandstones, marls.*

9 - Lower Devonian: *Byskarskaya series: variegated clastic sedimentary and tuffogenous rocks, flows and covers of trachybasalts, trachyandesites, trachyrhyodacites.*

10 - Paleogene-Quaternary volcanic pipes: *explosive and eruptive breccias of basaltic composition;*

11 - PreDevonian volcanogenic-sedimentary rocks;

12 - PreDevonian igneous rocks: *gabbroids (a), granitoids (b), syenitoids (c);*

13 - disjunctive dislocations;

14 - railway *- Abakan- Achinsk;*

15 - sample sites: *(a) boreholes and wells and (b) springs, and their numbers.*
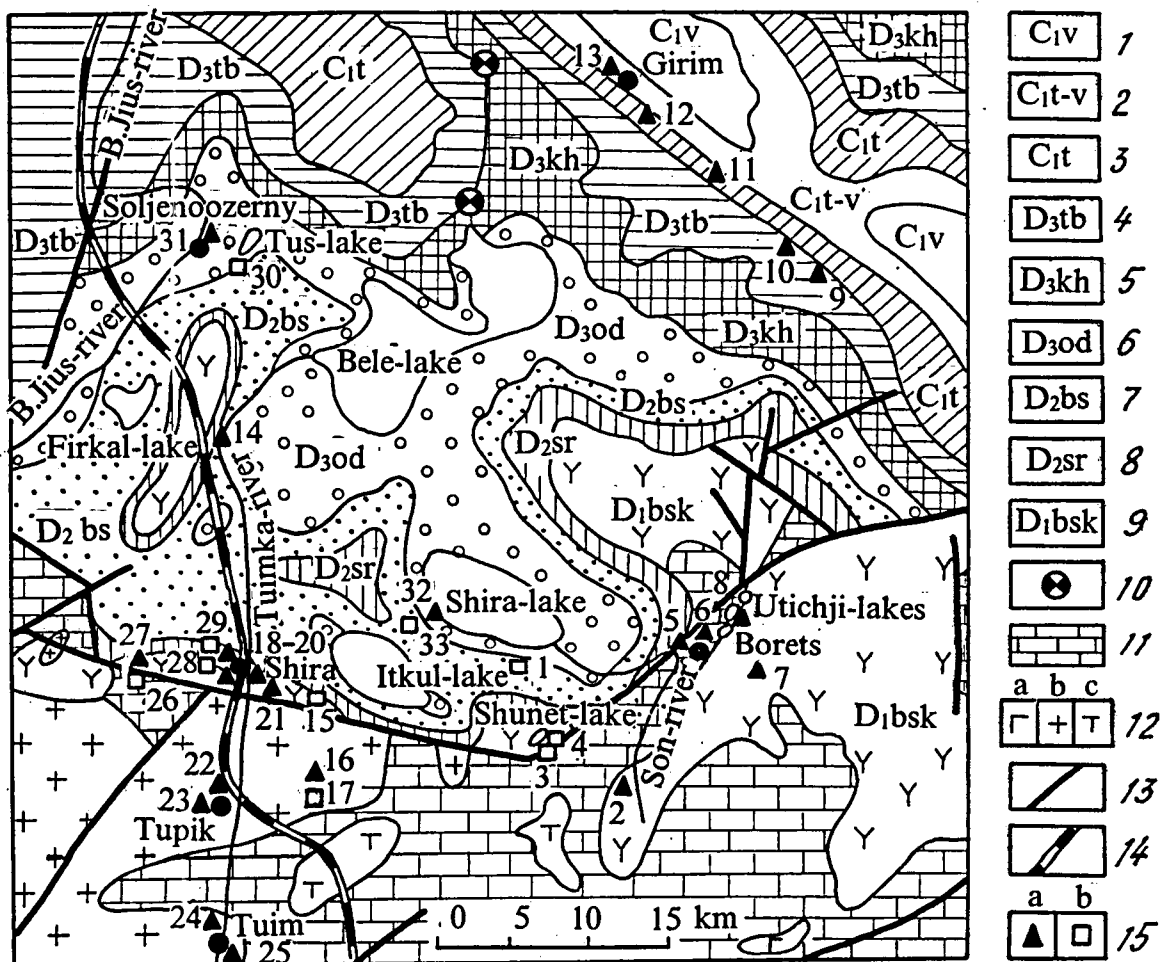
PART 5 - ANALYTICAL RESULTS FROM FIELD ANALYSES (pH, TEMPERATURE, Eh, ALKALINITY)

Samplenr	*Location	Rockcode	pH_field	T_field	Eh_field	Alk1	Alk2	Alk3	Alk_ave
1		4	7.3	4.5	145	7.8	7.7		7.75
2		3	7.55	6.2		5.8	5.6		5.7
3		3	7.66	6.2		7	7.1		7.05
4		3	7.37	3.7	172	7.2	7.4		7.3
5	Borets	1	7.6	7.5		6.9	6.9		6.9
6	Vlasyevo	1	7.74	6.6		11.8	11.6		11.7
7	Stary Borets	3	7.25	8		6.4	6.6		6.5
8		3	6.99	8.4		10.3	10.3		10.3
9	Vorota	5	7.75	7.5		5	5		5
10		5	7.46	4.4		6	6.2		6.1
11	Djirim no. 2/5	6	8.07	7.8		5.9	6.1		6
12	Djirim no. 2/1	6	8.16	6.5		6.3	6.3		6.3
13	Djirim town	6	8.03	6.7		10	10		10
14	Tselinni	5	7.49	6.8		6.8	6.8		6.8
15	Lake Itkul	3	7.5	3.5	135	5.1	5.2		5.15
16	TPU Baza	2	7.5	3.9		5.3	5.4		5.35
17	Lake Sakuchik	2	7.76	4.9		5	4.8		4.9
18	Shira stadium	3	7.41	5.6		6	6		6
19	Private, Shira	3	7.38	3.5		6.3	6.4		6.35
20	Shira North	4	7.33	5.4		5.3	5.2		5.25
21	Malii Spirin	3	7.53	3.7		5.6	5.7		5.65
22	Tupik Vostok	2	7.46	6.1		5.3	5.3		5.3
23	Tupik Zapad	2	7.22	4.6		8.4	8.3		8.35
24	Tuim town - centre	2	7.35	3.3		5.1	5.3		5.2
25	Tuim town - south	2	7.6	2.9		4.6	4.5		4.55
26	TGU field centre	1	7.52	3.7	150	4.1	4		4.05
27	Martsengash	3	7.62	3.6	190	3.7	3.6		3.65
28	Oz. Kruglaya S.	3	7.49	3.9		5.1	5	4.9	5
29	Oz. Kruglaya W.	4	7.38	4	225	6.3	6.6	6.4	6.43333
30	Oz. Tus S.	5	6.66	3.9	45	12.9	12.8		12.85
31	Solyonozyornoe	5	7.98	5.5		5.5	5.6		5.55
32	Oz. Shira kurort	5	7.55	4.8		3.3	3.4		3.35
33	Novosibirsk Univ. field centre	4	7.5	4.3	-20	8.2	8.4		8.3
34	Oz. Shira kurort (unfiltered)	5	7.55	4.8		3.3	3.4		3.35

IC results entered and checked 14/1/97
Field data and locations entered 14/1/97 and checked 15/1/97

T_field = field temperature in °C
Eh_field = field redox potential in mV
Alk1 - Alk 3 = duplicate determinations of alkalinity in meq/l
Alk_ave = average of duplicate determinations (meq/l)

PART 6 - ANALYTICAL RESULTS FROM ANALYSES PERFORMED AT NGU (ICP-AES, ATOMIC ADSORPTION AND ION CHROMATOGRAPHY)

The analytical value (17.6 mg/l) fluoride for Xa8F has been rejected due to the very high salinity of the sample and the inability of the laboratory to reproduce the original value.

Sample 32U is the unfiltered sample from site 32, also referred to as sample 34 in section 3.

NGU
Norges geologiske undersøkelse

Postboks 3006 - Lade
7002 TRONDHEIM
Tlf.: 73 90 40 11
Telefaks: 73 92 16 20

ANALYSERAPPORT

NORSK
AKKREDITERING
Nr. P020

ANALYSEKONTRAKT NR.: 1997.0155
NGU PROSJEKT NR.: 2716.00

OPPDRAGSGIVER: NGU, Grunnvannskvalitet i Grabenområdet

ADRESSE:

TLF.: 310

KONTAKTPERSON: David Banks

PRØVETYPE: Vann
ANTALL PRØVER: 34
IDENTIFIKASJON AV PRØVER: Iflg. liste fra oppdragsgiver
PRØVER MOTTATT: 02.07.97
ANMERKNINGER: Ingen

SPESIFIKASJON AV OPPDRAGET I HENHOLD TIL ANALYSEKONTRAKT:

METODE	DOKUMENTASJON *)	OMFATTES AV AKKREDITERING
ICP-AES vann	NGU-SD 3.1	Ja
GFAAS-As	NGU-SD 3.2	Ja
CVAAS-Hg	NGU-SD 3.3	Ja
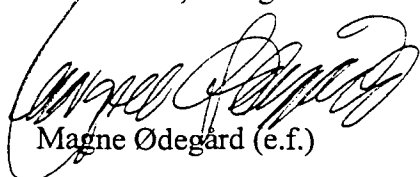
Endring av analyserapport 1997.0155.
Denne rapporten inneholder i alt 14 sider (de 5 siste sider er tillegg til rapport utsendt 15.07.97).
Rapporten må ikke gjengis i utdrag uten skriftlig godkjenning fra NGU-Lab.

Alle forhold ved prøvetaking, behandling og transport av prøvene før innlevering til NGU-Lab er underlagt oppdragsgivers ansvar. Analyseresultater framlagt i denne rapporten refererer derfor kun til det prøvematerialet som er mottatt av NGU-Lab.

Trondheim, 7. august 1997

Magne Ødegård (e.f.)

*) Fortegnelse over dokumentasjon finnes i NGU-Labs Kvalitetshåndbok, NGU-SD 0.1, som kan rekvireres fra NGU-Labs sekretariat.

NGU
Norges geologiske undersøkelse
NGU-Lab

Postboks 3006 - Lade
7002 TRONDHEIM
Tlf.: 73 90 40 11
Telefaks: 73 92 16 20

ICP-AES ANALYSER
VANN
Analysekontraktsnr:1997.0155

NORSK
AKKREDITERING
Nr. P020

INSTRUMENT TYPE :   **Thermo Jarrell Ash ICP 61**

NEDRE BESTEMMELSESGRENSER VANNANALYSER
(For vannprøver som tynnes, blir deteksjonsgrensene automatisk omregnet).

Si ppb	Al ppb	Fe ppb	Ti ppb	Mg ppb	Ca ppb	Na ppb	K ppb	Mn ppb	P ppb
20.-	20.-	10.-	5.-	50.-	20.-	50.-	500.-	1.-	100.-

Cu ppb	Zn ppb	Pb ppb	Ni ppb	Co ppb	V ppb	Mo ppb	Cd ppb	Cr ppb	Ba ppb
5.-	2.-	50.-	20.-	10.-	5.-	10.-	5.-	10.-	2.-

Sr ppb	Zr ppb	Ag ppb	B ppb	Be ppb	Li ppb	Sc ppb	Ce ppb	La ppb	Y ppb
1.-	5.-	10.-	10.-	1.-	5.0	1.-	50.-	10.-	1.-

ANALYSEUSIKKERHET: ± 20 rel. % for K, Pb, Cd, Li, Ce.
± 10 rel. % for Si, Al, Na, Mo, Cr, Zr, Ag, B og La.
± 5 rel. % for Fe, Ti, Mg, Ca, Mn, P, Cu, Zn, Ni, Co, V, Ba, Sr, Be, Sc, Y.

PRESISJON :   Det kjøres rutinemessig kontrollprøver, som føres i kontrolldiagram (X-diagram). Disse kan forevises om ønskelig.

ANTALL PRØVER: 34

ANMERKNINGER: B slettes p.g.a. forurensing av B i systemet.

Rapporten må ikke gjengis i utdrag uten skriftlig godkjenning fra NGU-Lab.

Ferdig analysert	3. juli 1997	Brit Inger Vongraven
	Dato	OPERATØR

NGU Norges geologiske undersøkelse NGU-Lab

Postboks 3006 - Lade
7002 TRONDHEIM
Tlf.: 73 90 40 11
Telefaks: 73 92 16 20

ICP-AES ANALYSER
VANN
Analysekontraktsnr:1997.0155

NORSK AKKREDITERING Nr. P020

	Xa1FA	Xa2FA	Xa3FA	Xa4FA	Xa5FA	Xa6FA	Xa7FA	Xa8FA	Xa9FA	Xa10FA
Si	5.0ppm	6.1ppm	6.7ppm	6.4ppm	4.1ppm	5.7ppm	6.8ppm	5.9ppm	3.9ppm	5.9ppm
Al	<20.0ppb	<20.0ppb	<20.0ppb	<20.0ppb	<20.0ppb	<20.0ppb	<20.0ppb	<20.0ppb	<20.0ppb	<20.0ppb
Fe	<10.0ppb	32.4ppb	<10.0ppb	<10.0ppb	12.9ppb	19.4ppb	86.3ppb	2.3ppm	12.9ppb	<10.0ppb
Ti	< 5.0ppb	< 5.0ppb	< 5.0ppb	< 5.0ppb	< 5.0ppb	< 5.0ppb	< 5.0ppb	5.9ppb	< 5.0ppb	< 5.0ppb
Mg	112ppm	26.5ppm	46.8ppm	48.7ppm	62.6ppm	181ppm	147ppm	0.11%wt	69.9ppm	34.0ppm
Ca	122ppm	62.6ppm	71.5ppm	72.7ppm	56.9ppm	96.2ppm	191ppm	384ppm	83.5ppm	51.9ppm
Na	338ppm	33.6ppm	98.2ppm	105ppm	65.5ppm	300ppm	210ppm	0.22%wt	212ppm	19.0ppm
K	5.2ppm	< 500ppb	1.5ppm	1.6ppm	2.5ppm	5.5ppm	4.8ppm	9.0ppm	3.0ppm	1.2ppm
Mn	3.0ppb	9.4ppb	<1.00ppb	2.0ppb	1.5ppb	362ppb	1.3ppm	1.2ppm	3.1ppb	<1.00ppb
P	< 100ppb	< 100ppb	< 100ppb	< 100ppb	< 100ppb	< 100ppb	155ppb	< 100ppb	< 100ppb	103ppb
Cu	< 5.0ppb	< 5.0ppb	< 5.0ppb	< 5.0ppb	< 5.0ppb	< 5.0ppb	< 5.0ppb	< 5.0ppb	< 5.0ppb	< 5.0ppb
Zn	7.4ppb	7.3ppb	< 2.0ppb	< 2.0ppb	24.5ppb	10.1ppb	4.4ppb	10.2ppb	11.4ppb	< 2.0ppb
Pb	59.5ppb	<50.0ppb	<50.0ppb	<50.0ppb	<50.0ppb	<50.0ppb	<50.0ppb	<50.0ppb	<50.0ppb	<50.0ppb
Ni	<20.0ppb	<20.0ppb	<20.0ppb	<20.0ppb	<20.0ppb	<20.0ppb	<20.0ppb	<20.0ppb	<20.0ppb	<20.0ppb
Co	<10.0ppb	<10.0ppb	<10.0ppb	<10.0ppb	<10.0ppb	<10.0ppb	<10.0ppb	<10.0ppb	<10.0ppb	<10.0ppb
V	6.5ppb	< 5.0ppb	< 5.0ppb	< 5.0ppb	< 5.0ppb	< 5.0ppb	6.5ppb	45.3ppb	9.8ppb	7.2ppb
Mo	25.6ppb	<10.0ppb	<10.0ppb	<10.0ppb	<10.0ppb	<10.0ppb	<10.0ppb	<10.0ppb	18.1ppb	<10.0ppb
Cd	< 5.0ppb	< 5.0ppb	< 5.0ppb	< 5.0ppb	< 5.0ppb	< 5.0ppb	< 5.0ppb	< 5.0ppb	< 5.0ppb	< 5.0ppb
Cr	<10.0ppb	<10.0ppb	<10.0ppb	<10.0ppb	<10.0ppb	<10.0ppb	<10.0ppb	<10.0ppb	<10.0ppb	<10.0ppb
Ba	3.2ppb	2.0ppb	16.6ppb	8.5ppb	35.6ppb	12.1ppb	7.3ppb	4.4ppb	8.9ppb	90.9ppb
Sr	6.1ppm	926ppb	1.3ppm	1.6ppm	757ppb	2.2ppm	5.6ppm	8.3ppm	7.1ppm	581ppb
Zr	< 5.0ppb	< 5.0ppb	< 5.0ppb	< 5.0ppb	< 5.0ppb	< 5.0ppb	< 5.0ppb	9.5ppb	< 5.0ppb	< 5.0ppb
Ag	<10.0ppb	<10.0ppb	<10.0ppb	<10.0ppb	<10.0ppb	<10.0ppb	<10.0ppb	<10.0ppb	<10.0ppb	<10.0ppb
Be	<1.00ppb	<1.00ppb	<1.00ppb	<1.00ppb	<1.00ppb	<1.00ppb	<1.00ppb	<1.00ppb	<1.00ppb	<1.00ppb
Li	90.5ppb	8.9ppb	6.9ppb	13.7ppb	11.0ppb	32.2ppb	50.8ppb	617ppb	36.4ppb	< 5.0ppb
Sc	<1.00ppb	<1.00ppb	<1.00ppb	<1.00ppb	<1.00ppb	<1.00ppb	<1.00ppb	<1.00ppb	<1.00ppb	<1.00ppb
Ce	74.2ppb	<50.0ppb	<50.0ppb	<50.0ppb	<50.0ppb	<50.0ppb	108ppb	191ppb	87.3ppb	<50.0ppb
La	<10.0ppb	<10.0ppb	<10.0ppb	<10.0ppb	<10.0ppb	<10.0ppb	<10.0ppb	<10.0ppb	<10.0ppb	<10.0ppb
Y	<1.00ppb	<1.00ppb	<1.00ppb	<1.00ppb	<1.00ppb	<1.00ppb	<1.00ppb	<1.00ppb	<1.00ppb	<1.00ppb

4

NGU
Norges geologiske undersøkelse
NGU-Lab

Postboks 3006 - Lade
7002 TRONDHEIM
Tlf.: 73 90 40 11
Telefaks: 73 92 16 20

ICP-AES ANALYSER
VANN
Analysekontraktsnr:1997.0155

NORSK
AKKREDITERING
Nr. P020

	Xa11FA	Xa12FA	Xa13FA	Xa14FA	Xa15FA	Xa16FA	Xa17FA	Xa18FA	Xa19FA	Xa20FA
Si	7.7ppm	6.2ppm	4.8ppm	5.4ppm	5.8ppm	5.9ppm	5.9ppm	7.1ppm	6.3ppm	8.1ppm
Al	<20.0ppb	<20.0ppb	<20.0ppb	<20.0ppb	<20.0ppb	<20.0ppb	<20.0ppb	<20.0ppb	<20.0ppb	<20.0ppb
Fe	10.8ppb	41.0ppb	43.2ppb	28.1ppb	<10.0ppb	19.4ppb	<10.0ppb	<10.0ppb	373ppb	15.1ppb
Ti	< 5.0ppb	< 5.0ppb	< 5.0ppb	< 5.0ppb	< 5.0ppb	< 5.0ppb	< 5.0ppb	< 5.0ppb	< 5.0ppb	< 5.0ppb
Mg	28.8ppm	25.9ppm	41.9ppm	42.0ppm	18.9ppm	27.8ppm	15.1ppm	29.2ppm	27.1ppm	60.4ppm
Ca	36.5ppm	16.8ppm	26.1ppm	86.5ppm	76.2ppm	70.8ppm	60.5ppm	93.8ppm	98.1ppm	125ppm
Na	48.2ppm	102ppm	423ppm	38.7ppm	14.0ppm	21.1ppm	12.4ppm	24.8ppm	20.4ppm	45.3ppm
K	< 500ppb	< 500ppb	1.2ppm	2.9ppm	1.1ppm	2.7ppm	963ppb	1.9ppm	2.7ppm	1.3ppm
Mn	1.8ppb	2.8ppb	6.9ppb	3.5ppb	<1.00ppb	1.3ppb	<1.00ppb	1.2ppb	11.2ppb	1.8ppb
P	< 100ppb	< 100ppb	119ppb	< 100ppb	< 100ppb	< 100ppb	< 100ppb	< 100ppb	< 100ppb	< 100ppb
Cu	< 5.0ppb	< 5.0ppb	< 5.0ppb	< 5.0ppb	< 5.0ppb	11.5ppb	< 5.0ppb	< 5.0ppb	< 5.0ppb	< 5.0ppb
Zn	2.8ppb	5.6ppb	5.3ppb	2.9ppb	4.7ppb	15.9ppb	2.8ppb	3.3ppb	7.6ppb	4.8ppb
Pb	<50.0ppb	<50.0ppb	<50.0ppb	<50.0ppb	<50.0ppb	<50.0ppb	<50.0ppb	<50.0ppb	<50.0ppb	<50.0ppb
Ni	<20.0ppb	<20.0ppb	<20.0ppb	<20.0ppb	<20.0ppb	<20.0ppb	<20.0ppb	<20.0ppb	<20.0ppb	<20.0ppb
Co	<10.0ppb	<10.0ppb	<10.0ppb	<10.0ppb	<10.0ppb	<10.0ppb	<10.0ppb	<10.0ppb	<10.0ppb	<10.0ppb
V	7.6ppb	12.8ppb	5.9ppb	< 5.0ppb	< 5.0ppb	5.6ppb	< 5.0ppb	< 5.0ppb	< 5.0ppb	9.7ppb
Mo	<10.0ppb	<10.0ppb	240ppb	<10.0ppb	<10.0ppb	<10.0ppb	<10.0ppb	<10.0ppb	<10.0ppb	<10.0ppb
Cd	< 5.0ppb	< 5.0ppb	< 5.0ppb	< 5.0ppb	< 5.0ppb	< 5.0ppb	< 5.0ppb	< 5.0ppb	< 5.0ppb	< 5.0ppb
Cr	<10.0ppb	<10.0ppb	<10.0ppb	<10.0ppb	<10.0ppb	<10.0ppb	<10.0ppb	<10.0ppb	<10.0ppb	<10.0ppb
Ba	14.9ppb	23.0ppb	8.9ppb	37.2ppb	33.9ppb	25.1ppb	72.3ppb	17.4ppb	63.4ppb	69.5ppb
Sr	1.3ppm	1.8ppm	1.8ppm	1.8ppm	961ppb	610ppb	704ppb	1.3ppm	956ppb	2.4ppm
Zr	< 5.0ppb	< 5.0ppb	< 5.0ppb	< 5.0ppb	< 5.0ppb	< 5.0ppb	< 5.0ppb	< 5.0ppb	< 5.0ppb	< 5.0ppb
Ag	<10.0ppb	<10.0ppb	<10.0ppb	<10.0ppb	<10.0ppb	<10.0ppb	<10.0ppb	<10.0ppb	<10.0ppb	<10.0ppb
Be	<1.00ppb	<1.00ppb	<1.00ppb	<1.00ppb	<1.00ppb	<1.00ppb	<1.00ppb	<1.00ppb	<1.00ppb	<1.00ppb
Li	11.7ppb	15.8ppb	134ppb	12.3ppb	10.3ppb	6.9ppb	5.5ppb	9.6ppb	6.9ppb	14.4ppb
Sc	<1.00ppb	<1.00ppb	<1.00ppb	<1.00ppb	<1.00ppb	<1.00ppb	<1.00ppb	<1.00ppb	<1.00ppb	<1.00ppb
Ce	<50.0ppb	<50.0ppb	<50.0ppb	<50.0ppb	<50.0ppb	<50.0ppb	<50.0ppb	<50.0ppb	62.9ppb	70.9ppb
La	<10.0ppb	<10.0ppb	<10.0ppb	<10.0ppb	<10.0ppb	<10.0ppb	<10.0ppb	<10.0ppb	<10.0ppb	<10.0ppb
Y	<1.00ppb	<1.00ppb	<1.00ppb	<1.00ppb	<1.00ppb	<1.00ppb	<1.00ppb	<1.00ppb	<1.00ppb	<1.00ppb

NGU
Norges geologiske undersøkelse
NGU-Lab

Postboks 3006 - Lade
7002 TRONDHEIM
Tlf.: 73 90 40 11
Telefaks: 73 92 16 20

ICP-AES ANALYSER
VANN
Analysekontraktsnr:1997.0155

NORSK
AKKREDITERING
Nr. P020

	Xa21FA	Xa22FA	Xa23FA	Xa24FA	Xa25FA	Xa26FA	Xa27FA	Xa28FA	Xa29FA	Xa30FA
Si	5.7ppm	6.4ppm	5.4ppm	5.9ppm	6.0ppm	5.0ppm	5.5ppm	8.5ppm	6.6ppm	6.5ppm
Al	<20.0ppb	<20.0ppb	<20.0ppb	<20.0ppb	24.7ppb	<20.0ppb	<20.0ppb	<20.0ppb	<20.0ppb	<20.0ppb
Fe	<10.0ppb	38.8ppb	62.6ppb	15.1ppb	<10.0ppb	<10.0ppb	<10.0ppb	<10.0ppb	<10.0ppb	1.6ppm
Ti	< 5.0ppb	< 5.0ppb	< 5.0ppb	< 5.0ppb	< 5.0ppb	< 5.0ppb	< 5.0ppb	< 5.0ppb	< 5.0ppb	8.4ppb
Mg	20.4ppm	16.2ppm	50.5ppm	16.9ppm	11.2ppm	13.3ppm	13.6ppm	20.0ppm	28.3ppm	686ppm
Ca	84.6ppm	85.7ppm	194ppm	89.6ppm	65.7ppm	53.9ppm	43.4ppm	85.4ppm	76.7ppm	467ppm
Na	12.4ppm	18.1ppm	17.5ppm	11.2ppm	6.4ppm	2.7ppm	9.5ppm	30.2ppm	19.2ppm	0.19%wt
K	3.1ppm	2.5ppm	6.6ppm	2.0ppm	1.5ppm	999ppb	950ppb	< 500ppb	1.6ppm	13.6ppm
Mn	<1.00ppb	6.9ppb	53.7ppb	1.2ppb	<1.00ppb	<1.00ppb	1.2ppb	<1.00ppb	<1.00ppb	26.6ppb
P	< 100ppb	< 100ppb	< 100ppb	111ppb	< 100ppb	< 100ppb	< 100ppb	< 100ppb	< 100ppb	< 100ppb
Cu	< 5.0ppb	< 5.0ppb	< 5.0ppb	< 5.0ppb	< 5.0ppb	< 5.0ppb	< 5.0ppb	< 5.0ppb	< 5.0ppb	< 5.0ppb
Zn	7.8ppb	6.1ppb	2.2ppb	4.4ppb	3.0ppb	< 2.0ppb	2.3ppb	< 2.0ppb	2.1ppb	7.6ppb
Pb	<50.0ppb	<50.0ppb	<50.0ppb	<50.0ppb	<50.0ppb	<50.0ppb	<50.0ppb	<50.0ppb	<50.0ppb	<50.0ppb
Ni	<20.0ppb	<20.0ppb	<20.0ppb	<20.0ppb	<20.0ppb	<20.0ppb	<20.0ppb	<20.0ppb	<20.0ppb	<20.0ppb
Co	<10.0ppb	<10.0ppb	<10.0ppb	<10.0ppb	<10.0ppb	<10.0ppb	<10.0ppb	<10.0ppb	<10.0ppb	<10.0ppb
V	< 5.0ppb	< 5.0ppb	8.4ppb	< 5.0ppb	< 5.0ppb	< 5.0ppb	< 5.0ppb	12.8ppb	5.9ppb	33.6ppb
Mo	<10.0ppb	<10.0ppb	<10.0ppb	<10.0ppb	<10.0ppb	<10.0ppb	<10.0ppb	<10.0ppb	<10.0ppb	<10.0ppb
Cd	< 5.0ppb	< 5.0ppb	< 5.0ppb	< 5.0ppb	< 5.0ppb	< 5.0ppb	< 5.0ppb	< 5.0ppb	< 5.0ppb	< 5.0ppb
Cr	<10.0ppb	<10.0ppb	<10.0ppb	<10.0ppb	<10.0ppb	<10.0ppb	<10.0ppb	<10.0ppb	<10.0ppb	<10.0ppb
Ba	57.0ppb	46.5ppb	87.7ppb	48.1ppb	33.5ppb	97.4ppb	17.0ppb	20.6ppb	29.1ppb	3.2ppb
Sr	803ppb	668ppb	1.2ppm	731ppb	457ppb	228ppb	1.3ppm	1.3ppm	1.8ppm	8.6ppm
Zr	< 5.0ppb	< 5.0ppb	< 5.0ppb	< 5.0ppb	< 5.0ppb	< 5.0ppb	< 5.0ppb	< 5.0ppb	< 5.0ppb	< 5.0ppb
Ag	<10.0ppb	<10.0ppb	<10.0ppb	<10.0ppb	<10.0ppb	<10.0ppb	<10.0ppb	<10.0ppb	<10.0ppb	<10.0ppb
Be	<1.00ppb	<1.00ppb	<1.00ppb	<1.00ppb	<1.00ppb	<1.00ppb	<1.00ppb	<1.00ppb	<1.00ppb	<1.00ppb
Li	6.9ppb	< 5.0ppb	< 5.0ppb	< 5.0ppb	< 5.0ppb	< 5.0ppb	6.2ppb	7.5ppb	10.3ppb	503ppb
Sc	<1.00ppb	<1.00ppb	<1.00ppb	<1.00ppb	<1.00ppb	<1.00ppb	<1.00ppb	<1.00ppb	<1.00ppb	<1.00ppb
Ce	52.5ppb	62.3ppb	120ppb	54.5ppb	<50.0ppb	<50.0ppb	<50.0ppb	<50.0ppb	<50.0ppb	257ppb
La	<10.0ppb	<10.0ppb	<10.0ppb	<10.0ppb	<10.0ppb	<10.0ppb	<10.0ppb	<10.0ppb	<10.0ppb	<10.0ppb
Y	<1.00ppb	<1.00ppb	<1.00ppb	<1.00ppb	<1.00ppb	<1.00ppb	<1.00ppb	<1.00ppb	<1.00ppb	<1.00ppb

6

NGU
Norges geologiske undersøkelse
NGU-Lab

Postboks 3006 - Lade
7002 TRONDHEIM
Tlf.: 73 90 40 11
Telefaks: 73 92 16 20

ICP-AES ANALYSER
VANN
Analysekontraktsnr:1997.0155

NORSK
AKKREDITERING
Nr. P020

	XA31FA	Xa32FA	Xa32UA	Xa33FA
Si	3.4ppm	3.5ppm	3.5ppm	3.9ppm
Al	<20.0ppb	<20.0ppb	<20.0ppb	<20.0ppb
Fe	86.3ppb	309ppb	1.2ppm	<10.0ppb
Ti	< 5.0ppb	< 5.0ppb	< 5.0ppb	< 5.0ppb
Mg	42.6ppm	73.1ppm	71.5ppm	62.8ppm
Ca	28.4ppm	150ppm	147ppm	46.6ppm
Na	81.7ppm	450ppm	441ppm	181ppm
K	3.7ppm	3.2ppm	2.7ppm	5.9ppm
Mn	4.3ppb	37.6ppb	37.9ppb	27.4ppb
P	< 100ppb	< 100ppb	120ppb	< 100ppb
Cu	< 5.0ppb	< 5.0ppb	< 5.0ppb	< 5.0ppb
Zn	5.2ppb	8.2ppb	10.9ppb	< 2.0ppb
Pb	<50.0ppb	<50.0ppb	<50.0ppb	<50.0ppb
Ni	<20.0ppb	<20.0ppb	<20.0ppb	<20.0ppb
Co	<10.0ppb	<10.0ppb	<10.0ppb	<10.0ppb
V	< 5.0ppb	8.2ppb	8.0ppb	< 5.0ppb
Mo	11.8ppb	18.0ppb	14.3ppb	24.6ppb
Cd	< 5.0ppb	< 5.0ppb	< 5.0ppb	< 5.0ppb
Cr	<10.0ppb	<10.0ppb	<10.0ppb	<10.0ppb
Ba	19.8ppb	3.2ppb	3.2ppb	18.6ppb
Sr	2.7ppm	4.5ppm	4.4ppm	7.5ppm
Zr	< 5.0ppb	< 5.0ppb	< 5.0ppb	< 5.0ppb
Ag	<10.0ppb	<10.0ppb	<10.0ppb	<10.0ppb
Be	<1.00ppb	<1.00ppb	<1.00ppb	<1.00ppb
Li	30.2ppb	110ppb	107ppb	49.4ppb
Sc	<1.00ppb	<1.00ppb	<1.00ppb	<1.00ppb
Ce	<50.0ppb	108ppb	88.6ppb	<50.0ppb
La	<10.0ppb	<10.0ppb	<10.0ppb	<10.0ppb
Y	<1.00ppb	<1.00ppb	<1.00ppb	<1.00ppb

NGU

ATOMABSORPSJONS-ANALYSE (As- Grafittovn teknikk)
Vann
Analysekontraktsnr:1997.0155

NORSK
AKKREDITERING
Nr. P020

NGU - Lab

INSTRUMENT TYPE : Perkin Elmer type SIMAA 6000

NEDRE BESTEMMELSES GRENSER : As 3 µg/l (3ppb)

ANALYSEUSIKKERHET   Analyseusikkerheten er gitt i tabellen under

Element	Usikkerhet
As	± 20 % rel.

PRESISJON :   Det kjøres rutinemessig kontrollprøver, som føres i kontrolldiagram (X-diagram). Disse kan forevises om ønskelig.

ANTALL PRØVER: 34

ANMERKNINGER: Ingen

Rapporten må ikke gjengis i utdrag uten skriftlig godkjenning fra NGU-Lab.

Ferdig analysert	14. juli 1997	Frank Berge
	Dato	OPERATØR

ATOMABSORPSJONS-ANALYSE (As- Grafittovn teknikk)
Vann
Analysekontraktsnr:1997.0155

NGU - Lab

Prøve nr:	As µg/l
Xa 1FA	<3.0
Xa 2FA	<3.0
Xa 3FA	<3.0
Xa 4FA	<3.0
Xa 5FA	<3.0
Xa 6FA	<3.0
Xa 7FA	<3.0
Xa 8FA	<3.0
Xa 9FA	<3.0
Xa 10FA	<3.0
Xa 11FA	12.6
Xa 12FA	18.8
Xa 13FA	<3.0
Xa 14FA	<3.0
Xa 15FA	<3.0
Xa 16FA	<3.0
Xa 17FA	<3.0

Prøve nr:	As µg/l
Xa 18FA	<3.0
Xa 19FA	<3.0
Xa 20FA	<3.0
Xa 21FA	<3.0
Xa 22FA	<3.0
Xa 23FA	<3.0
Xa 24FA	<3.0
Xa 25FA	<3.0
Xa 26FA	<3.0
Xa 27FA	<3.0
Xa 28FA	<3.0
Xa 29FA	<3.0
Xa 30FA	<3.0
Xa 31FA	<3.0
Xa 32FA	<3.0
Xa 32UA	<3.0
Xa 33FA	<3.0

NGU
Norges geologiske undersøkelse
NGU-Lab

Postboks 3006 - Lade
7002 TRONDHEIM
Tlf.: 73 90 40 11
Telefaks: 73 92 16 20

ICP-AES ANALYSER
VANN
Analysekontraktsnr:1997 0155

NORSK
AKKREDITERING
Nr. P020

INSTRUMENT TYPE : Thermo Jarrell Ash ICP 61

NEDRE BESTEMMELSESGRENSER VANNANALYSER
(For vannprøver som tynnes, blir deteksjonsgrensene automatisk omregnet).

Si ppb	Al ppb	Fe ppb	Ti ppb	Mg ppb	Ca ppb	Na ppb	K ppb	Mn ppb	P ppb
20.-	20.-	10.-	5.-	50.-	20.-	50.-	500.-	1.-	100.-

Cu ppb	Zn ppb	Pb ppb	Ni ppb	Co ppb	V ppb	Mo ppb	Cd ppb	Cr ppb	Ba ppb
5.-	2.-	50.-	20.-	10.-	5.-	10.-	5.-	10.-	2.-

Sr ppb	Zr ppb	Ag ppb	B ppb	Be ppb	Li ppb	Sc ppb	Ce ppb	La ppb	Y ppb
1.-	5.-	10.-	10.-	1.-	5.0	1.-	50.-	10.-	1.-

ANALYSEUSIKKERHET: ± 20 rel. % for K, Pb, Cd, Li, Ce.

± 10 rel. % for Si, Al, Na, Mo, Cr, Zr, Ag, B og La.

± 5 rel. % for Fe, Ti, Mg, Ca, Mn, P, Cu, Zn, Ni, Co, V, Ba, Sr, Be, Sc, Y.

PRESISJON :   Det kjøres rutinemessig kontrollprøver, som føres i kontrolldiagram (X-diagram). Disse kan forevises om ønskelig.

ANTALL PRØVER: 34

ANMERKNINGER: Bare B rapporteres, øvrige elementer levert tidligere.

Rapporten må ikke gjengis i utdrag uten skriftlig godkjenning fra NGU-Lab.

Ferdig analysert	7. august 1997	Brit Inger Vongraven
	Dato	OPERATØR

ICP-AES ANALYSER
VANN
Analysekontraktsnr:1997 0155

NORSK
AKKREDITERING
Nr. P020

	Xa1FA	Xa2FA	Xa3FA	Xa4FA	Xa5FA	Xa6FA	Xa7FA	Xa8FA	Xa9FA	Xa10Fa
B	429ppb	63.6ppb	117ppb	139ppb	174ppb	293ppb	160ppb	613ppb	869ppb	49.6ppb

11

NGU

Norges geologiske undersøkelse
NGU-Lab

Postboks 3006 - Lade
7002 TRONDHEIM
Tlf.: 73 90 40 11
Telefaks: 73 92 16 20

ICP-AES ANALYSER
VANN
Analysekontraktsnr:1997 0155

NORSK
AKKREDITERING
Nr. P020

	Xa11FA	Xa12FA	Xa13FA	Xa14FA	Xa15FA	XA16FA	Xa17FA	Xa18FA	Xa19FA	Xa20FA
B	75.4ppb	121ppb	269ppb	94.8ppb	49.6ppb	60.3ppb	51.7ppb	58.2ppb	47.4ppb	69.0ppb

NGU

Norges geologiske undersøkelse
NGU-Lab

Postboks 3006 - Lade
7002 TRONDHEIM
Tlf.: 73 90 40 11
Telefaks: 73 92 16 20

ICP-AES ANALYSER
VANN
Analysekontraktsnr:1997 0155

NORSK
AKKREDITERING
Nr. P020

	Xa21FA	Xa22FA	Xa23FA	Xa24FA	Xa25FA	Xa26FA	Xa27FA	Xa28FA	Xa29FA	Xa30FA
B	47.4ppb	92.7ppb	45.3ppb	47.4ppb	34.5ppb	32.3ppb	71.1ppb	69.0ppb	73.3ppb	252ppb

NGU

Norges geologiske undersøkelse
NGU-Lab

Postboks 3006 - Lade
7002 TRONDHEIM
Tlf.: 73 90 40 11
Telefaks: 73 92 16 20

ICP-AES ANALYSER
VANN
Analysekontraktsnr:1997 0155

NORSK
AKKREDITERING
Nr. P020

	Xa31FA	Xa32FA	Xa33FA	Xa32UA
B	528ppb	1.0ppm	325ppb	961ppb

14

NGU
Norges geologiske undersøkelse

Postboks 3006 - Lade
7002 TRONDHEIM
Tlf.: 73 90 40 11
Telefaks: 73 92 16 20

ANALYSERAPPORT

NORSK
AKKREDITERING
Nr. P020

OPPDRAGSGIVER: NGU, Grunnvannskvalitet i Grabenområdet

ADRESSE:

TLF.: 310

KONTAKTPERSON: David Banks

PRØVETYPE: Vann
ANTALL PRØVER: 34
IDENTIFIKASJON AV PRØVER: Iflg. liste fra oppdragsgiver
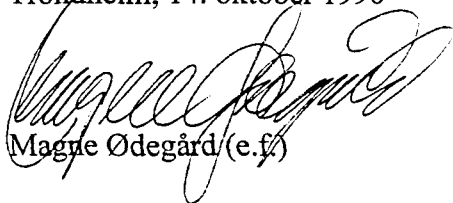PRØVER MOTTATT: 29.08.96
ANMERKNINGER: Ingen

SPESIFIKASJON AV OPPDRAGET I HENHOLD TIL ANALYSEKONTRAKT:

METODE	DOKUMENTASJON *)	OMFATTES AV AKKREDITERING
IC	NGU-SD 3.4	Ja

Denne rapporten inneholder i alt 5 sider. Rapporten må ikke gjengis i utdrag uten skriftlig godkjenning fra NGU-Lab.

Alle forhold ved prøvetaking, behandling og transport av prøvene før innlevering til NGU-Lab er underlagt oppdragsgivers ansvar. Analyseresultater framlagt i denne rapporten refererer derfor kun til det prøvematerialet som er mottatt av NGU-Lab.

Trondheim, 14. oktober 1996

Magne Ødegård (e.f.)

*) Fortegnelse over dokumentasjon finnes i NGU-Labs Kvalitetshåndbok, NGU-SD 0.1, som kan rekvireres fra NGU-Labs sekretariat.

NGU

Norges geologiske undersøkelse
NGU-Lab

Postboks 3006 - Lade
7002 TRONDHEIM
Tlf.: 73 90 40 11
Telefaks: 73 92 16 20

IC- ANALYSER
VANN
Analysekontraktsnr:1996.0162

NORSK
AKKREDITERING
Nr. P020

7 ANIONER : F^-, Cl^-, NO_2^-, Br^-, NO_3^-, PO_4^{3-}, SO_4^{2-}

INSTRUMENT TYPE :   DIONEX IONEKROMATOGRAF 2120i

NEDRE BESTEMMELSESGRENSER

ION	F^-	Cl^-	NO_2^-*	Br^-	NO_3^-	PO_4^{3-}	SO_4^{2-}
Nedre bestemmelsesgrense - mg/l	0.05	0.1	0.05	0.1	0.05	0.2	0.1

ANALYSEUSIKKERHET :   10 % rel. for alle ionene

PRESISJON :   Det kjøres rutinemessig kontrollprøver, som føres i kontrolldiagram (X-diagram). Disse kan forevises om ønskelig.

ANTALL PRØVER: 34

ANMERKNINGER:

                    * NGU-LAB er ikke akkreditert for NO_2^- *

Rapporten må ikke gjengis i utdrag uten skriftlig godkjenning fra NGU-Lab.

Ferdig analysert	14. oktober 1996	Egil Kvam
	Dato	OPERATØR

3

NGU

Norges geologiske undersøkelse
NGU-Lab

Postboks 3006 - Lade
7002 TRONDHEIM
Tlf.: 73 90 40 11
Telefaks: 73 92 16 20

IC- ANALYSER
VANN
Analysekontraktsnr:1996.0162

NORSK
AKKREDITERING
Nr. P020

Prøve Id.	F⁻ [mg/l]	Cl⁻ [mg/l]	NO₂⁻ [mg/l]	Br⁻ [mg/l]	NO₃⁻ [mg/l]	PO₄³⁻ [mg/l]	SO₄²⁻ [mg/l]
162/96 - Xa F 1	0.630	122	< 0.05	0.709	21.8	< 0.2	982
162/96 - Xa F 2	0.436	5.42	< 0.05	< 0.1	7.34	< 0.2	58.0
162/96 - Xa F 3	0.596	31.9	< 0.05	0.417	7.87	< 0.2	224
162/96 - Xa F 4	0.582	35.7	< 0.05	0.453	8.12	< 0.2	241
162/96 - Xa F 5	0.298	38.2	< 0.05	0.295	82.1	< 0.2	127
162/96 - Xa F 6	0.358	259	< 0.05	0.897	189	< 0.2	714
162/96 - Xa F 7	0.262	346	< 0.05	1.49	14.1	< 0.2	887
162/96 - Xa F 8	17.6	2968	< 0.05	14.3	< 0.05	< 0.2	6248
162/96 - Xa F 9	0.111	131	< 0.05	0.470	112	< 0.2	632
162/96 - Xa F 10	0.322	6.14	< 0.05	< 0.1	11.4	< 0.2	29.7
162/96 - Xa F 11	0.195	4.57	< 0.05	< 0.1	9.05	< 0.2	38.5
162/96 - Xa F 12	0.448	8.03	< 0.05	0.258	4.27	< 0.2	86.8
162/96 - Xa F 13	0.921	118	< 0.05	0.534	28.7	< 0.2	563
162/96 - Xa F 14	0.509	70.6	< 0.05	0.270	17.9	< 0.2	91.1
162/96 - Xa F 15	0.571	20.2	< 0.05	< 0.1	7.54	< 0.2	41.4
162/96 - Xa F 16	0.927	14.4	< 0.05	< 0.1	26.7	< 0.2	72.5
162/96 - Xa F 17	0.643	1.66	< 0.05	< 0.1	9.78	< 0.2	18.9
162/96 - Xa F 18	0.500	49.3	< 0.05	< 0.1	56.7	< 0.2	59.6
162/96 - Xa F 19	0.477	51.9	< 0.05	< 0.1	30.6	< 0.2	59.1
162/96 - Xa F 20	0.317	306	< 0.05	0.267	81.9	< 0.2	68.7
162/96 - Xa F 21	0.494	20.2	< 0.05	< 0.1	16.0	< 0.2	46.9
162/96 - Xa F 22	0.314	42.8	< 0.05	< 0.1	6.95	< 0.2	44.3
162/96 - Xa F 23	0.223	202	< 0.05	< 0.1	76.7	< 0.2	39.8
162/96 - Xa F 24	0.382	22.8	< 0.05	< 0.1	28.6	< 0.2	56.1
162/96 - Xa F 25	0.381	3.95	< 0.05	< 0.1	15.1	< 0.2	15.1
162/96 - Xa F 26	0.132	0.297	< 0.05	< 0.1	2.23	< 0.2	7.17
162/96 - Xa F 27	0.201	0.836	< 0.05	< 0.1	1.91	< 0.2	20.0
162/96 - Xa F 28	0.229	39.5	< 0.05	0.336	8.18	< 0.2	91.9
162/96 - Xa F 29	0.249	10.7	< 0.05	< 0.1	7.16	< 0.2	53.2
162/96 - Xa F 30	0.249	2851	< 0.05	7.64	< 0.05	< 0.2	3232
162/96 - Xa F 31	1.08	33.6	< 0.05	0.298	60.6	< 0.2	118
162/96 - Xa F 32	< 0.05	200	< 0.05	0.940	25.4	< 0.2	1532

4

NGU
Norges geologiske undersøkelse
NGU-Lab

Postboks 3006 - Lade
7002 TRONDHEIM
Tlf.: 73 90 40 11
Telefaks: 73 92 16 20

IC- ANALYSER
VANN
Analysekontraktsnr:1996.0162

NORSK
AKKREDITERING
Nr. P020

Prøve Id.	F^- [mg/l]	Cl^- [mg/l]	NO_2^- [mg/l]	Br^- [mg/l]	NO_3^- [mg/l]	PO_4^{3-} [mg/l]	SO_4^{2-} [mg/l]
162/96 - Xa F 33	1.07	31.2	< 0.05	0.330	0.196	< 0.2	405
162/96 - Xa U 32	< 0.05	199	< 0.05	0.915	24.3	< 0.2	1488

5

IC

Original analyse ga fluorid konsentrasjon av 17 mg/l. Etter spørsmaål fra D. Banks, ble prøven omkjørt med tilsetting av standard fluorid løsning.

Resultatene for 5-ganger fortynnet prøve med tilsett fluorid var som følger (konsentrasjoner er omregnet til å gi konsentrasjoner i ufortynnet prøve):

Konsentrasjon F i 5-ganger fortynnet prøve ppm	Konsentrasjon tilsett F ppm	Forventet omregnet konsentrasjon for ufortynnet prøve + tilsett F ppm	Aktuelle konsentrasjon målte for ufoertynnet prøve + tilsett F ppm
4.3 (ufortynnet omkjørt ga 21.6 ppm)	0	21.6	21.6
4.3	2.5	34	28
4.3	5.0	46.5	34.9
4.3	10	71.5	54.8
4.3	25	147	123.3

Fr-results tabell ser det ut som det er noe inn i prøven som kanskje binder tilsett fluorid så at målte verdier ble for lav. Det er også sannsynlig at «F-» toppen innholder noen annet enn bare fluorid.

F ISE

På grunn av de ovrige resultater, prøven var analysert ved F ion selektiv elektrode, ved bruk av standard additions. Standard additions metode tar hensyn til prøvens matrix og så skulle være mer nøyaktig enn lesing av verdier direkte fra graph konstruert fra standard løsninger. Resultater var som følger:

	Volum 10 mg/l standard F løsning tilsett	mV	Omregnet F konsentrasjon
2-ganger fortynnet prøve	0	163	0.23**
2-ganger fortynnet prøve	+ 0.50 ml	159	0.286
2-ganger fortynnet prøve	+ 0.50 ml + 0.50 ml	155.7	0.292
2-ganger fortynnet prøve	+ 0,50 ml + 0,50 ml + 0,50 ml	152.5	0.284
Gjennomsnitt fra standard additions for 2-ganger fortynnet prøve			0.287 ± 0.003
Omregnet konsentrasjon for ufortynnet prøve			0.574

** Leste fra graph med S = 57

Verdier omregnet under standard additions, regnet ved bruk av formål:

$$C_x = \frac{C_s (V_s/V_x)}{(\log^{-1} \Delta E/S) - 1}$$

hvor

C_s = konsentrasjon av standard

V_s = volum av standard ,

osv.

§

---

§ C:\s.banks\reports\19960162.doc

PART 7 - ANALYTICAL RESULTS FROM ANALYSES PERFORMED AT THE UNIVERSITY OF KIEL (ICP-MS)

See Figures 8.20 and 8.21 for a comparison of selected parameters analysed by ICP-AES. AA and ICP-MS.

Sample 32U is the unfiltered sample from site 32, also referred to as sample 34 in section 3.

Thomas Arpe
**Geologisch-Paläontologisches Institut und Museum
der Christian-Albrechts-Universität zu Kiel
ICP-MS Labor**

**Olshausenstr. 40-60
D-24118 Kiel, 13.06.97
F.R. Germany
Phone: (0431) 880-2688
Telefax: (0431) 880-4376**

Geol.-Paläontolog. Institut, Olshausenstr. 40, 24118 KIEL_____e-mail: ta@gpi.uni-kiel.de

to
**S. Banks
Geological Survey of Norway**
Postboks 3006 Lade
**N 7002 Trondheim
Norwegen**

-
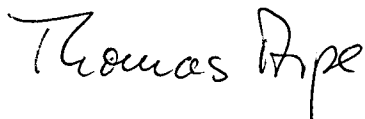
13. Juni 1997

Russian groundwater samples

Dear Mrs. Banks,

inclosed you will find the 34 russian groundwater samples and a copy of the results. The samples are all acidified with 2 ml conc. HNO_3 (subboiled).

Sincerely yours

(i. A. Thomas Arpe)

Banks		Xa 1 F ‹s	Xa 2 F ‹s	Xa 3 F ‹s	Xa 4 F ‹s	Xa 5 F ‹s	Xa 6 F ‹s	Xa 7 F ‹s	Xa 8 F ‹s	Xa 9 F i	Xa 10 F i	Xa 11 F i	Xa 12 F i	Xa 13 F i	Xa 14 F i	Xa 15 F i	Xa 16 F i	Xa 17 F
Lithium	µg l-1	259	27	25	43	39	98	146	1810	102	11	27	49	406	35	26	16	13
Scandium	µg l-1	3.5	4.3	4.4	4.4	3.6	4.8	4.4	4.6	3.0	4.1	4.3	3.5	3.6	4.2	3.0	4.0	2.9
Vanadium	µg l-1	5.6	5.2	3.8	8.9	1.9	14.9	11.5	63.5	11.4	5.5	4.3	10.4	10.2	14.1	1.6	1.8	1.3
Chromium	µg l-1	1.5	1.6	1.4	1.6	2.1	3.0	1.5	2.7	1.4	1.5	1.5	1.6	2.3	1.3	1.2	1.1	1.0
Manganese	µg l-1	2.0	13.8	1.9	4.6	3.9	592	1504	1977	3.2	0.9	2.3	4.9	10.9	7.4	0.6	1.1	0.4
Cobalt	µg l-1	0.2	0.2	0.2	0.2	0.2	0.3	1.5	1.3	0.2	0.2	0.1	0.1	0.1	0.2	0.1	0.2	0.1
Nickel	µg l-1	< 0.5	1.0	< 0.5	< 0.5	< 0.5	0.7	1.3	4.9	< 0.5	< 0.5	< 0.5	< 0.5	< 0.5	< 0.5	< 0.5	< 0.5	< 0.5
Copper	µg l-1	5.8	5.3	6.2	11.5	2.3	4.6	5.7	8.1	4.0	3.4	2.2	2.6	3.8	14.1	1.4	9.7	1.2
Zinc	µg l-1	4.9	4.9	1.8	1.6	16.2	7.0	3.4	2.2	7.2	3.9	1.7	4.2	4.9	2.8	4.0	10.0	3.0
Gallium	µg l-1	0.19	0.16	0.25	0.52	0.06	0.23	0.38	0.38	0.07	0.09	0.11	0.14	0.10	1.09	0.09	0.11	0.04
Arsenic	µg l-1	5.36	2.11	3.36	10.7	2.48	20.1	12.3	87.9	6.72	1.84	2.97	14.6	28.6	17.4	1.84	1.10	0.49
Rubidium	µg l-1	1.71	0.18	1.48	2.38	0.70	3.10	2.77	9.74	0.91	0.85	1.57	1.47	1.05	0.58	0.39	0.16	0.27
Strontium	µg l-1	8724	1326	1979	2312	1171	3272	8689	13558	10058	935	2046	2797	3015	2905	1508	985	1049
Yttrium	µg l-1	< 0.03	< 0.03	< 0.03	0.03	< 0.03	0.08	< 0.03	0.45	< 0.03	0.04	< 0.03	0.03	< 0.03	< 0.03	< 0.03	< 0.03	< 0.03
Zirconium	µg l-1	0.10	0.04	0.07	0.07	< 0.03	1.39	0.03	9.06	0.16	0.12	< 0.03	< 0.03	0.11	0.08	< 0.03	0.04	< 0.03
Molybdenum	µg l-1	38.0	3.47	6.37	5.34	6.44	10.5	1.76	7.86	22.9	1.45	2.56	7.16	311	7.85	7.49	12.0	9.83
Silver	µg l-1	< 0.03	< 0.03	< 0.03	< 0.03	< 0.03	< 0.03	< 0.03	0.04	< 0.03	< 0.03	< 0.03	< 0.03	< 0.03	< 0.03	< 0.03	< 0.03	< 0.03
Cadmium	µg l-1	0.06	0.12	< 0.05	< 0.05	< 0.05	< 0.05	0.05	< 0.05	< 0.05	< 0.05	< 0.05	< 0.05	0.31	< 0.05	< 0.05	0.32	< 0.05
Tin	µg l-1	< 0.03	< 0.03	< 0.03	< 0.03	< 0.03	< 0.03	< 0.03	0.05	< 0.03	< 0.03	< 0.03	< 0.03	< 0.03	< 0.03	< 0.03	< 0.03	< 0.03
Antimony	µg l-1	< 0.05	< 0.05	0.07	0.09	0.06	< 0.05	< 0.05	0.17	< 0.05	0.09	0.06	0.26	0.28	0.10	0.07	0.06	0.05
Caesium	µg l-1	< 0.05	0.05	0.10	0.18	0.05	0.12	0.05	0.36	< 0.05	< 0.05	0.20	< 0.05	< 0.05	< 0.05	< 0.05	< 0.05	< 0.05
Barium	µg l-1	5.37	3.72	21.9	12.1	46.8	15.8	10.9	7.65	11.4	116	19.1	28.0	12.0	47.4	41.6	32.6	85.5
Lanthanum	µg l-1	< 0.03	< 0.03	< 0.03	< 0.03	< 0.03	< 0.03	< 0.03	0.09	< 0.03	< 0.03	< 0.03	< 0.03	< 0.03	< 0.03	< 0.03	< 0.03	< 0.03
Cerium	µg l-1	< 0.03	< 0.03	< 0.03	< 0.03	< 0.03	< 0.03	< 0.03	0.13	< 0.03	< 0.03	< 0.03	< 0.03	< 0.03	< 0.03	< 0.03	< 0.03	< 0.03
Praeseodymium	µg l-1	< 0.03	< 0.03	< 0.03	< 0.03	< 0.03	< 0.03	< 0.03	0.02	< 0.03	< 0.03	< 0.03	< 0.03	< 0.03	< 0.03	< 0.03	< 0.03	< 0.03
Neodymium	µg l-1	< 0.03	< 0.03	< 0.03	< 0.03	< 0.03	< 0.03	< 0.03	0.09	< 0.03	< 0.03	< 0.03	< 0.03	< 0.03	< 0.03	< 0.03	< 0.03	< 0.03
Samarium	µg l-1	< 0.03	< 0.03	< 0.03	< 0.03	< 0.03	< 0.03	< 0.03	0.04	< 0.03	< 0.03	< 0.03	< 0.03	< 0.03	< 0.03	< 0.03	< 0.03	< 0.03
Europium	µg l-1	< 0.03	< 0.03	< 0.03	< 0.03	< 0.03	< 0.03	< 0.03	0.01	< 0.03	< 0.03	< 0.03	< 0.03	< 0.03	< 0.03	< 0.03	< 0.03	< 0.03
Gadolinium	µg l-1	< 0.03	< 0.03	< 0.03	< 0.03	< 0.03	< 0.03	< 0.03	0.07	< 0.03	< 0.03	< 0.03	< 0.03	< 0.03	< 0.03	< 0.03	< 0.03	< 0.03
Terbium	µg l-1	< 0.03	< 0.03	< 0.03	< 0.03	< 0.03	< 0.03	< 0.03	0.01	< 0.03	< 0.03	< 0.03	< 0.03	< 0.03	< 0.03	< 0.03	< 0.03	< 0.03
Dysprosium	µg l-1	< 0.03	< 0.03	< 0.03	< 0.03	< 0.03	< 0.03	< 0.03	0.06	< 0.03	< 0.03	< 0.03	< 0.03	< 0.03	< 0.03	< 0.03	< 0.03	< 0.03
Holmium	µg l-1	< 0.03	< 0.03	< 0.03	< 0.03	< 0.03	< 0.03	< 0.03	0.02	< 0.03	< 0.03	< 0.03	< 0.03	< 0.03	< 0.03	< 0.03	< 0.03	< 0.03
Erbium	µg l-1	< 0.03	< 0.03	< 0.03	< 0.03	< 0.03	< 0.03	< 0.03	0.05	< 0.03	< 0.03	< 0.03	< 0.03	< 0.03	< 0.03	< 0.03	< 0.03	< 0.03
Thulium	µg l-1	< 0.03	< 0.03	< 0.03	< 0.03	< 0.03	< 0.03	< 0.03	0.01	< 0.03	< 0.03	< 0.03	< 0.03	< 0.03	< 0.03	< 0.03	< 0.03	< 0.03
Ytterbium	µg l-1	< 0.03	< 0.03	< 0.03	< 0.03	< 0.03	< 0.03	< 0.03	0.04	< 0.03	< 0.03	< 0.03	< 0.03	< 0.03	< 0.03	< 0.03	< 0.03	< 0.03
Lutetium	µg l-1	< 0.03	< 0.03	< 0.03	< 0.03	< 0.03	< 0.03	< 0.03	0.01	< 0.03	< 0.03	< 0.03	< 0.03	< 0.03	< 0.03	< 0.03	< 0.03	< 0.03
Tungsten	µg l-1	0.06	0.07	0.06	0.07	0.14	0.13	0.05	0.67	< 0.05	0.67	< 0.05	0.11	0.17	0.07	0.06	0.38	0.11
Thallium	µg l-1	< 0.03	< 0.03	< 0.03	< 0.03	< 0.03	< 0.03	< 0.03	< 0.03	< 0.03	< 0.03	< 0.03	< 0.03	0.07	< 0.03	< 0.03	< 0.03	< 0.03
Lead	µg l-1	< 0.05	< 0.05	< 0.05	< 0.05	0.07	0.07	< 0.05	< 0.05	< 0.05	< 0.05	< 0.05	0.06	0.05	< 0.05	< 0.05	< 0.05	< 0.05
Bismuth	µg l-1	< 0.03	< 0.03	< 0.03	< 0.03	< 0.03	< 0.03	< 0.03	< 0.03	< 0.03	< 0.03	< 0.03	< 0.03	< 0.03	< 0.03	< 0.03	< 0.03	< 0.03
Thorium	µg l-1	< 0.03	< 0.03	< 0.03	< 0.03	< 0.03	< 0.03	< 0.03	< 0.03	< 0.03	< 0.03	< 0.03	< 0.03	< 0.03	< 0.03	< 0.03	< 0.03	< 0.03
Uranium	µg l-1	7.54	6.42	9.45	9.65	6.27	13.2	8.32	10.1	27.9	3.74	11.0	18.6	16.3	7.07	6.42	5.69	16.1

	Xa 18 F	Xa 19 F	Xa 20 F	Xa 21 F	Xa 22 F	Xa 23 F	Xa 24 F	Xa 25 F	Xa 26 F	Xa 27 F	Xa 28 F	Xa 29 F	Xa 31 F	Xa 32 F	Xa 32 U	Xa 33 F
Lithium	24	15	39	10	4	<3	6	<3	<3	17	21	26	79	304	319	148
Scandium	4.3	4.2	4.5	3.9	4.2	3.4	4.3	4.4	3.0	3.3	4.3	4.3	1.9	2.4	2.6	3.5
Vanadium	4.4	2.5	21.0	2.7	2.5	10.1	3.1	5.3	1.0	2.0	10.6	2.9	2.3	8.1	12.1	2.0
Chromium	1.2	1.0	1.7	1.0	1.1	1.4	3.9	1.0	0.8	1.0	1.5	1.4	1.3	0.9	1.1	1.9
Manganese	1.2	18.9	3.1	1.0	11.0	84.3	2.6	1.9	0.8	2.1	1.7	0.8	5.1	55.5	62.3	42.9
Cobalt	0.2	0.3	0.3	0.2	0.2	0.4	0.2	0.1	0.1	0.1	0.1	0.1	0.1	0.3	0.3	0.2
Nickel	<0.5	<0.5	0.8	<0.5	<0.5	1.3	<0.5	<0.5	<0.5	<0.5	<0.5	<0.5	<0.5	0.8	1.0	<0.5
Copper	2.1	2.6	2.7	2.7	2.0	4.8	7.2	10.3	1.1	2.8	3.2	2.0	0.8	4.6	5.8	2.9
Zinc	3.1	6.7	4.7	5.9	4.7	3.2	4.1	2.8	3.4	1.7	1.3	1.9	3.8	4.5	7.0	2.1
Gallium	0.07	0.08	0.09	0.15	0.07	0.14	0.23	0.50	0.05	0.17	0.09	0.15	0.01	0.11	0.17	0.09
Arsenic	2.18	2.07	15.8	1.60	1.90	9.08	3.09	5.87	0.74	3.63	3.01	2.04	1.25	6.93	9.19	2.39
Rubidium	0.38	0.16	0.97	0.16	0.10	0.30	0.08	0.05	0.08	0.18	0.26	0.34	1.91	0.87	0.78	2.61
Strontium	2019	1584	3977	1304	1108	1964	1222	709	345	2161	2180	2952	4045	7168	7546	10938
Yttrium	<0.03	<0.03	<0.03	<0.03	<0.03	<0.03	<0.03	<0.03	<0.03	<0.03	<0.03	<0.03	<0.03	<0.03	<0.03	<0.03
Zirconium	0.03	0.04	0.03	0.03	0.03	0.04	0.03	<0.03	<0.03	<0.03	<0.03	<0.03	<0.03	0.04	0.07	0.03
Molybdenum	8.77	9.08	5.96	9.63	5.64	5.80	17.4	4.55	3.65	7.98	2.69	5.12	17.1	24.8	26.6	34.8
Silver	<0.03	<0.03	<0.03	<0.03	<0.03	<0.03	<0.03	<0.03	<0.03	<0.03	<0.03	<0.03	<0.03	<0.03	<0.03	<0.03
Cadmium	<0.05	<0.05	0.06	<0.05	0.08	<0.05	<0.05	<0.05	<0.05	<0.05	<0.05	<0.05	0.06	<0.05	<0.05	<0.05
Tin	<0.03	<0.03	<0.03	<0.03	<0.03	<0.03	<0.03	<0.03	<0.03	<0.03	<0.03	<0.03	<0.03	<0.03	<0.03	<0.03
Antimony	0.07	0.09	<0.05	0.10	0.37	0.17	0.23	0.59	0.05	0.05	<0.05	0.05	<0.05	<0.05	<0.05	0.07
Caesium	<0.05	<0.05	<0.05	<0.05	<0.05	<0.05	<0.05	<0.05	<0.05	<0.05	<0.05	<0.05	<0.05	<0.05	<0.05	0.07
Barium	22.9	79.6	89.6	71.2	58.7	110	62.1	40.2	114	20.3	26.1	36.4	24.2	4.62	4.91	23.3
Lanthanum	<0.03	<0.03	<0.03	<0.03	<0.03	0.04	<0.03	<0.03	<0.03	<0.03	<0.03	<0.03	<0.03	<0.03	<0.03	<0.03
Cerium	<0.03	<0.03	<0.03	<0.03	<0.03	0.03	<0.03	<0.03	<0.03	<0.03	<0.03	<0.03	<0.03	<0.03	<0.03	<0.03
Praeseodymium	<0.03	<0.03	<0.03	<0.03	<0.03	0.01	<0.03	<0.03	<0.03	<0.03	<0.03	<0.03	<0.03	<0.03	<0.03	<0.03
Neodymium	<0.03	<0.03	<0.03	<0.03	<0.03	0.03	<0.03	<0.03	<0.03	<0.03	<0.03	<0.03	<0.03	<0.03	<0.03	<0.03
Samarium	<0.03	<0.03	<0.03	<0.03	<0.03	0.02	<0.03	<0.03	<0.03	<0.03	<0.03	<0.03	<0.03	<0.03	<0.03	<0.03
Europium	<0.03	<0.03	<0.03	<0.03	<0.03	0.01	<0.03	<0.03	<0.03	<0.03	<0.03	<0.03	<0.03	<0.03	<0.03	<0.03
Gadolinium	<0.03	<0.03	<0.03	<0.03	<0.03	0.03	<0.03	<0.03	<0.03	<0.03	<0.03	<0.03	<0.03	<0.03	<0.03	<0.03
Terbium	<0.03	<0.03	<0.03	<0.03	<0.03	0.00	<0.03	<0.03	<0.03	<0.03	<0.03	<0.03	<0.03	<0.03	<0.03	<0.03
Dysprosium	<0.03	<0.03	<0.03	<0.03	<0.03	0.01	<0.03	<0.03	<0.03	<0.03	<0.03	<0.03	<0.03	<0.03	<0.03	<0.03
Holmium	<0.03	<0.03	<0.03	<0.03	<0.03	0.00	<0.03	<0.03	<0.03	<0.03	<0.03	<0.03	<0.03	<0.03	<0.03	<0.03
Erbium	<0.03	<0.03	<0.03	<0.03	<0.03	0.01	<0.03	<0.03	<0.03	<0.03	<0.03	<0.03	<0.03	<0.03	<0.03	<0.03
Thulium	<0.03	<0.03	<0.03	<0.03	<0.03	0.00	<0.03	<0.03	<0.03	<0.03	<0.03	<0.03	<0.03	<0.03	<0.03	<0.03
Ytterbium	<0.03	<0.03	<0.03	<0.03	<0.03	0.01	<0.03	<0.03	<0.03	<0.03	<0.03	<0.03	<0.03	<0.03	<0.03	<0.03
Lutetium	<0.03	<0.03	<0.03	<0.03	<0.03	0.00	<0.03	<0.03	<0.03	<0.03	<0.03	<0.03	<0.03	<0.03	<0.03	<0.03
Tungsten	0.06	0.08	0.05	0.09	0.17	0.27	0.24	0.08	<0.05	0.05	<0.05	0.05	<0.05	0.52	0.52	0.06
Thallium	<0.03	<0.03	<0.03	<0.03	<0.03	<0.03	<0.03	<0.03	<0.03	<0.03	<0.03	<0.03	<0.03	<0.03	<0.03	0.06
Lead	<0.05	0.08	<0.03	<0.03	<0.03	0.05	0.03	0.04	<0.03	0.06	<0.03	<0.03	<0.03	<0.03	<0.03	<0.03
Bismuth	<0.03	<0.03	<0.03	<0.03	<0.03	<0.03	<0.03	<0.03	<0.03	<0.03	<0.03	<0.03	<0.03	<0.03	<0.03	<0.03
Thorium	<0.03	<0.03	<0.03	<0.03	<0.03	<0.03	<0.03	<0.03	<0.03	<0.03	<0.03	<0.03	<0.03	<0.03	<0.03	<0.03
Uranium	6.42	5.16	9.61	7.94	4.34	4.56	6.88	3.23	1.09	5.62	3.41	5.06	11.5	13.2	13.1	5.78

PART 8 - MISCELLANEOUS PRESENTATIONS OF DATA (NOT INCLUDED IN PART 2)

For all data below the analytical detection limit, data have been set to a value of half the detection limit for the purposes of statistical analysis and data presentation.

Where ratios are considered and either component of the ratio is below analytical detection limit, that sample is excluded from further statistical analysis and plotting (this applies to ratios involving the parameters K and Br⁻).

Figure 8.1   Boxplots showing distribution of elements Al, Ba, Ca, Ce, Cu, Fe, K, Li, Mg, Mn, Mo and Na, as analysed by ICP-AES. All concentrations in mg/l. 1st and 3rd columns show distribution according to geological units; 2nd and 4th columns show distribution according to surrounding land use.

Figure 8.2   Boxplots showing distribution of elements P, Pb, Si, Sr, Ti, V, Zn, Zr, as analysed by ICP-AES, and also As by atomic adsorption, sum of anions (Cl⁻, $SO_4^=$, NO_3^- and alkalinity) and sum of cations (Na, K, Mg, Ca and Fe [assumed +II]). All concentrations in mg/l, except As in µg/l and the two ionic sums in meq/l. 1st and 3rd columns show distribution according to geological units; 2nd and 4th columns show distribution according to surrounding land use.

Figure 8.3   Boxplots showing distribution of parameters pH (field), temperature (°C - field), Eh (mV - field), alkalinity (meq/l - field), Br⁻, Cl⁻, F⁻, NO_3^-, $SO_4^=$ (all mg/l, by ion chromatography), $\log_{10}Cl^-$ and $\log_{10}SO_4^=$. 1st and 3rd columns show distribution according to geological units; 2nd and 4th columns show distribution according to surrounding land use.

Figure 8.4   Boxplots showing distribution of the mass ratios Sr/Ca, Na/Cl⁻ , Na/Ca and $SO_4^=$/Cl⁻ according to geological units.

Figure 8.5   x-y plots showing distribution of the mass ratios Sr/Ca, Na/Cl⁻ , Na/Ca and $SO_4^=$/Cl⁻ according to geological units and pH.

Figure 8.6   x-y plots showing distribution of the mass ratios Sr/Ca, Na/Cl⁻ , Na/Ca and $SO_4^=$/Cl⁻ according to geological units and chloride.

Figure 8.7   x-y plots showing Na vs. Cl⁻, Na vs. $SO_4^=$, Mg vs. Ca and Mg vs. $SO_4^=$, according to geological units.

Figure 8.8   x-y plots showing P vs. NO_3^-, K vs. NO_3^-, Fe vs. NO_3^- and Br⁻/Cl⁻ mass ratio vs. NO_3^- according to surrounding land use. Note detection limits for P (0.1 mg/l), K (0.5 mg/l)

73

and Fe (0.01 mg/l). A Br/Cl ratio has only been calculated where both parameters are above analytical detection limit.

Figure 8.9   x-y plots showing (top) distribution of ion balance error ([sum cations - sum anions]*100% / [sum cations + sum anions]) versus sum of anions (meq/l) according to geological unit. The point marked "kurort-unfiltered" is the unfiltered parallel sample of Xa32F; (bottom) Br/Cl mass ratio vs. Cl (mg/l). A Br/Cl ratio has only been calculated where both parameters are above analytical detection limit. The sum of anions is based on Cl, $SO_4^=$, NO_3^- and alkalinity. The sum of cations is based on Na, K, Mg and Ca.

Figure 8.10   x-y plots showing $SO_4^=$ vs. Cl, K vs. Cl, Ca vs. Cl, and Mg vs. Cl according to geological units. All concentrations in meq/l.

Figure 8.11   x-y plots showing alkalinity vs. Cl, Na/K (meq ratio) vs. Cl, Ca/Mg (meq ratio) vs. Cl, and Ca/alkalinity (meq ratio) vs. Cl according to geological units. All concentrations in meq/l.

Figure 8.12   x-y plots showing Na/Cl (meq ratio) vs. Cl, Na/$SO_4^=$ (meq ratio) vs. $SO_4^=$, Na vs. Cl, and Na vs. $SO_4^=$ according to geological units. All concentrations in meq/l.

Figure 8.13   Boxplots showing distribution of Na/$SO_4^=$ equivalent ratio according to geological units.

Figure 8.14   x-y plots showing $SO_4^=$ vs. Cl, Sr vs. Ca, Ba vs. $SO_4^=$, and Ca vs F according to geological units. All concentrations in mg/l. The line shows a simple saturation line for CaF_2 fluorite (uncorrected for activity or speciation).

Figure 8.15   "Draftsman" presentation of correlations between different parameters. Alkave = field alkalinity (average of duplicate determinations), Ehfield = Eh (mV, field), suffix AES signifies analysis by ICPAES.

Figure 8.16   Boxplots showing distribution of selected elements analysed by ICP-MS (and fluoride by ion chromatography), according to geological units.

Figure 8.17   Boxplots comparing pH, alkalinity, calcium, sodium, uranium, fluoride, copper, zinc, Na/Ca mass ratio and lead for four different granites (C_O granites of Khakassia, the Precambrian Iddefjord Granite of Hvaler, SE Norway (Banks et al. 1997), the Carboniferous granite of the Isles of Scilly, UK (Banks et al. 1997) and the Permian granites of Vestfold (dominated by the Drammen granite - Reimann et al. 1996). For the Khakassian groundwaters, Pb, U, Cu and Zn are analysed by ICPMS, Ca and Na by ICPAES, F by ion chromatography, pH and alkalinity in the field.

Figure 8.18   Boxplots comparing iron, manganese and beryllium for the four different granites (as for Fig. 8.17) For the Khakassian groundwaters, Fe, Mn and Be were analysed by

ICPAES. Note all the Khakassian groundwaters have concentrations of Be below the analytical detection limit of 1 μg/l.

Figure 8.19   Durov diagram based only on meq/l concentrations of Na, Mg, Ca, $SO_4^=$, Cl⁻, and alkalinity (HCO_3^-) (i.e. not NO_3^- and K), sorted according to geological units.

Figure 8.20   x-y diagrams comparing eight selected parameters analysed by ICP-AES and ICP-MS techniques. Li, Mo and Ba all give rather good correspondences, although ICP-MS gives consistently slightly higher results for Ba. Sr gives extremely good correlation between the two methods, although the ICP-MS results are consistently higher. For Zn, a fair correlation is also observed but the ICP-AES results are higher in this case. V gives a poorer correlation, but the concentrations returned are approximately corresponding. Cu compares poorly for the two methods, with significantly higher results being returned by ICP-MS for most samples. The most serious divergence in results occurs with Ce where results show up to three orders of magnitude difference (ICP-AES yielding the high results). It must be pointed out that this dataset is particularly challenging to analyse, containing a number of very high salinity samples.

Figure 8.21   x-y diagrams comparing six selected parameters analysed by ICP-AES, AA and ICP-MS techniques. Mn gives a good correlation although results by ICP-MS are consistently higher. Zr and Y yield no discrepancies (all samples < detection limit of 1 μg/l for Y by ICPAES). For Pb only one sample gives a serious discrepancy, with a much higher concentration being returned by ICPAES. For As, the two samples where As was detected by AA yield similar results for ICP-MS, although for other samples, ICP-MS often yields higher concentrations than the detection limit by AA. For Sc all ICPMS analyses return concentrations > 1 μg/l, whereas for ICPAES all samples return < 1μg/l.

Figures 8.22 and 8.23 Boxplots showing distributions of concentrations according to geological units for all elements analysed by ICP-MS, all concentrations in μg/l. LogZr = $log_{10}Zr$, with Zr in μg/l.

Reimann, C., Hall, G.E.M., Siewers, U., Bjorvatn, K., Morland, G., Skarphagen, H. & Strand, T. (1996): Radon, fluoride and 62 elements as determined by ICP-MS in 145 Norwegian hard rock groundwater samples. *Science of the Total Environment*, 192, 1-19.

Banks, D., Reimann, C., Skarphagen, H. & Watkins, D. (1997): The comparative hydrogeochemistry of two granitic island aquifers: the Isles of Scilly, UK and the Hvaler Islands, Norway. *Norges Geol. Unders. Report* 97.070.

Lithological codes:

V_C: Vendian-Cambrian metasediments and meta-volcanics.
C_O: Cambro-Ordovician igneous (granitoid) complex
D1: Lower Devonian sediments and volcanics

D2: Middle Devonian carbonate-dominated sediments

D3: Upper Devonian sediments.

C1: Lower Carboniferous sediments.

Figure 8.1

Figure 8.2

Figure 8.3

For all samples:

NO2 < 0.05 mg/l

PO4 < 0.2 mg/l
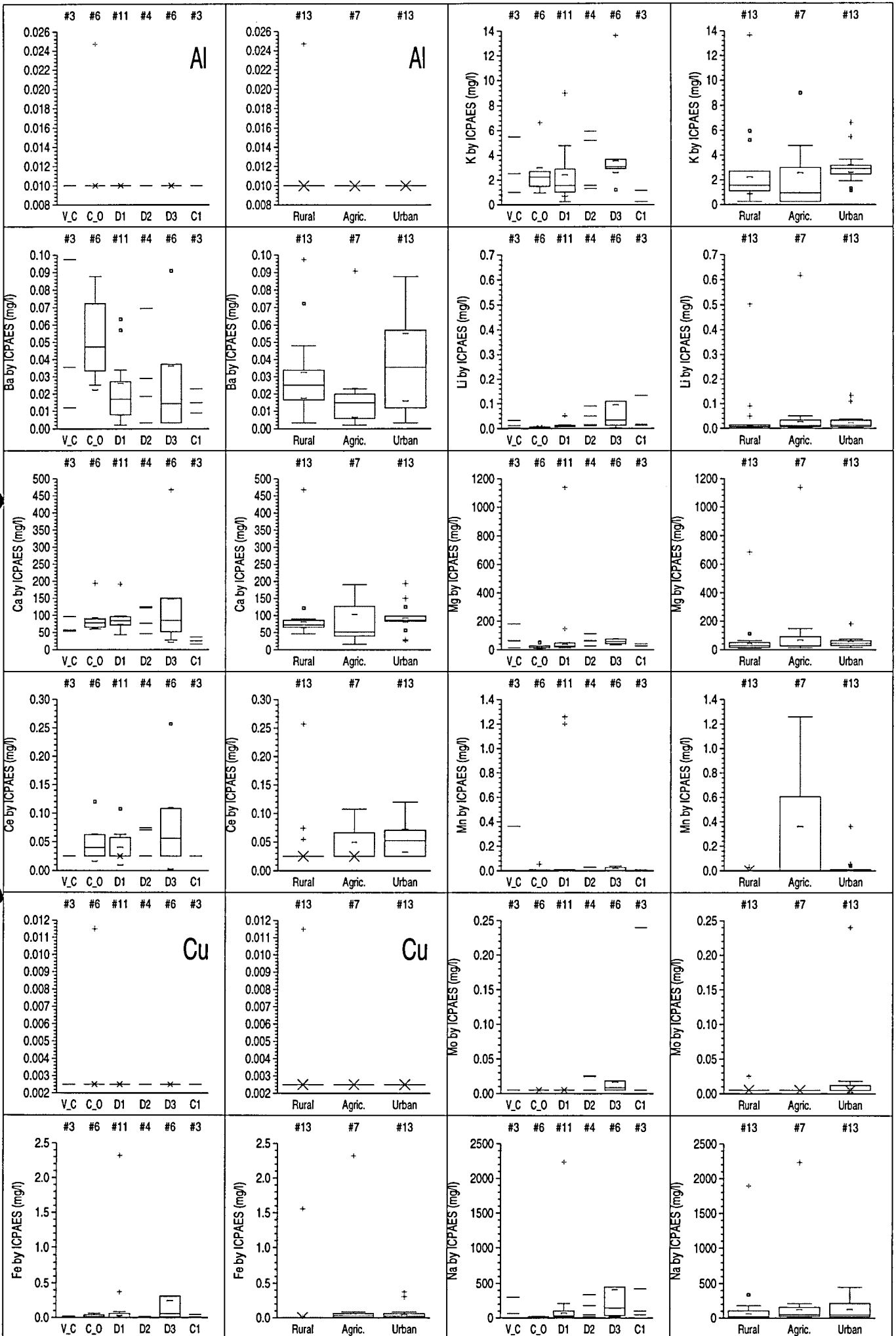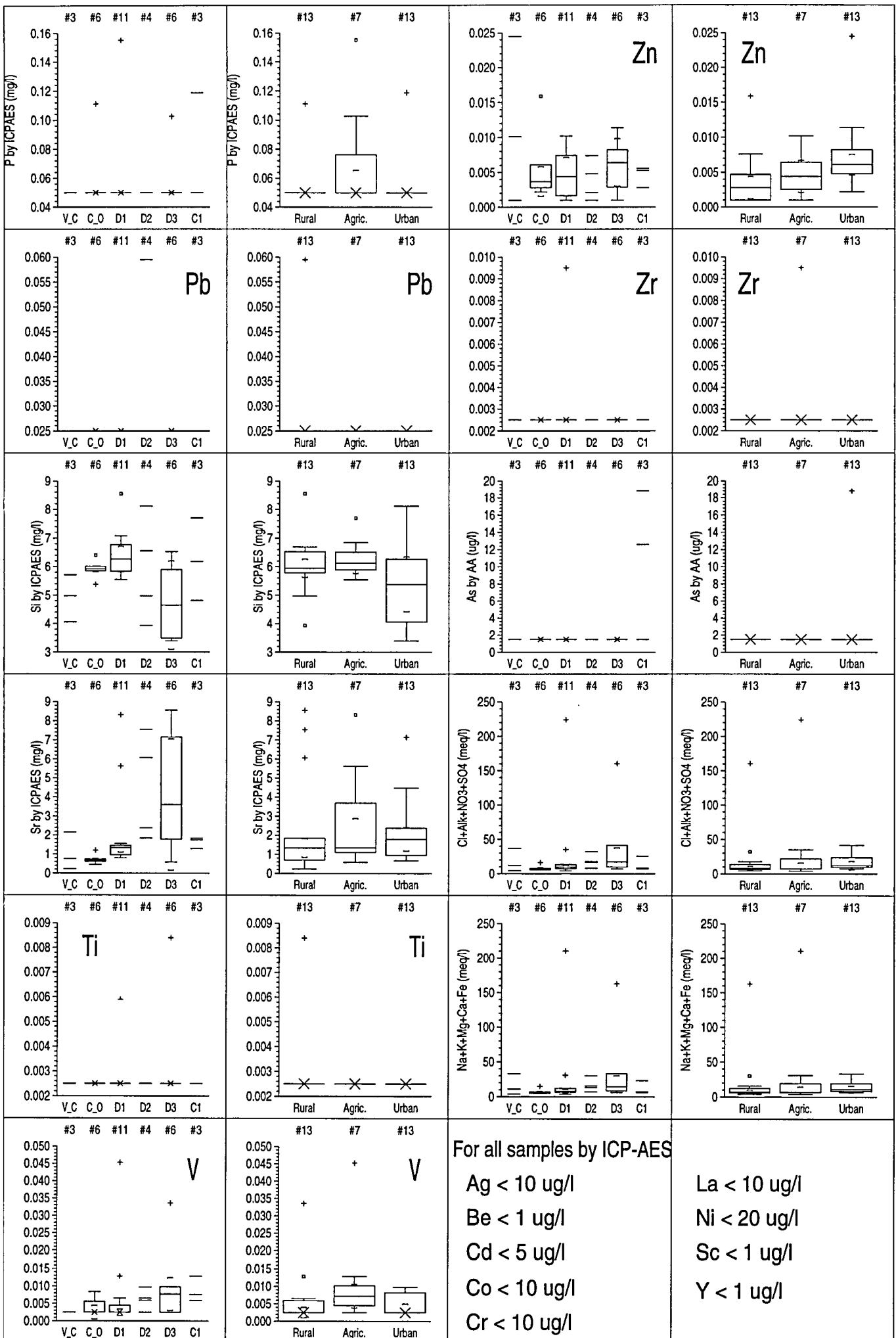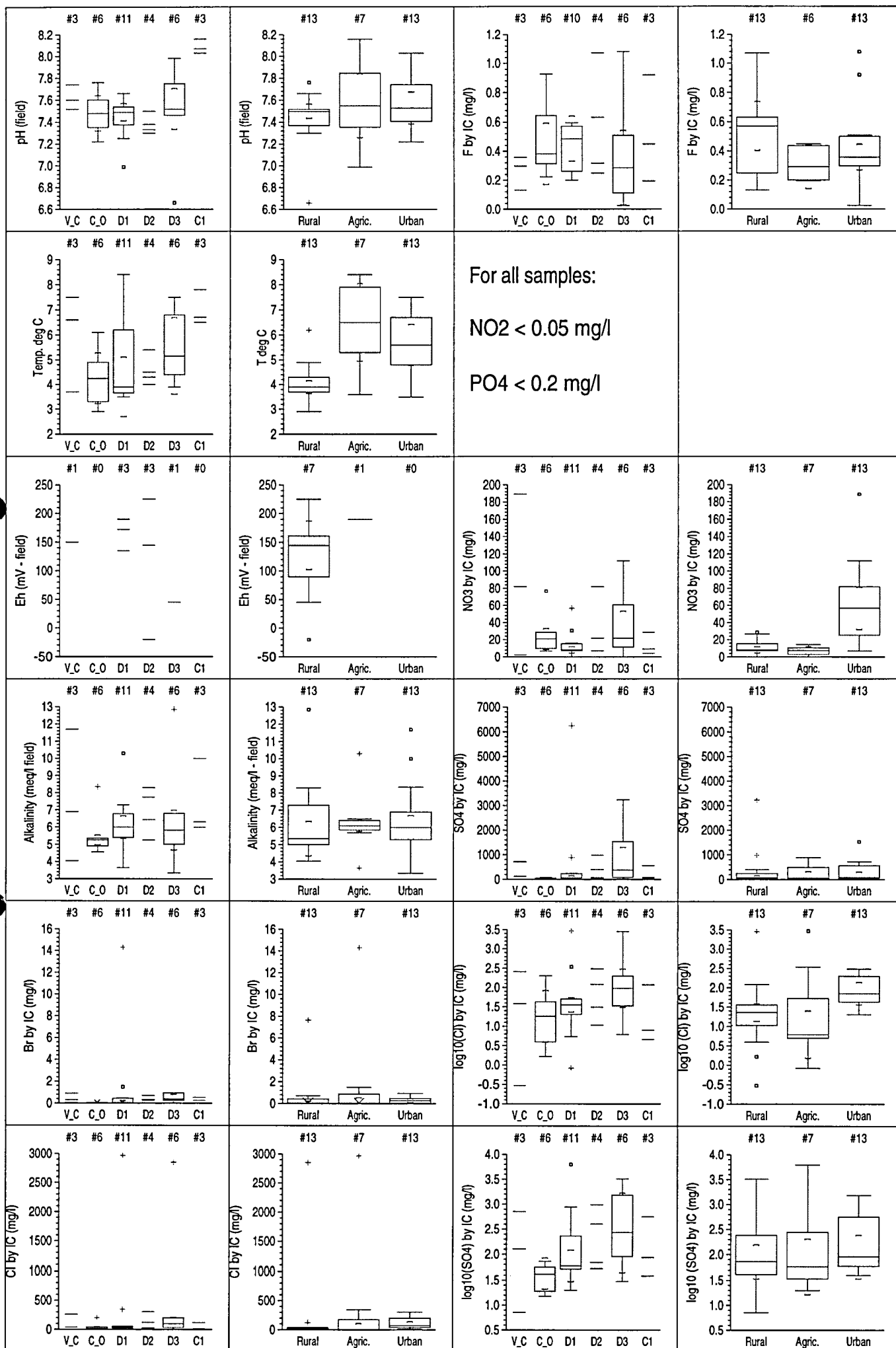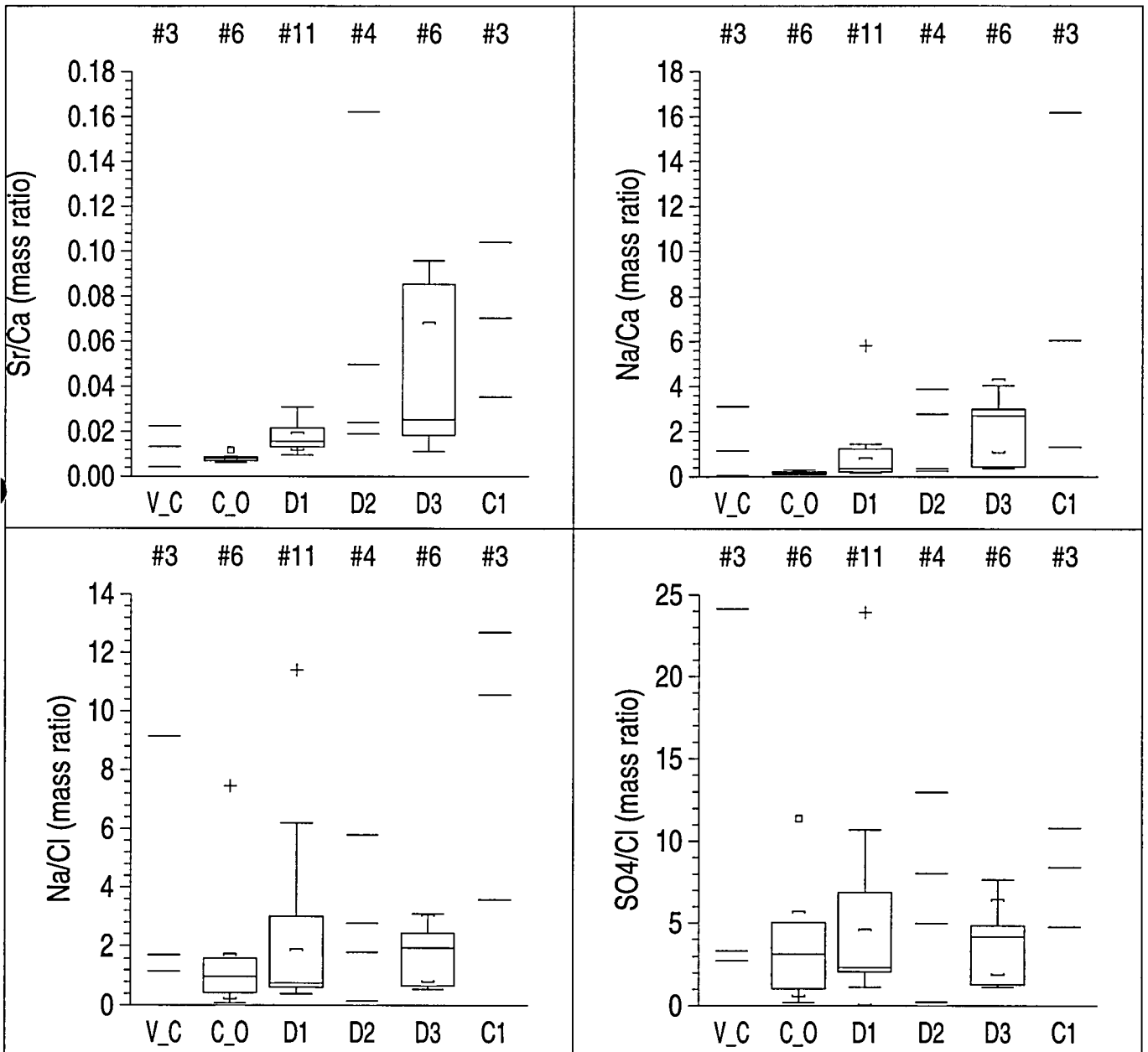
Figure 8.4

Figure 8.5

Sample numbers indicated for selected points
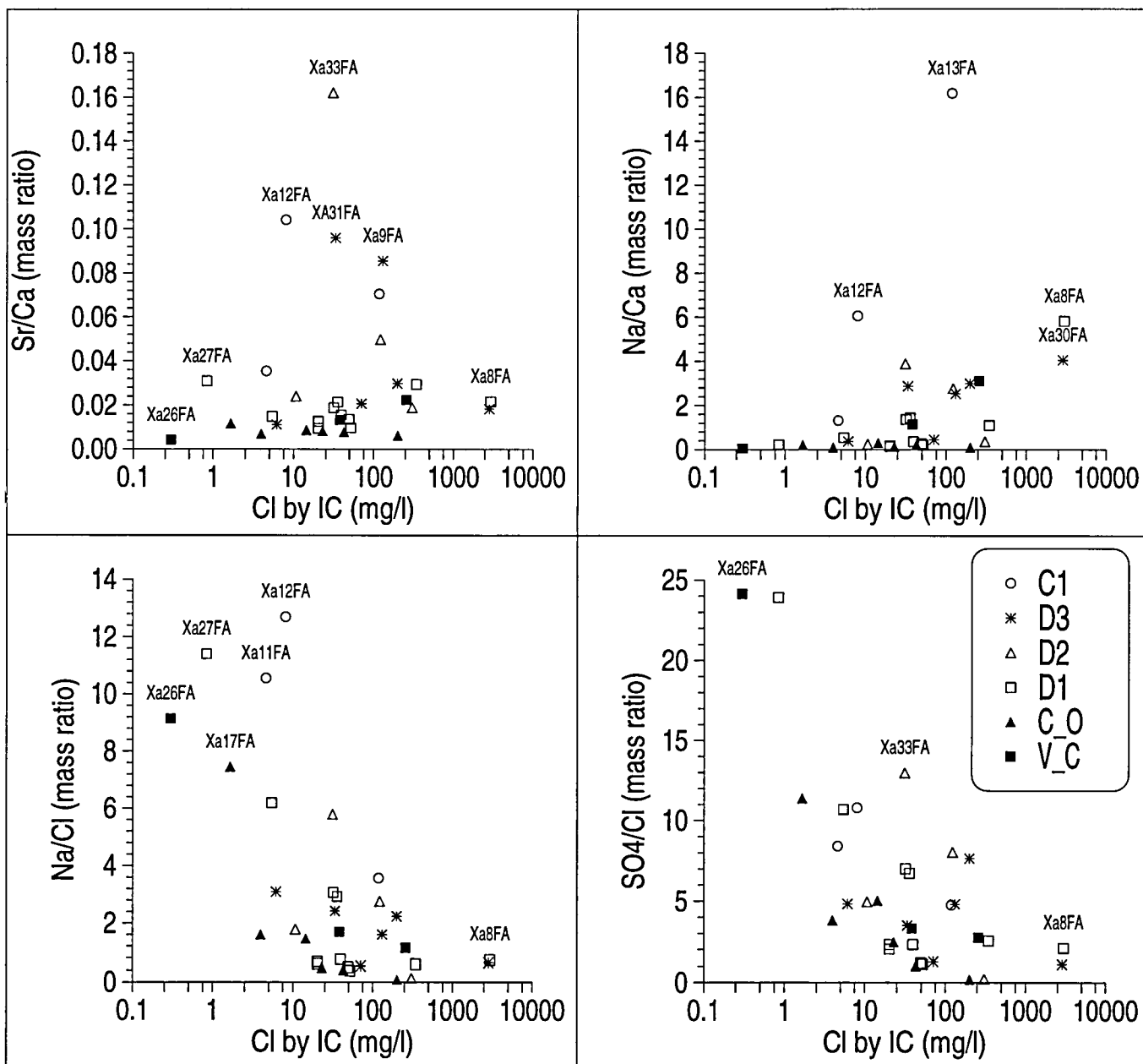Xa12FA = sample 12, filtered and acidified.
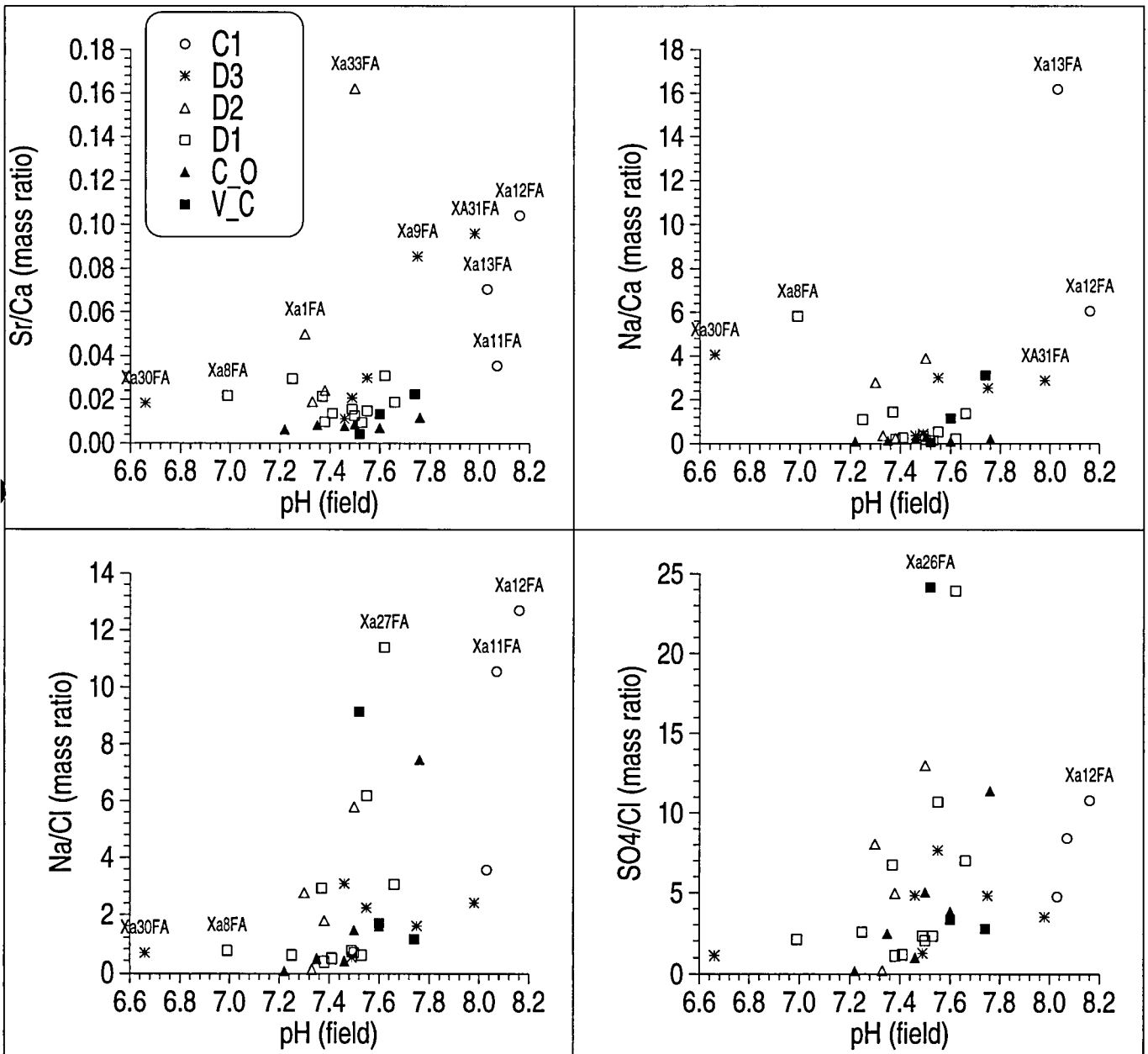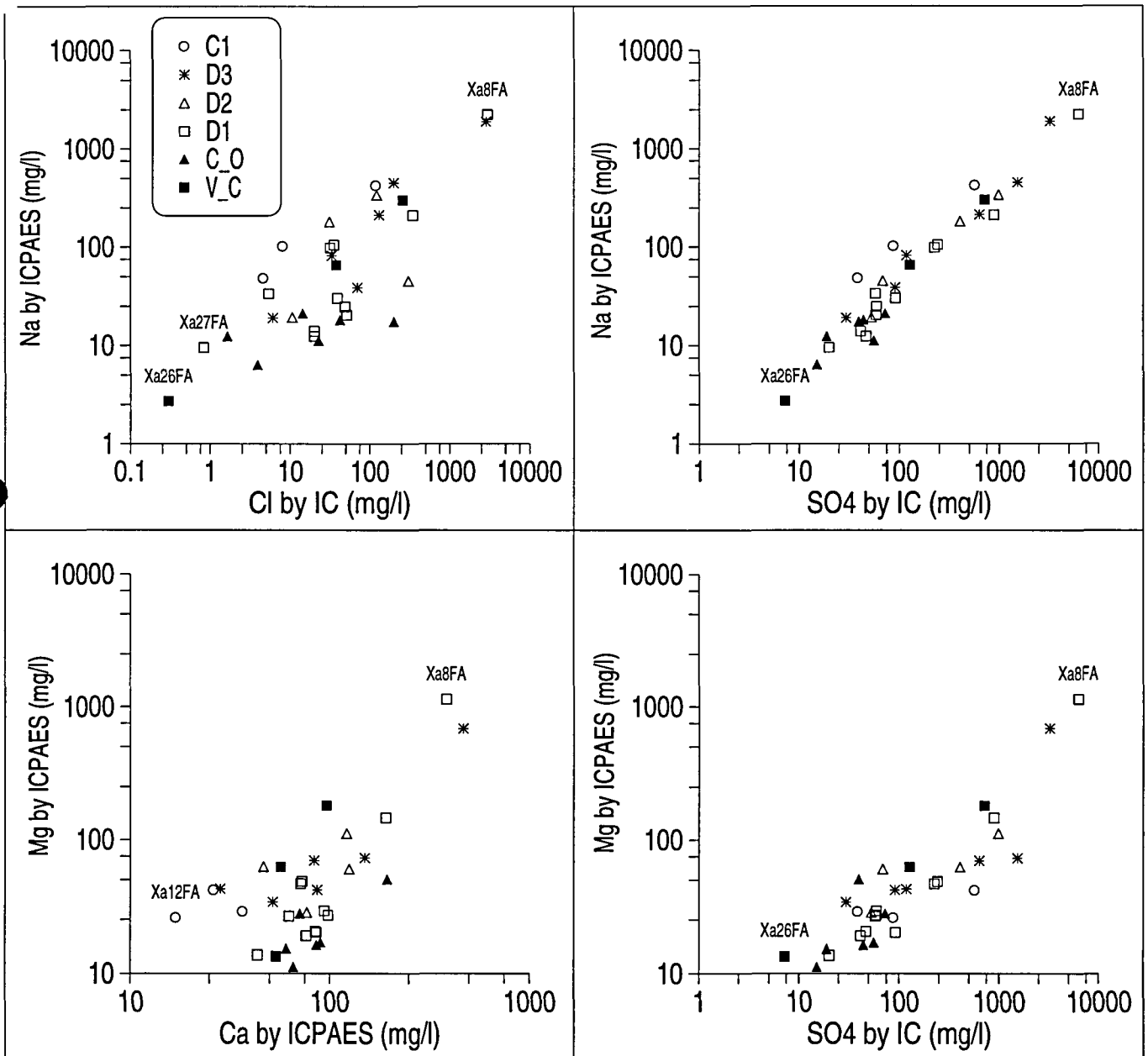
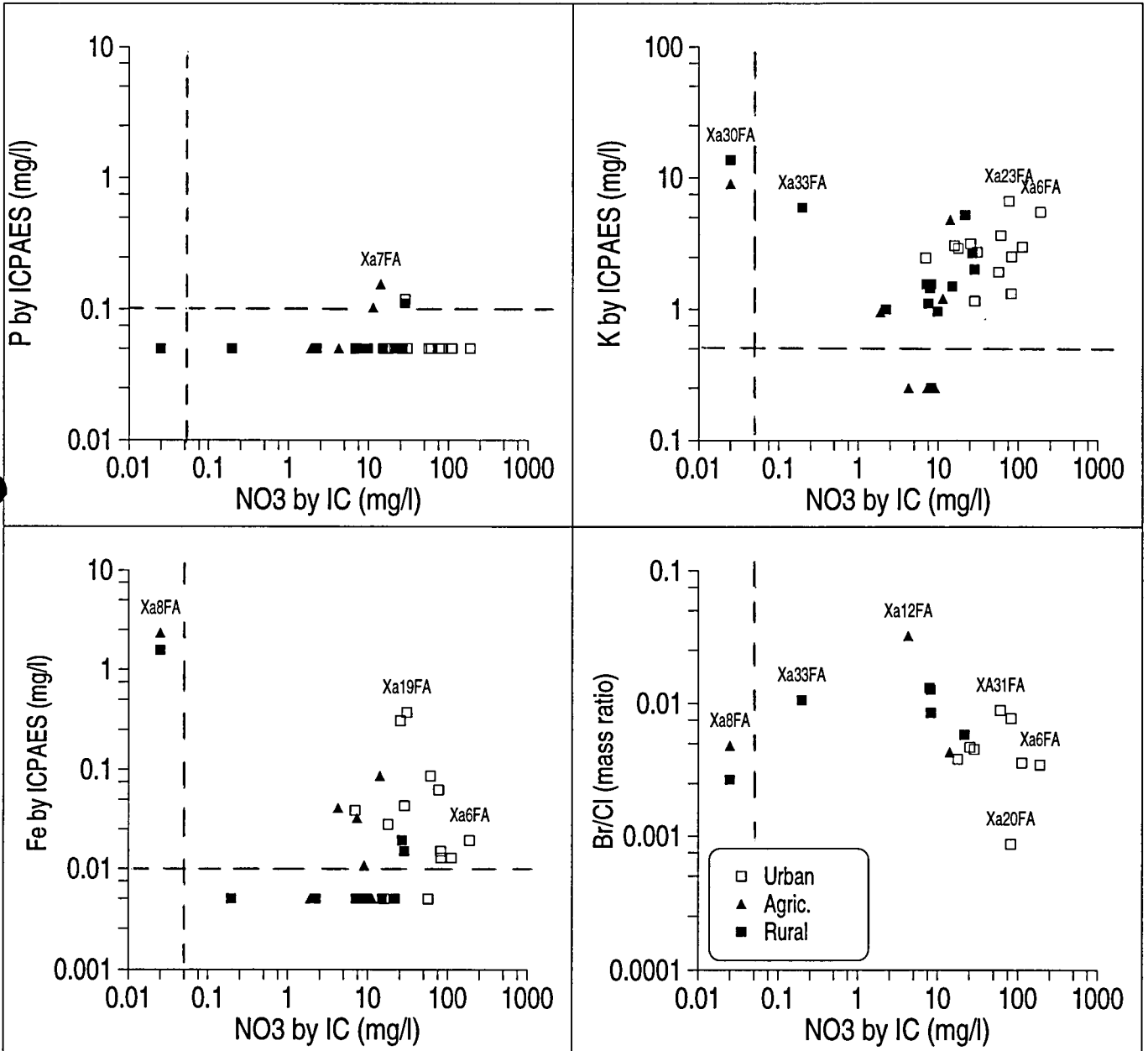Figure 8.6

Figure 8.6

Figure 8.7
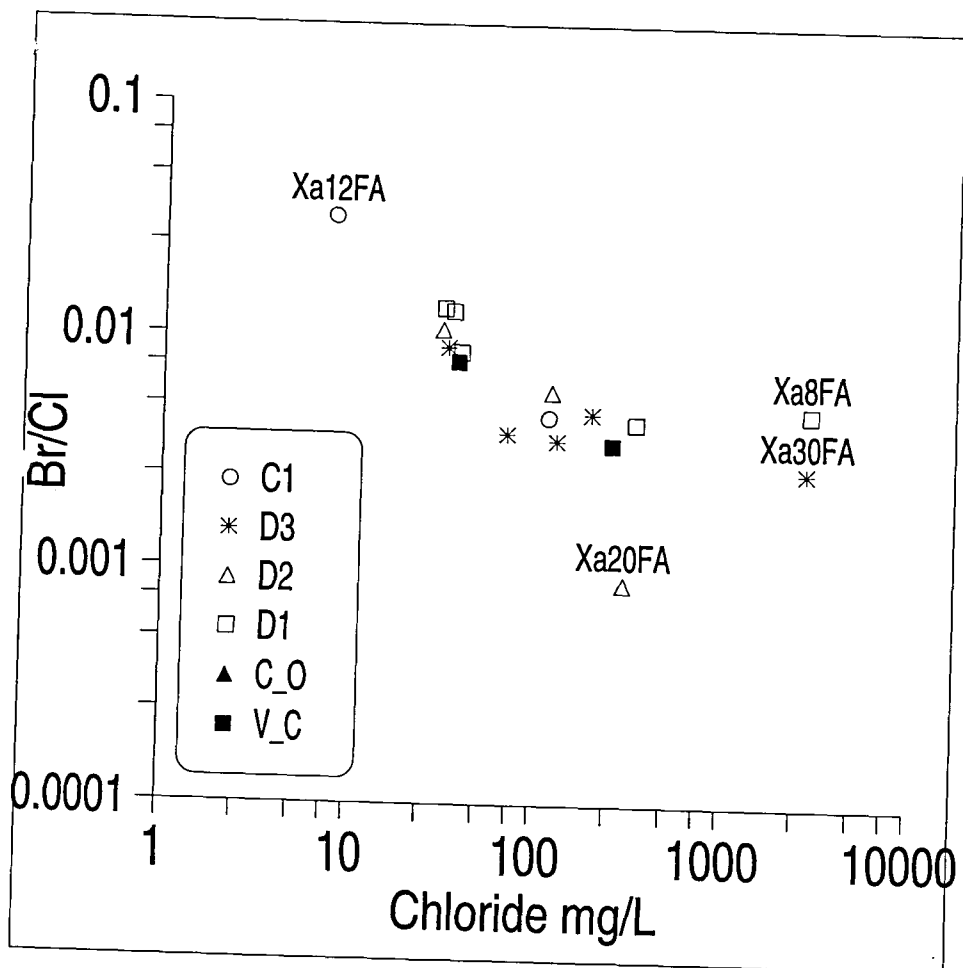
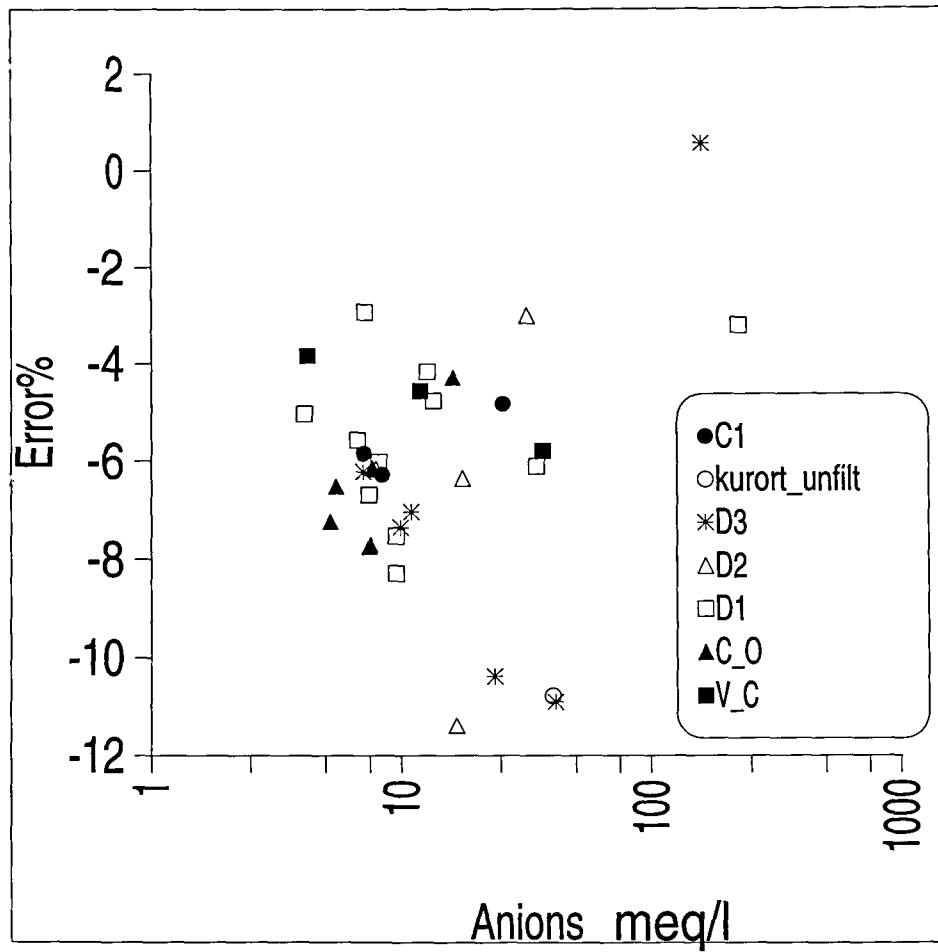Figure 8.8
(Dashed lines show detection limits)
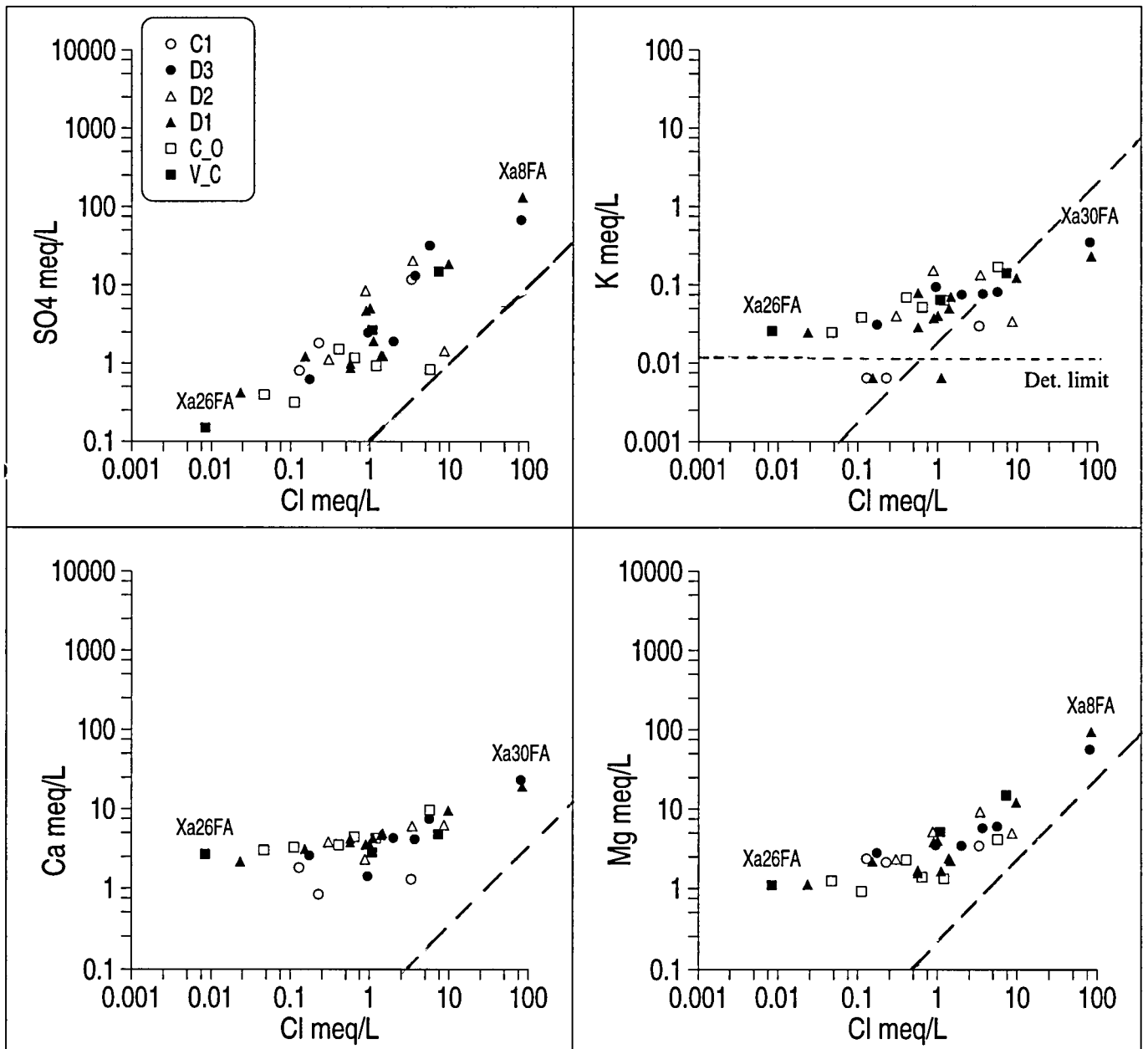
Figure 8.9

Figure 8.10
(Lines show seawater dilution)

Figure 8.11

Figure 8.12
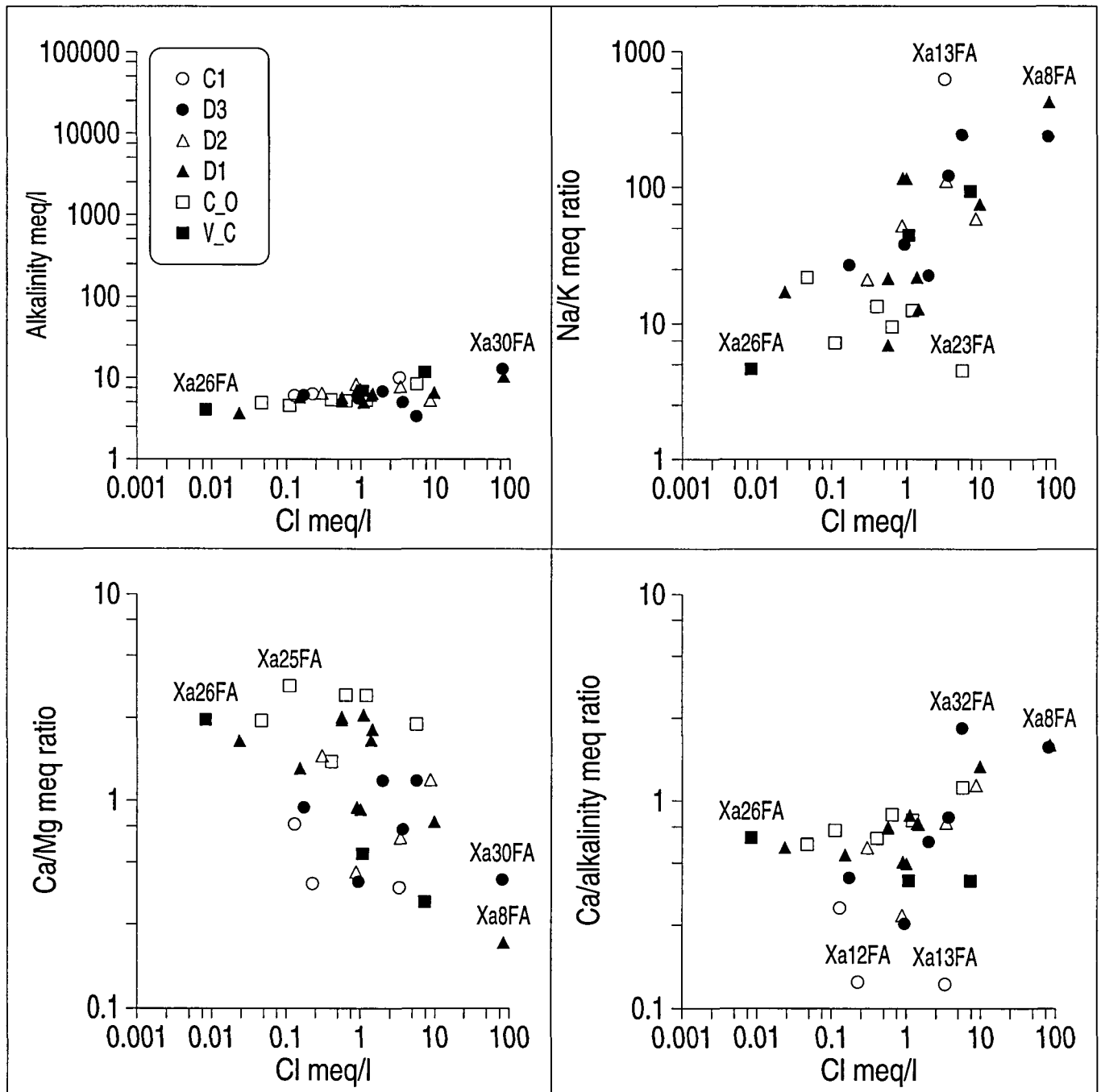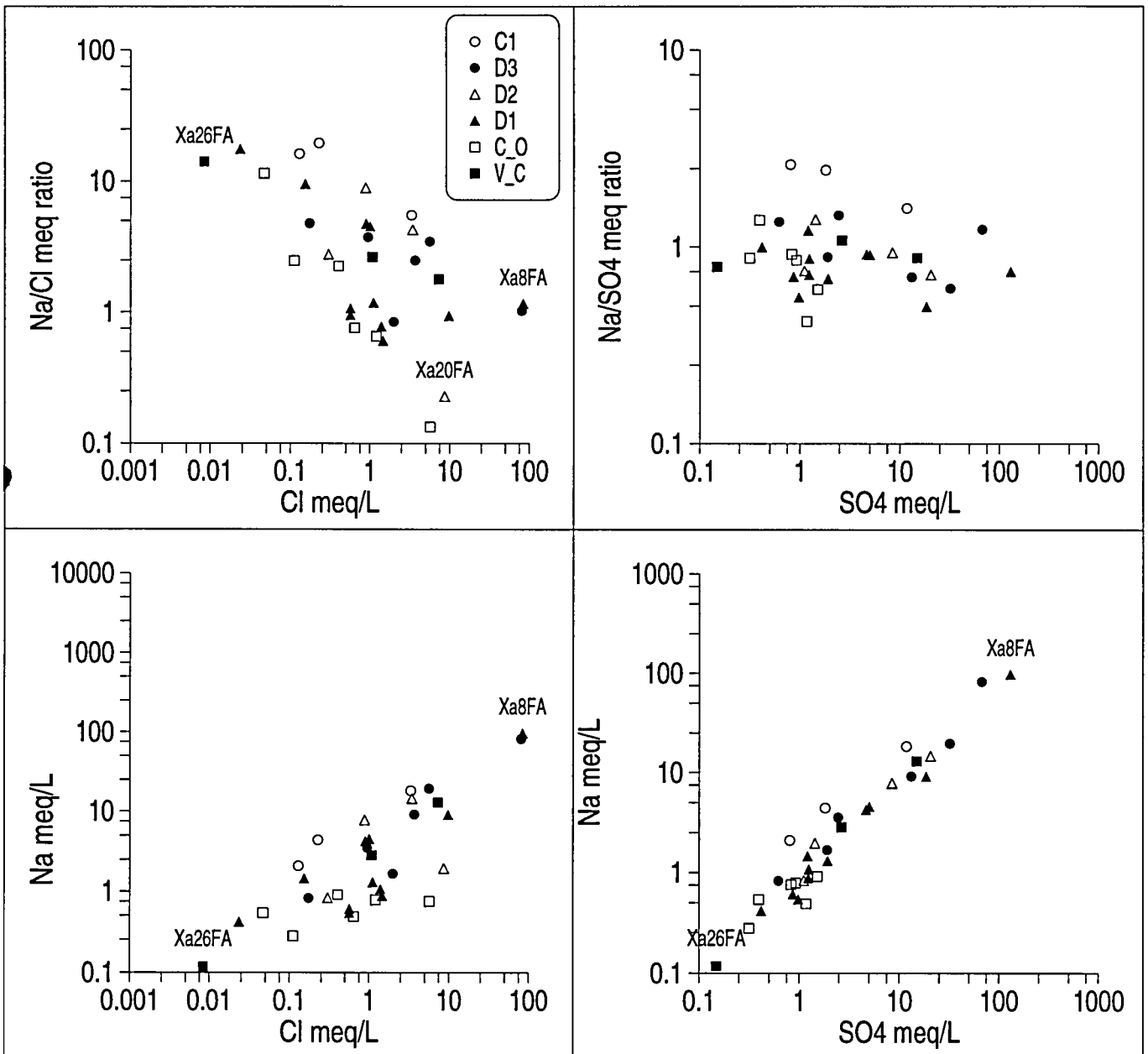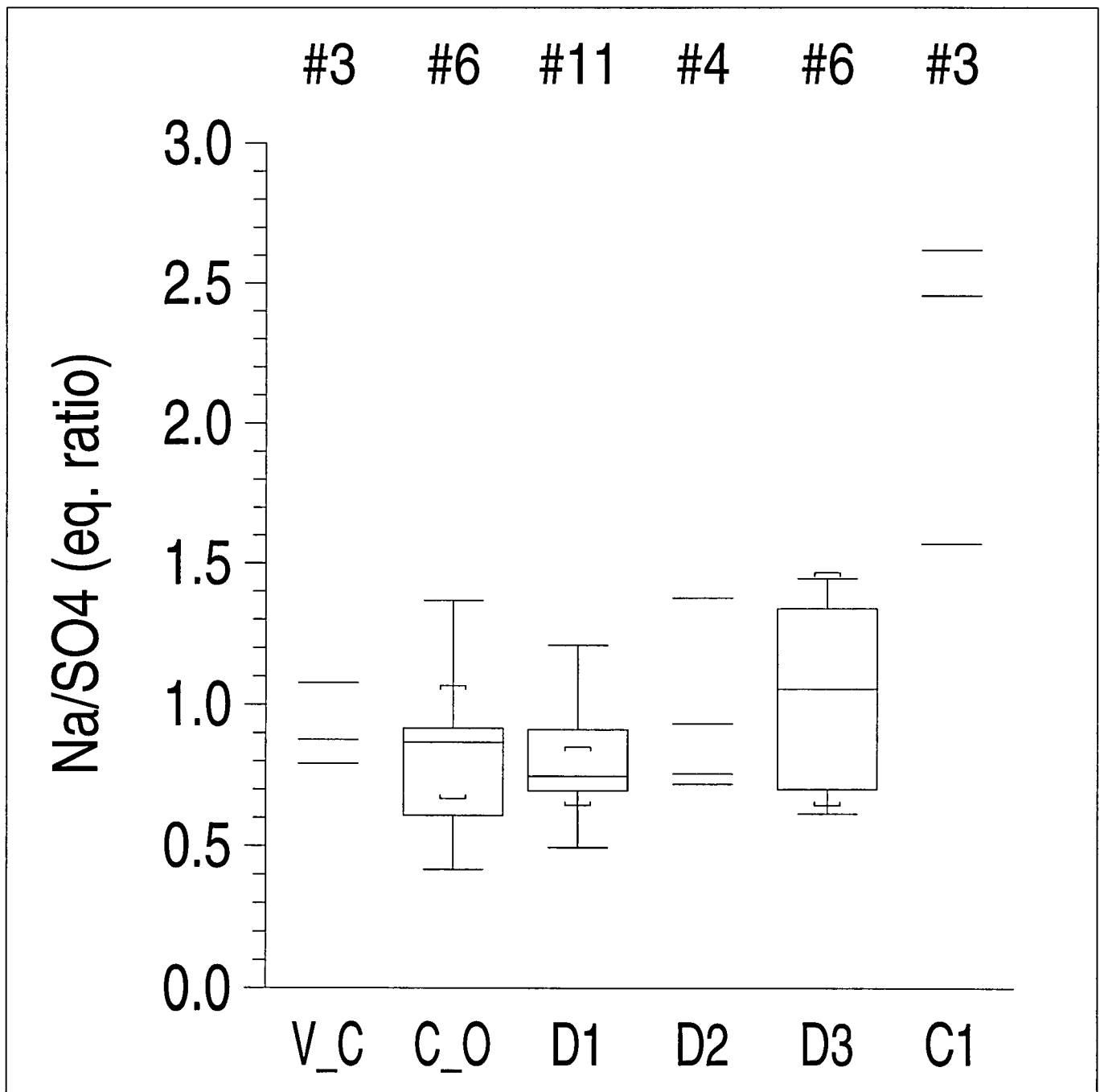
Figure 8.13

Figure 8.14

Lines show approximate fluorite saturation (uncorrected for activity)
Upper pair of lines pK_s = 10.4 (Krauskopf 1979) - dashed = 25°C, unbroken = 6°C
Lower pair of lines pK_s = 10.96 (Nordström & Jenne 1977) - dashed = 25°C, unbroken = 6°C
Saturation lines for 6°C calculated via the Van't Hoff isotherm.

Krauskopf, K.B. 1979. *Introduction to Geochemistry. 2nd Edn.* McGraw-Hill.

Nordström, D.K. & Jenne, E.A. 1977. Fluorite solubility equilibria in selected geothermal waters. *Geochimica et Cosmochimica Acta* 53, 1727-1740.

Figure 8.15

n = 33
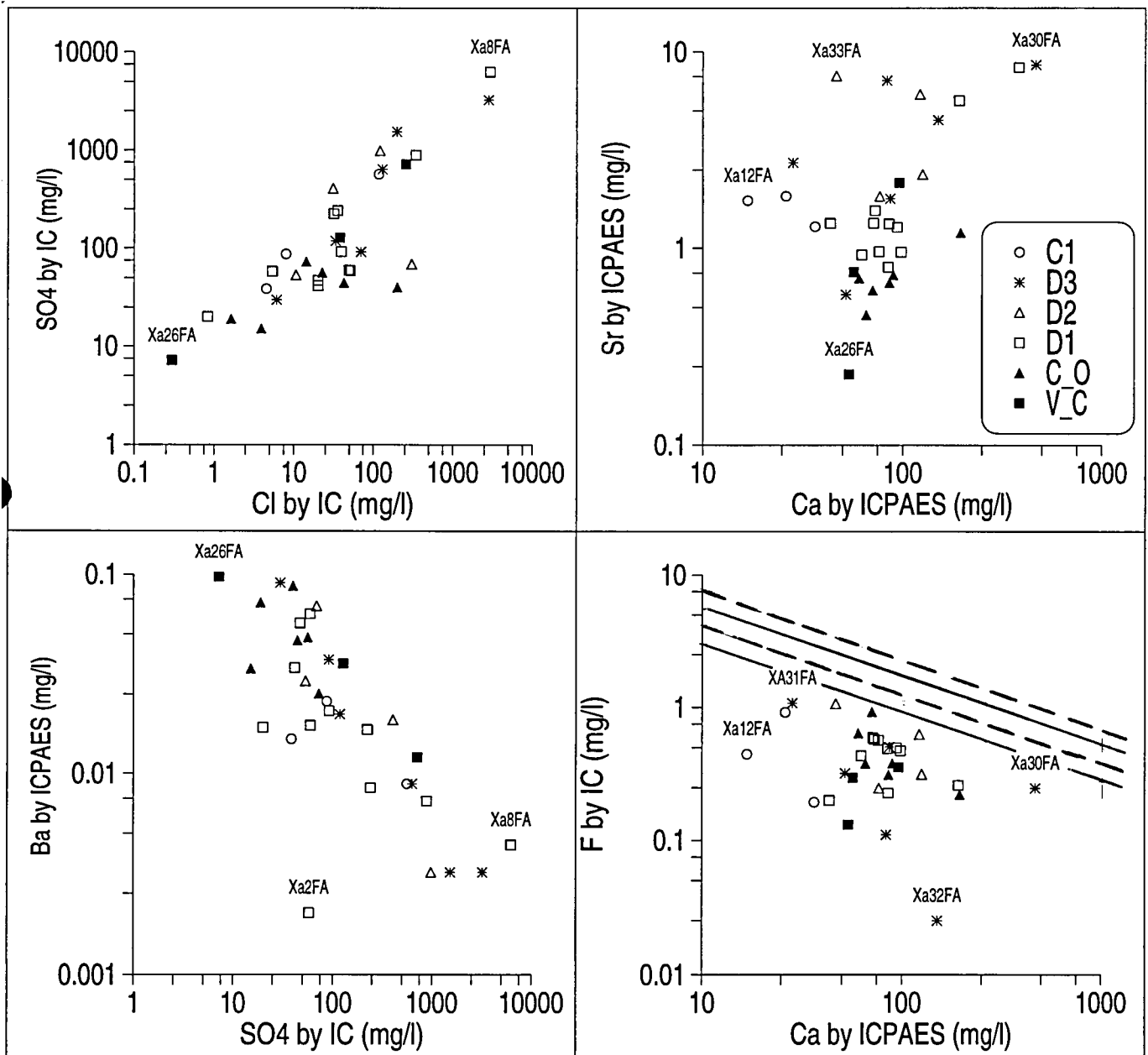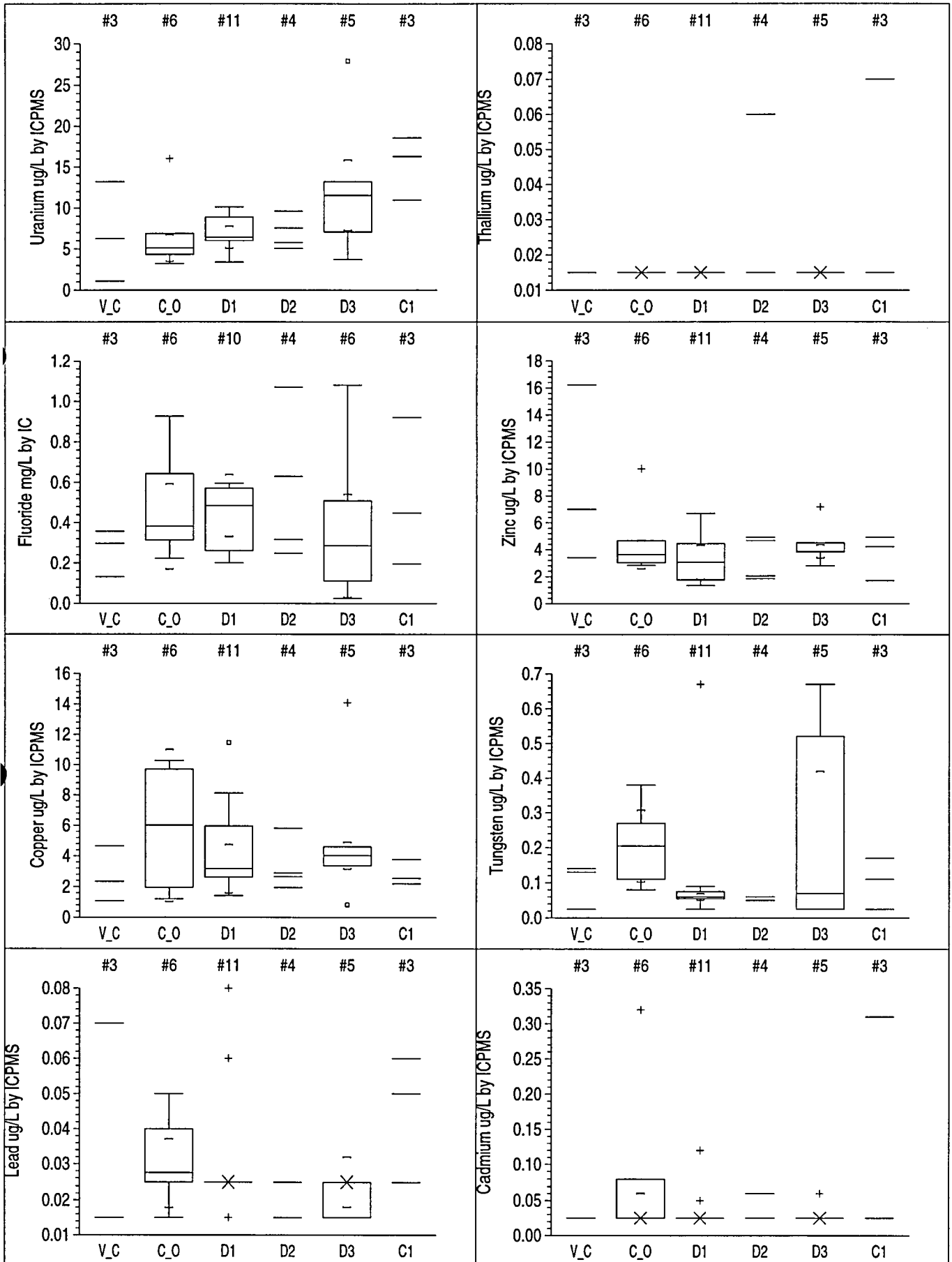
Figure 8.16

Figure 8.17
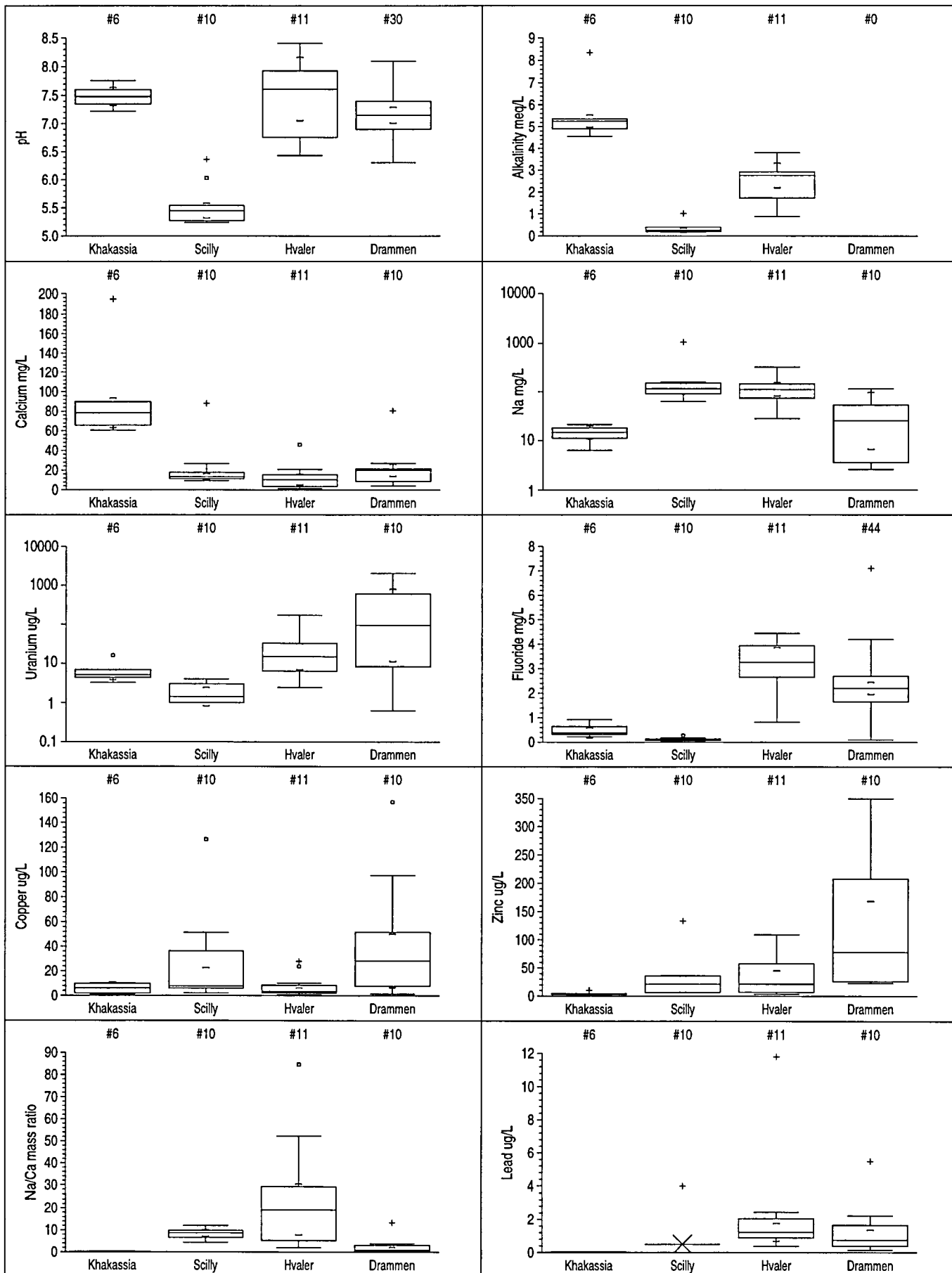
Figure 8.18
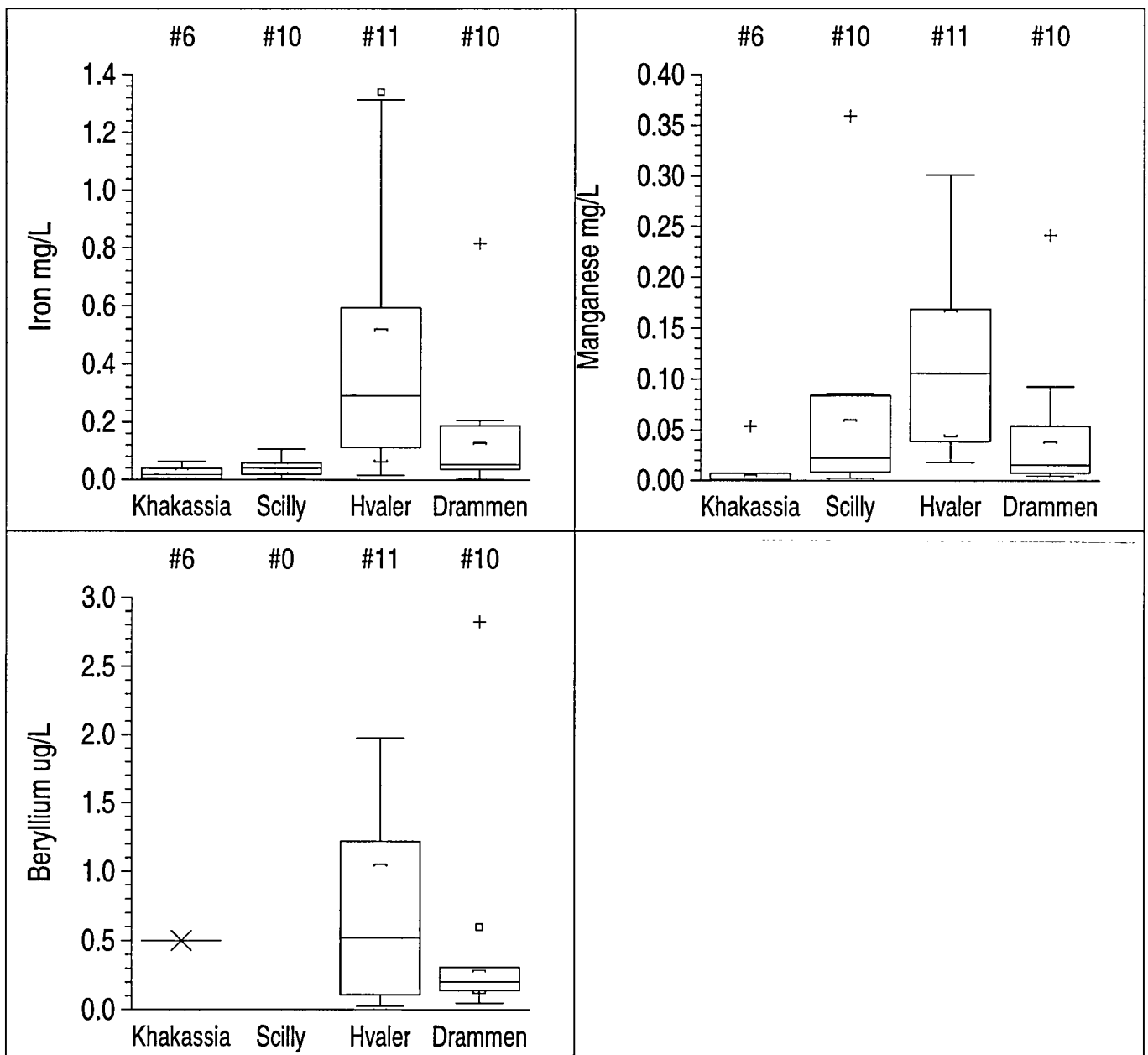
Figure 8.19

Khakassian gw without NO3 /K
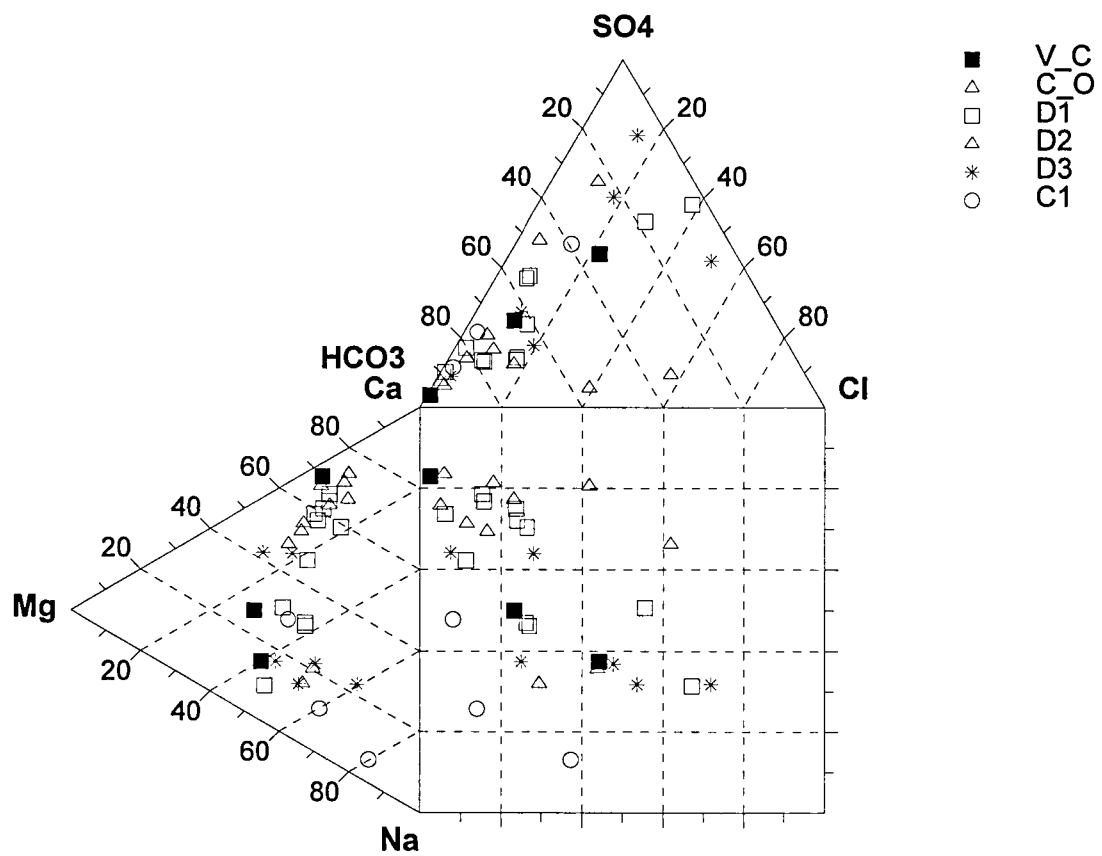
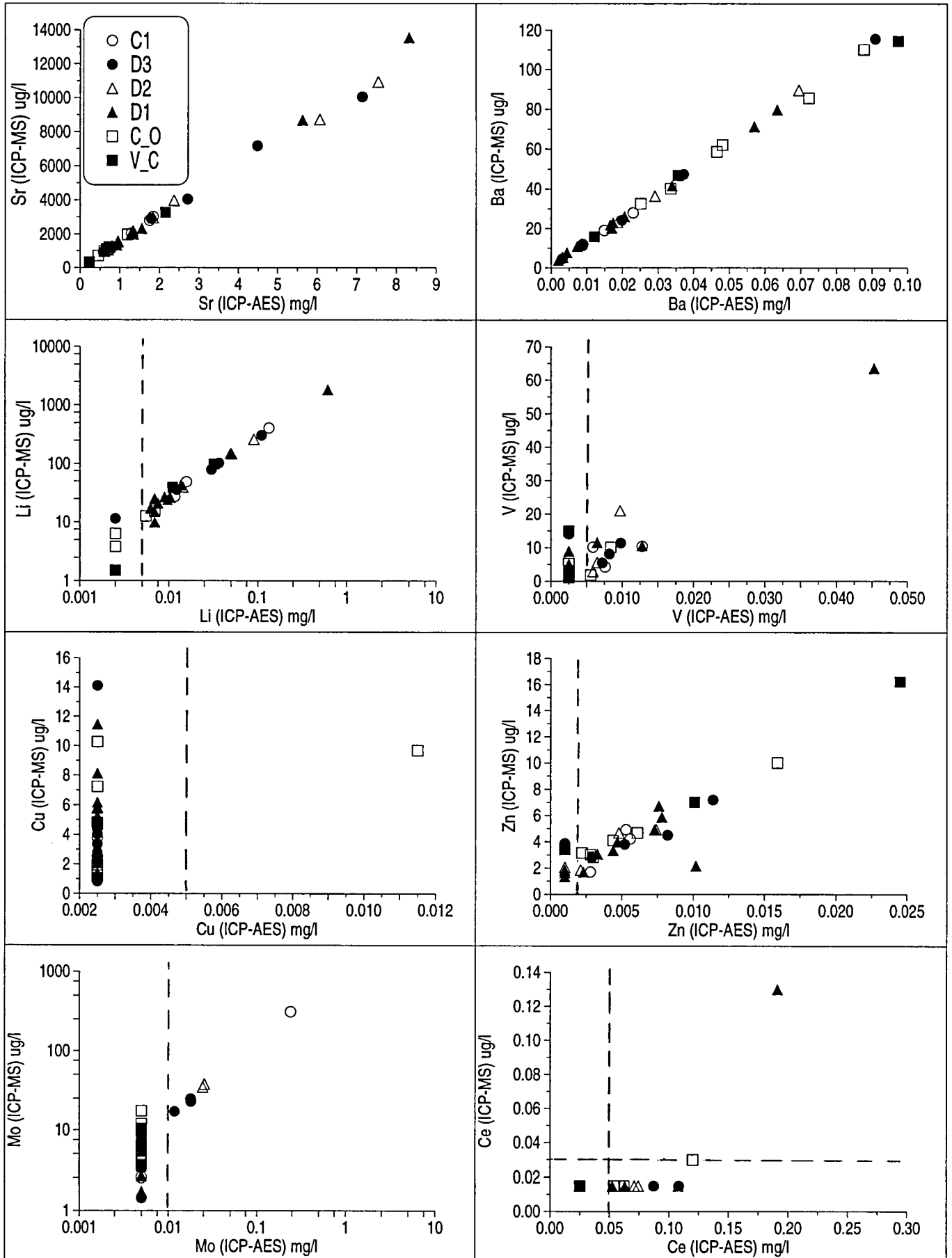Figure 8.20
(Lines show detection limits by ICP-AES)
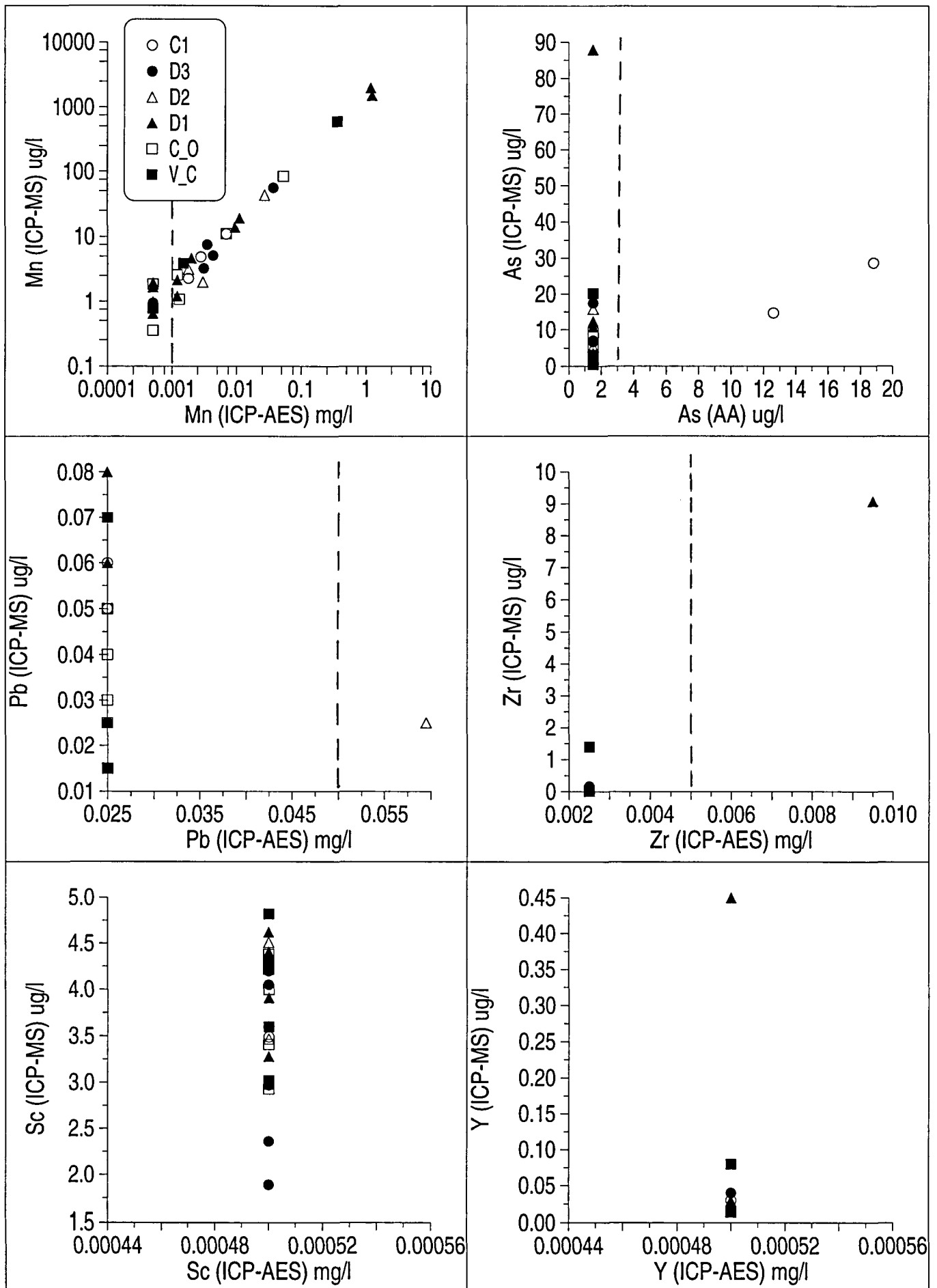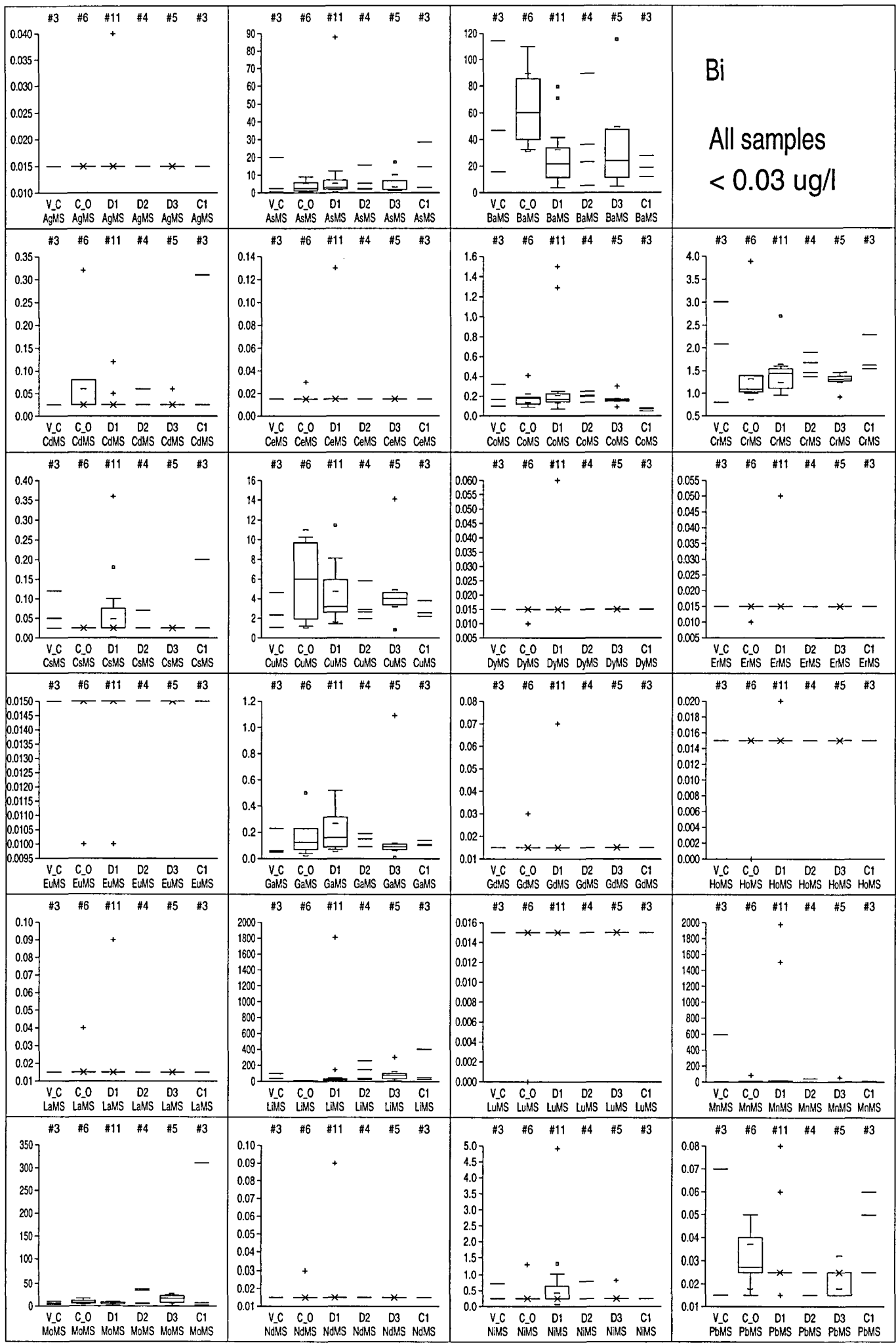
Figure 8.21
(Lines show detection limits by ICP-AES)

Figure 8.22

e.g. AgMS = Ag by ICP-MS in µg/l

Figure 8.23

Th

All samples

< 0.03 ug/l

All concentrations

in ug/l